Magnetic Properties and Superconductivity

Course code: 053311 PHY 3101
Course title: Electrical Engineering Materials
Bachelor of Science in Electrical and Electronic Engineering
Jashore University of Science and Technology

Content

Magnetic properties of materials, Magnetic moment, magnetization and relative permitivity, different types of magnetic materials, origin of ferromagnetism and magnetic domains. Introduction to superconductivity, Zero resistance and Meissner effect, Type I and Type II superconductors and critical current density.

References

Principles of Electronic Materials and Devices – S. O. Kasap
Electrical Engineering Materials – A. J. Dekker
Superconductivity: Basics and Applications to Magnets – R.G. Sharma

CHAPTER

8

Magnetic Properties and Superconductivity

Many electrical engineering devices such as inductors, transformers, rotating machines, and ferrite antennas are based on utilizing the magnetic properties of materials. There are many instances where permanent magnets are also used either on their own or as part of a device such as a rotating machine or a loud speaker. The majority of engineering devices make use of the ferromagnetic and ferrimagnetic properties, which are therefore treated in much more detail than other magnetic properties such as diamagnetism and paramagnetism. Although superconductivity involves the vanishing of the resistivity of a conductor at low temperatures and is normally explained within quantum mechanics, we treat the subject in this chapter because all superconductors are perfect diamagnets and, further, they have present or potential uses that involve magnetic fields. The advent of high-T_c superconductivity, discovered in 1986 by George Bednorz and Alex Müller at IBM Research Laboratories in Zürich, is undoubtedly one of the most significant discoveries over the last 50. High-T_c superconductors are already finding applications in such devices as superconducting solenoids, sensitive magnetometers, and high-Q microwave filters, power cables and superconducting current limiters and so on. Giant magnetoresistance (GMR) is probably one of the most exciting discoveries in the field of sprintronics, that is, spin transport electronics. GMR is a phenomenon that depends on the spin of the electron as it passes from one thin ferromagnetic layer to an adjacent antiferromagnetic layer. Its best known application is in the read heads of magnetic hard drives.

8.1 MAGNETIZATION OF MATTER

8.1.1 MAGNETIC DIPOLE MOMENT

Magnetic properties of materials involve concepts based on the magnetic dipole moment. Consider a current loop, as shown in Figure 8.1, where the circulating current is I. This may, for example, be a coil carrying a current. For simplicity we will assume that the current loop lies within a single plane. The area enclosed by the current is A. Suppose that $\mathbf{u}_n$ is a unit vector coming out from the area A. The direction of $\mathbf{u}_n$ is such that looking along it, the current circulates clockwise. Then the **magnetic dipole moment,** or simply the **magnetic moment** $\boldsymbol{\mu}_m$, is defined by[1]

Definition of magnetic moment

$$\boldsymbol{\mu}_m = IA\mathbf{u}_n \qquad [8.1]$$

When a magnetic moment is placed in a magnetic field, it experiences a torque that tries to rotate the magnetic moment to align its axis with the magnetic field, as depicted in Figure 8.2. Moreover, since a magnetic moment is a current loop, it gives rise to a magnetic field **B** around it, as shown in Figure 8.3, which is similar to the magnetic field around a bar magnet. We can find the field **B** from the current I and

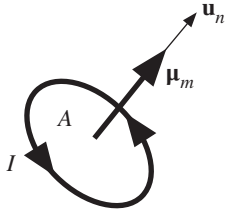


Figure 8.1 Definition of a magnetic dipole moment.

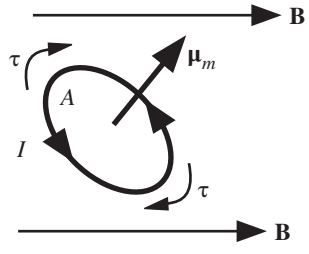


Figure 8.2 A magnetic dipole moment in an external field experiences a torque.

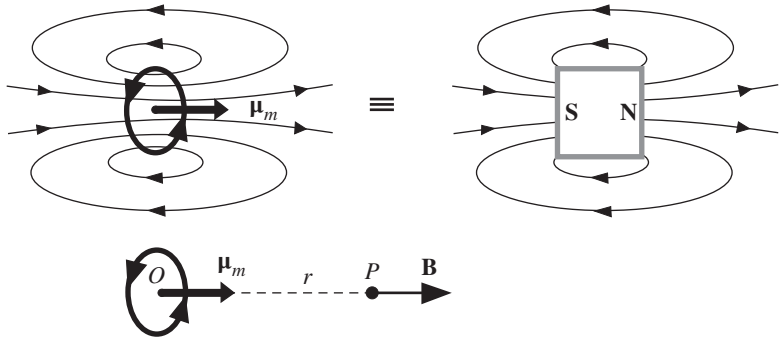


Figure 8.3 A magnetic dipole moment creates a magnetic field just like a bar magnet. The field **B** depends on $\boldsymbol{\mu}_m$.

[1] The symbol $\boldsymbol{\mu}$ for the magnetic dipole moment should not be confused with the permeability. Absolute and relative permeabilities will be denoted by μ_o and μ_r.

its geometry, which are treated in various physics textbooks. For example, the field **B** at a point P at a distance r along the axis of the coil from the center, as shown in Figure 8.3, is directly proportional to the magnitude of the magnetic moment but inversely proportional to r^3, that is, $\mathbf{B} \propto \boldsymbol{\mu}_m / r^3$.

8.1.2 Atomic Magnetic Moments

An orbiting electron in an atom behaves much like a current loop and has a magnetic dipole moment associated with it, called the **orbital magnetic moment** (μ_{orb}), as illustrated in Figure 8.4. If ω is the angular frequency of the electron, then the current I due to the orbiting electron is

$$I = \text{Charge flowing per unit time} = -\frac{e}{\text{Period}} = -\frac{e\omega}{2\pi}$$

If r is the radius of the orbit, then the magnetic dipole moment is

$$\mu_{\text{orb}} = I(\pi r^2) = -\frac{e\omega r^2}{2}$$

But the velocity v of the electron is ωr and its orbital angular momentum is

$$L = (m_e v)r = m_e \omega r^2$$

Using this in μ_{orb}, we get

Orbital magnetic moment of the electron

$$\mu_{\text{orb}} = -\frac{e}{2m_e} L \qquad [8.2]$$

We see that the magnetic moment is proportional to the orbital angular momentum through a factor that has the charge to mass ratio of the electron. The numerical factor, in this case $e/2m_e$, relating the angular momentum to the magnetic moment, is called the **gyromagnetic ratio.** The negative sign in Equation 8.2 indicates that μ_{orb} is in the opposite direction to L and is due to the negative charge of the electron.

The electron also has an intrinsic angular momentum S, that is, spin. The spin of the electron has a **spin magnetic moment,** denoted by μ_{spin}, but the relationship between μ_{spin} and S is not the same as that in Equation 8.2. The gyromagnetic ratio is a factor of 2 greater,

Spin magnetic moment of the electron

$$\mu_{\text{spin}} = -\frac{e}{m_e} S \qquad [8.3]$$

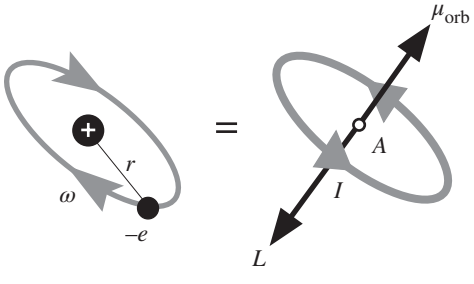


Figure 8.4 An orbiting electron is equivalent to a magnetic dipole moment μ_{orb}.

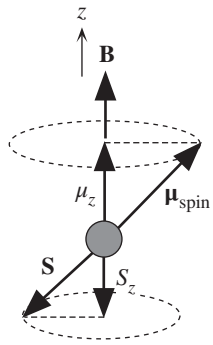


Figure 8.5 The spin magnetic moment precesses about an external magnetic field along z and has a value μ_z along z.

The overall magnetic moment of the electron consists of $\boldsymbol{\mu}_{orb}$ and $\boldsymbol{\mu}_{spin}$ appropriately added. We cannot simply add them numerically as they are vector quantities. Furthermore, the overall magnetic moment $\boldsymbol{\mu}_{atom}$ of the atom itself depends on the orbital motions and spins of *all* the electrons. Electrons in closed subshells, however, do not contribute to the overall magnetic moment because for every electron with a given **L** (or **S**), there is another one with an opposite **L** (or **S**). The reason is that the direction of **L** is space quantized by m_ℓ and all negative and positive values of m_ℓ are occupied in a closed shell. Similarly, there are as many electrons spinning up as there are spinning down, so there is no net electron spin in a closed shell and no net $\boldsymbol{\mu}_{spin}$. Thus, only **unfilled subshells** contribute to the overall magnetic moment of an atom.

Consider an atom that has closed inner shells and a single electron in an s orbital ($\ell = 0$). This means that the orbital magnetic moment is zero and the atom has a magnetic moment due to the spin of the electron alone, $\boldsymbol{\mu}_{atom} = \boldsymbol{\mu}_{spin}$. In the presence of an external magnetic field along the z direction, the magnetic moment cannot simply rotate and align with the field because quantum mechanics requires the spin angular momentum to be space quantized, that is, S_z (the component of **S** along z) must be $m_s\hbar$ where $m_s = \pm\frac{1}{2}$ is the spin magnetic quantum number. The torque experienced by the spinning electron causes the spin magnetic moment to precess about the external magnetic field, as shown in Figure 8.5. This precession is such that $S_z = -\frac{1}{2}\hbar$ and leads to an average magnetic moment μ_z along the field given by Equation 8.3 with S_z, that is,

Magnetic moment along the field

$$\mu_z = -\frac{e}{m_e}S_z = -\frac{e}{m_e}(m_s\hbar) = \frac{e\hbar}{2m_e} = \beta \qquad [8.4]$$

The quantity $\beta = e\hbar/2m_e$ is called the **Bohr magneton** and has the value 9.27×10^{-24} A m^2 or J T^{-1}.

Thus, the spin of a single electron has a magnetic moment of one Bohr magneton along the field.

8.1.3 MAGNETIZATION VECTOR M

Consider a tightly wound long solenoid, ideally infinitely long, with free space (or vacuum) as the medium inside the solenoid, as shown in Figure 8.6a. The magnetic

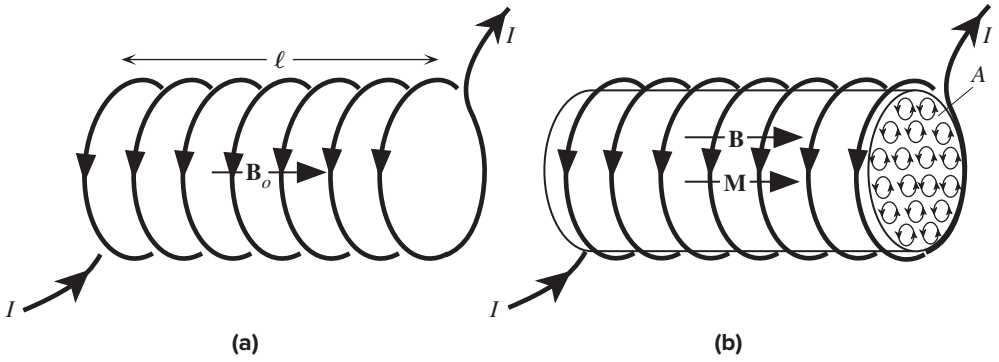


Figure 8.6 (a) Consider a long solenoid. With free space as the medium inside, the magnetic field is $\mathbf{B}_o$. (b) A material medium inserted into the solenoid develops a magnetization **M**.

field inside the solenoid is denoted by $\mathbf{B}_o$ to specifically identify this field as in free space. This field depends on the current I through the solenoid wire and the number of turns per unit length n and is given by[2]

Free space field inside solenoid

$$B_o = \mu_o nI = \mu_o I' \qquad [8.5]$$

where I' is the current per unit length of the solenoid, that is, $I' = nI$, and μ_o is the absolute permeability of free space in henries per meter, H m^{-1}.

If we now place a cylindrical material medium to fill the inside of this solenoid, as in Figure 8.6b, we find that the magnetic field has changed. The new magnetic field in the presence of a medium is denoted as **B**. We will take $\mathbf{B}_o$ to be the applied magnetic field into which the material medium is placed.

Each atom of the material responds to the applied field $\mathbf{B}_o$ and develops, or acquires, a net magnetic moment $\boldsymbol{\mu}_m$ along the applied field. We can view each magnetic moment $\boldsymbol{\mu}_m$ as the result of the precession of each atomic magnetic moment about $\mathbf{B}_o$. The medium therefore develops a net magnetic moment along the field and becomes **magnetized.** The magnetic vector **M** describes the extent of magnetization of the medium. **M** is defined as the **magnetic dipole moment per unit volume.** Suppose that there are N atoms in a small volume ΔV and each atom i has a magnetic moment $\boldsymbol{\mu}_{mi}$ (where $i = 1$ to N). Then **M** is defined by

Magnetization vector

$$\mathbf{M} = \frac{1}{\Delta V}\sum_{i=1}^{N}\boldsymbol{\mu}_{mi} = n_{\text{at}}\boldsymbol{\mu}_{\text{av}} \qquad [8.6]$$

where n_{at} is the number of atoms per unit volume and $\boldsymbol{\mu}_{\text{av}}$ is the average magnetic moment per atom. We can assume that each atom acquires a magnetic moment $\boldsymbol{\mu}_{\text{av}}$ along $\mathbf{B}_o$. Each of these magnetic moments along $\mathbf{B}_o$ can be viewed as an elementary current loop at the atomic scale, as schematically depicted in Figure 8.6b. These elementary current loops are due to electronic currents within the atom and arise from both orbital and spin motions of the electrons. Each current loop has its current plane normal to $\mathbf{B}_o$.

[2] The proof of this comes out from Ampere's law and can be found in any textbook of electromagnetism.

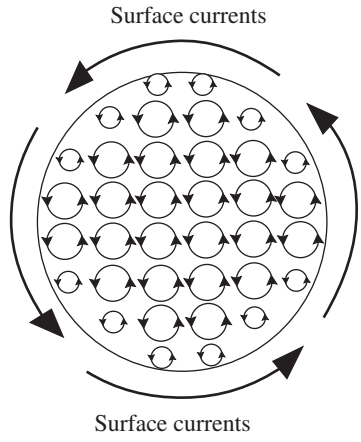


Figure 8.7 Elementary current loops result in surface currents. There is no internal current, as adjacent currents on neighboring loops are in opposite directions.

Consider a cross section of the magnetized medium, as in Figure 8.7. All the elementary current loops in this plane have the current circulation in the same direction inasmuch as each atom acquires the same magnetic moment $\boldsymbol{\mu}_{av}$. All neighboring loops in the bulk have adjacent currents in opposite directions that cancel each other, as apparent in Figure 8.7. Thus, there are no net bulk currents, or internal currents, within the bulk of the material. However, the currents at the surface in the surface loops cannot be canceled and this leads to a net **surface current,** as depicted in Figure 8.7. The surface currents are induced by the magnetization of the medium by the applied magnetic field and therefore depend on the magnetization M of the specimen.

From the definition of M, the total magnetic moment of the cylindrical specimen is

$$\text{Total magnetic moment} = M\ (\text{Volume}) = MA\ell$$

Suppose that the magnetization current on the surface per unit length of the specimen is I_m. Then the total circulating surface current is $I_m\ell$ and the total magnetic moment of the specimen, by definition, is

$$\text{Total magnetic moment} = (\text{Total current}) \times (\text{Cross-sectional area}) = I_m\ell A$$

Magnetization and surface currents

Equating the two total magnetic moments, we find

$$M = I_m \qquad [8.7]$$

We derived this for a particular sample geometry, a cylindrical specimen, in which **M** is along the axis of the cylindrical specimen and I_m flows in a plane perpendicular to **M**. The relationship, however, is more general, as derived in more advanced texts. It should be emphasized that the magnetization current I_m is not due to the flow of free charge carriers, as in a current-carrying copper wire, but due to localized electronic currents within the atoms of the solid at the surface. Equation 8.7 states that we can represent the magnetization of a medium by a surface current per unit length I_m that is equal to M.

8.1.4 MAGNETIZING FIELD OR MAGNETIC FIELD INTENSITY H

The magnetized specimen in Figure 8.6b placed inside the solenoid develops magnetization currents on the surface. It therefore behaves like a solenoid. We can now regard the solenoid with medium inside, as depicted in Figure 8.8. The magnetic field within the medium now arises from not only the conduction current per unit length I' in the solenoid wires but also from the magnetization current I_m on the surface. The magnetic field B inside the solenoid is now given by the usual solenoid expression but with a current that includes both I' and I_m, as shown in Figure 8.8:

$$B = \mu_o(I' + I_m) = B_o + \mu_o M$$

Magnetic field in a magnetized medium

This relationship is generally valid and can be written in vector form as

$$\mathbf{B} = \mathbf{B}_o + \mu_o \mathbf{M} \qquad [8.8]$$

The field at a point inside a magnetized material is the sum of the applied field $\mathbf{B}_o$ and a contribution from the magnetization $\mathbf{M}$ of the material. The magnetization arises from the application of $\mathbf{B}_o$ due to the current of free carriers in the solenoid wires, called the **conduction current,** which we can externally adjust. It becomes useful to introduce a vector field that represents the effect of the external or conduction current alone. In general, $\mathbf{B} - \mu_o\mathbf{M}$ at a point is the contribution of the external currents alone to the magnetic field at that point inside the material that we called $\mathbf{B}_o$. $\mathbf{B} - \mu_o\mathbf{M}$ represents a magnetizing field because it is the field of the external currents that magnetize the material. The **magnetizing field H** is defined as

$$\mathbf{H} = \frac{1}{\mu_o}\mathbf{B} - \mathbf{M} \qquad [8.9]$$

Definition of the magnetizing field

or

$$\mathbf{H} = \frac{1}{\mu_o}\mathbf{B}_o$$

The magnetizing field is also known as the **magnetic field intensity** and is measured in A m^{-1}. The reason for the division by μ_o is that the resulting vector field $\mathbf{H}$ becomes simply related to the external conduction currents (through Ampere's law). Since in the solenoid $\mathbf{B}_o$ is $\mu_o nI$, we see that the magnetizing field in a solenoid is

$$H = nI = \text{Total conduction current per unit length} \qquad [8.10]$$

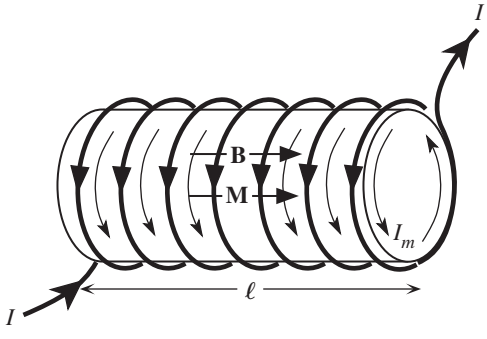


Figure 8.8 The field **B** in the material inside the solenoid is due to the conduction current *I* through the wires and the magnetization current I_m on the surface of the magnetized medium, or $\mathbf{B} = \mathbf{B}_o + \mu_o\mathbf{M}$.

It is generally helpful to imagine **H** as the *cause* and **B** as the *effect*. The cause **H** depends only on the external conduction currents, whereas the effect **B** depends on the magnetization **M** of matter.

8.1.5 MAGNETIC PERMEABILITY AND MAGNETIC SUSCEPTIBILITY

Suppose that at a point P in a material, the magnetic field is **B** and the magnetizing field is **H**. We let $\mathbf{B}_o$ be the magnetic field at P in the absence of any material (*i.e.*, in free space). The magnetic permeability of the medium at P is defined as the magnetic field per unit magnetizing field,

Definition of magnetic permeability

$$\mu = \frac{B}{H} \tag{8.11}$$

It relates the effect B to the cause H at the same point P inside a material. In simple qualitative terms, μ represents to what extent a medium is permeable by magnetic fields. Relative permeability μ_r of a medium is the fractional increase in the magnetic field with respect to the field in free space when a material medium is introduced. For example, suppose that the field in a solenoid with free space in it is B_o but with material inserted it is B. Then μ_r is defined by

Definition of relative permeability

$$\mu_r = \frac{B}{B_o} = \frac{B}{\mu_o H} \tag{8.12}$$

From Equations 8.11 and 8.12, clearly,

Total permeability

$$\mu = \mu_o \mu_r \tag{8.13}$$

The magnetization **M** produced in a material depends on the net magnetic field **B**. It would be natural to proceed as in dielectrics by relating **M** to **B** analogously to relating P (polarization) to E (electric field). However, for historic reasons, **M** is related to **H**, the magnetizing field. Suppose that the medium is isotropic (same properties in all directions), then magnetic susceptibility χ_m of the medium is defined simply by

Definition of magnetic susceptibility

$$\mathbf{M} = \chi_m \mathbf{H} \tag{8.14}$$

This relationship is not obeyed by all magnetic materials. For example, as we will see later, ferromagnetic materials do not obey Equation 8.12. Since the magnetic field

Magnetic and magnetizing fields and magnetization

$$\mathbf{B} = \mu_o(\mathbf{H} + \mathbf{M}) \tag{8.15}$$

we have

$$B = \mu_o H + \mu_o M = \mu_o H + \mu_o \chi_m H = \mu_o(1 + \chi_m)H$$

and

Relative permeability and susceptibility

$$\mu_r = 1 + \chi_m \tag{8.16}$$

The presence of a magnetizable material is conveniently accounted for by using the relative permeability μ_r, or $(1 + \chi_m)$, to simply multiply μ_o. Alternatively, one can simply replace μ_o with $\mu = \mu_o \mu_r$. For example, the inductance of the solenoid with a magnetic medium inside increases by a factor of μ_r.

Table 8.1 provides a summary of various important magnetic quantities, their definitions, and units.

Table 8.1 Magnetic quantities and their units

Magnetic Quantity	Symbol	Definition	Units	Comment
Magnetic field; magnetic induction	$\mathbf{B}$	$\mathbf{F} = q\mathbf{v} \times \mathbf{B}$	T = tesla = webers m^{-2}	Produced by moving charges or currents, acts on moving charges or currents.
Magnetic flux	Φ	$\Delta\Phi = B_{\text{normal}}\,\Delta A$	Wb = weber	$\Delta\Phi$ is flux through ΔA and B_{normal} is normal to ΔA. Total flux through any closed surface is zero.
Magnetic dipole moment	$\boldsymbol{\mu}_m$	$\mu_m = IA$	A m^2	Experiences a torque in $\mathbf{B}$ and a net force in a nonuniform $\mathbf{B}$.
Bohr magneton	β	$\beta = e\hbar/2m_e$	A m^2 or J T^{-1}	Magnetic moment due to the spin of the electron. $\beta = 9.27 \times 10^{-24}$ A m^2
Magnetization vector	$\mathbf{M}$	Magnetic moment per unit volume	A m^{-1}	Net magnetic moment in a material per unit volume.
Magnetizing field; magnetic field intensity	$\mathbf{H}$	$\mathbf{H} = \mathbf{B}/\mu_o - \mathbf{M}$	A m^{-1}	$\mathbf{H}$ is due to external conduction currents only and is the cause of $\mathbf{B}$ in a material.
Magnetic susceptibility	χ_m	$\mathbf{M} = \chi_m\mathbf{H}$	None	Relates the magnetization of a material to the magnetizing field $\mathbf{H}$.
Absolute permeability	μ_o	$c = [\varepsilon_o\mu_o]^{-1/2}$	H m^{-1} = Wb m^{-1} A^{-1}	A fundamental constant in magnetism. In free space, $\mu_o = B/H$.
Relative permeability	μ_r	$\mu_r = B/\mu_o H$	None	
Magnetic permeability	μ	$\mu = \mu_o\mu_r$	H m^{-1}	Not to be confused with magnetic moment.
Inductance	L	$L = \Phi_{\text{total}}/I$	H (henries)	Total flux threaded per unit current.
Magnetostatic energy density	E_{vol}	$dE_{\text{vol}} = H\,dB$	J m^{-3}	dE_{vol} is the energy required per unit volume in changing B by dB.

EXAMPLE 8.1

AMPERE'S LAW AND THE INDUCTANCE OF A TOROIDAL COIL Ampere's law provides a relationship between the conduction current I and the magnetic field intensity H threading this current. The conduction current I is the current due to the flow of free charge carriers through a conductor and not due to the magnetization of any medium. Consider an arbitrary closed path C around a conductor carrying a current I, as shown in Figure 8.9. The tangential component of $\mathbf{H}$ to the curve C at point P is H_t. If dl is an infinitesimally small path length of C at P, as shown in Figure 8.9, then the summation of $H_t\,dl$ around the path C gives the conduction current enclosed within C. This is **Ampere's law,**

$$\oint_C H_t\,dl = I \qquad [8.17]$$

Ampere's law

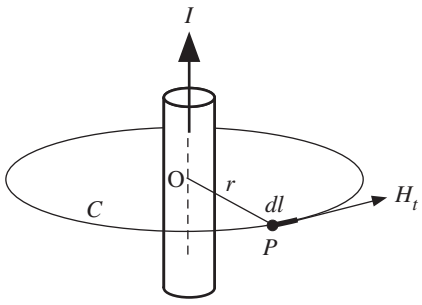


Figure 8.9 Ampere's circuital law.

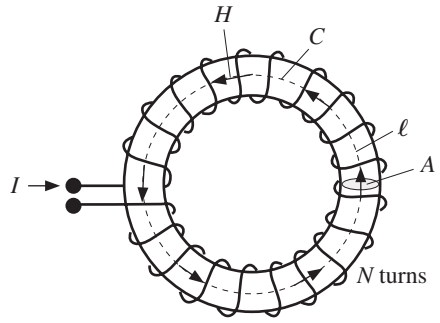


Figure 8.10 A toroidal coil with *N* turns.

Consider the toroidal coil with N turns shown in Figure 8.10. First assume that the toroid core is air ($\mu_r \approx 1$). Suppose that the current through the coils is I. By symmetry, the magnetic field intensity H inside the toroidal core is the same everywhere and is directed along the circumference. Suppose that l is the length of the mean circumference C. The current is linked N times by the circumference C, so Equation 8.17 is

$$\oint_C H_t \, dl = H\ell = NI$$

or

$$H = \frac{NI}{\ell}$$

The magnetic field B_o with air as core material is then simply

$$B_o = \mu_o H = \frac{\mu_o NI}{\ell}$$

When the toroidal coil has a magnetic medium with a relative permeability μ_r, the magnetic field intensity is still H because the conduction current I has not changed. But the magnetic field B is now different than B_o and is given by

Magnetic field inside toroidal coil

$$B = \mu_o \mu_r H = \frac{\mu_o \mu_r NI}{\ell} \qquad [8.18]$$

If A is the cross-sectional area of the toroid, then the total flux Φ through the core is BA or $\mu_o \mu_r NAI/\ell$. The current I in Figure 8.10 threads the flux N times. The inductance L of the toroidal coil, by definition, is then

Inductance of toroidal coil

$$L = \frac{\text{Total flux threaded}}{\text{Current}} = \frac{N\Phi}{I} = \frac{\mu_o \mu_r N^2 A}{\ell} \qquad [8.19]$$

Having a magnetic material as the toroid core increases the inductance by a factor of μ_r in the same way a dielectric material increases the capacitance by a factor of ε_r.

EXAMPLE 8.2 **MAGNETOSTATIC ENERGY PER UNIT VOLUME** Consider a toroidal coil with N turns that is energized from a voltage supply through a rheostat, as shown in Figure 8.11. The core of the toroid may be any material. Suppose that by adjusting the rheostat we increase the current

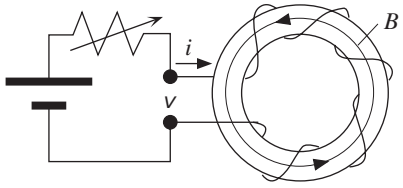


Figure 8.11 Energy required to magnetize a toroidal coil.

i supplied to the coil. The current i produces magnetic flux Φ in the core, which is BA, where B is the magnetic field and A is the cross-sectional area. We can now use Ampere's law for H to relate the current i to H, as in Example 8.1. If ℓ is the mean circumference, then

$$H\ell = Ni \qquad [8.20]$$

The changing current means that the flux is also changing (both increasing). We know from Faraday's law that a changing flux that threads a circuit generates a voltage v in that circuit given by the rate of change of total threaded flux, or $N\Phi$. Lenz's law makes the polarity of the induced voltage oppose the applied voltage. Suppose that in a time interval δt seconds, the magnetic field within the core changes by δB; then $\delta\Phi = A\delta B$ and

$$v = \frac{\delta(\text{Total flux threaded})}{\delta t} = \frac{N\delta\Phi}{\delta t} = NA\frac{\delta B}{\delta t} \qquad [8.21]$$

The battery has to supply the current i against this induced voltage v, which means that it has to do electrical work iv every second. In other words, the battery has to do work $iv\ \delta t$ in a time interval δt to supply the necessary current to increase the magnetic field by δB. The electric energy δE that is input into the coil in time δt is then, using Equations 8.20 and 8.21,

$$\delta E = iv\ \delta t = \left(\frac{H\ell}{N}\right)\left(NA\frac{\delta B}{\delta t}\right)\delta t = (A\ell)H\ \delta B$$

This energy δE is the work done in increasing the field in the core by δB. The volume of the toroid is $A\ell$. Therefore, the total energy or work required per unit volume to increase the magnetic field from an initial value B_1 to a final value B_2 in the toroid is

Work done per unit volume during magnetization

$$E_{\text{vol}} = \int_{B_1}^{B_2} H\ dB \qquad [8.22]$$

where the integration limits are determined by the initial and final magnetic field. This is the expression for calculating the **energy density** (energy per unit volume) required to change the field from B_1 to B_2. It should be emphasized that Equation 8.22 is valid for *any medium*. We conclude that an incremental energy density of $dE_{\text{vol}} = H\ dB$ is required to increase the magnetic field by dB at a point in any medium including free space.

We can now consider a core material that we can represent by a *constant* relative permeability μ_r. This means we can exclude those materials that do not have a linear relationship between B and H, such as ferromagnetic and ferrimagnetic materials, which we will discuss later. If the core is free space or air, then $\mu_r = 1$.

Suppose that we increase the current in Figure 8.11 from zero to some final value I so that the magnetic field changes from zero to some final value B. Since the medium has a constant relative permeability μ_r, we can write

$$B = \mu_r\mu_o H$$

and use this in Equation 8.22 to integrate and find the energy per unit volume needed to establish the field B or field intensity H

Energy density of a magnetic field

$$E_{\text{vol}} = \frac{1}{2}\mu_r\mu_o H^2 = \frac{B^2}{2\mu_r\mu_o} \qquad [8.23]$$

This is the energy absorbed from the battery per unit volume of core medium to establish the magnetic field. This energy is stored in the magnetic field and is called **magnetostatic energy density.** It is a form of magnetic potential energy. If we were to suddenly remove the battery and short those terminals, the current will continue to flow for a short while (determined by L/R) and do external work in heating the resistor. This external work comes from the stored energy in the magnetic field. If the medium is free space, or air, then the energy density is

Magnetostatic energy density in free space

$$E_{\text{vol}}(\text{air}) = \frac{1}{2}\mu_o H^2 = \frac{B^2}{2\mu_o}$$

A magnetic field of 2 T corresponds to a magnetostatic energy density of 1.6 MJ m^{-3} or 1.6 J cm^{-3}. The energy in a magnetic field of 2 T in a 1 cm^3 volume (size of a thimble) has the work ability (potential energy) to raise an average-sized apple roughly by 5 feet, or 1.6 m. We should note that as long as the core material is linear, that is, μ_r is independent of the magnetic field itself, magnetostatic energy density can also be written as

Magnetostatic energy in a linear magnetic medium

$$E_{\text{vol}} = \frac{1}{2}HB \qquad [8.24]$$

8.2 MAGNETIC MATERIAL CLASSIFICATIONS

In general, magnetic materials are classified into five distinct groups: diamagnetic, paramagnetic, ferromagnetic, antiferromagnetic, and ferrimagnetic. Table 8.2 provides a summary of the magnetic properties of these classes of materials.

8.2.1 DIAMAGNETISM

Typical diamagnetic materials have a magnetic susceptibility that is negative and small. For example, the silicon crystal is diamagnetic with $\chi_m = -5.2 \times 10^{-6}$. The relative permeability of diamagnetic materials is slightly less than unity. When a diamagnetic substance such as a silicon crystal is placed in a magnetic field, the magnetization vector **M** in the material is in the *opposite* direction to the applied field $\mu_o\mathbf{H}$ and the resulting field **B** within the material is less than $\mu_o\mathbf{H}$. The negative susceptibility can be interpreted as the diamagnetic substance trying to expel the applied field from the material. When a diamagnetic specimen is placed in a nonuniform magnetic field, the magnetization **M** of the material is in the opposite direction to **B** and the specimen experiences a net force toward smaller fields, as depicted in Figure 8.12. A substance exhibits diamagnetism whenever the constituent atoms in the material have closed subshells and shells. This means that each constituent atom has no permanent magnetic moment in the absence of an applied field. Covalent crystals and many ionic crystals are typical diamagnetic materials because the

Table 8.2 Classification of magnetic materials

Type	χ_m (typical values)	χ_m versus T	Comments and Examples
Diamagnetic	Negative and small (-10^{-6})	T independent	Atoms of the material have closed shells. Organic materials, *e.g.*, many polymers; covalent solids, *e.g.*, Si, Ge, diamond; some ionic solids, *e.g.*, alkalihalides; some metals, *e.g.*, Cu, Ag, Au.
	Negative and large (-1)	Below a critical temperature	Superconductors
Paramagnetic	Positive and small (10^{-5}–10^{-4})	Independent of T	Due to the alignment of spins of conduction electrons. Alkali and transition metals.
	Positive and small (10^{-5})	Curie or Curie–Weiss law, $\chi_m = C/(T - T_C)$	Materials in which the constituent atoms have a permanent magnetic moment, *e.g.*, gaseous and liquid oxygen; ferromagnets (Fe), antiferromagnets (Cr), and ferrimagnets (Fe_3O_4) at high temperatures.
Ferromagnetic	Positive and very large	Ferromagnetic below and paramagnetic above the Curie temperature	May possess a large permanent magnetization even in the absence of an applied field. Some transition and rare earth metals, Fe, Co, Ni, Gd, Dy.
Antiferromagnetic	Positive and small	Antiferromagnetic below and paramagnetic above the Néel temperature	Mainly salts and oxides of transition metals, *e.g.*, MnO, NiO, MnF_2, and some transition metals, α–Cr, Mn.
Ferrimagnetic	Positive and very large	Ferrimagnetic below and paramagnetic above the Curie temperature	May possess a large permanent magnetization even in the absence of an applied field. Ferrites.

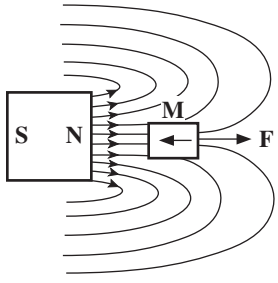


Figure 8.12 A diamagnetic material placed in a nonuniform magnetic field experiences a force toward smaller fields.

This repels the diamagnetic material away from a permanent magnet.

constituent atoms have no unfilled subshells. Superconductors, as we will discuss later, are perfect diamagnets with $\chi_m = -1$ and totally expel the applied field from the material.

8.2.2 PARAMAGNETISM

Paramagnetic materials have a small positive magnetic susceptibility. For example, oxygen gas is paramagnetic with $\chi_m = 2.1 \times 10^{-6}$ at atmospheric pressure and room temperature. Each oxygen molecule has a net magnetic dipole moment $\boldsymbol{\mu}_{\text{mol}}$. In the absence of an applied field, these molecular moments are randomly oriented due to the random collisions of the molecules, as depicted in Figure 8.13a. The magnetization of the gas is zero. In the presence of an applied field, the molecular magnetic moments take various alignments with the field, as illustrated in Figure 8.13b. The degree of alignment of $\boldsymbol{\mu}_{\text{mol}}$ with the applied field and hence magnetization **M** increases with the strength of the applied field $\mu_o\mathbf{H}$. Magnetization M typically decreases with increasing temperature because at higher temperatures there are more molecular collisions, which destroy the alignments of molecular magnetic moments with the applied field. When a paramagnetic substance is placed in a nonuniform magnetic field, the induced magnetization **M** is along **B** and there is a net force toward greater fields. For example, when liquid oxygen is poured close to a strong magnet, as depicted in Figure 8.14, the liquid becomes attracted to the magnet.

Many metals are also paramagnetic, such as magnesium with $\chi_m = 1.2 \times 10^{-5}$. The origin of paramagnetism (called **Pauli spin paramagnetism**) in these metals is due to the alignment of the majority of spins of conduction electrons with the field.

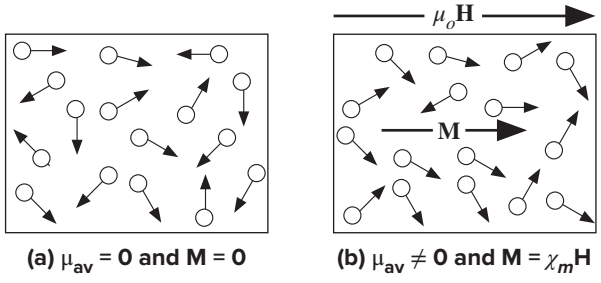


Figure 8.13 (a) In a paramagnetic material, each individual atom possesses a permanent magnetic moment, but due to thermal agitation there is no average moment per atom and **M** = 0. (b) In the presence of an applied field, individual magnetic moments take alignments along the applied field and **M** is finite and along **B**.

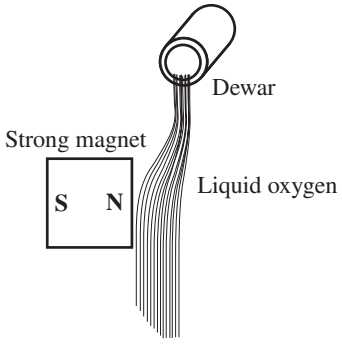


Figure 8.14 A paramagnetic material placed in a nonuniform magnetic field experiences a force toward greater fields.

This attracts the paramagnetic material (*e.g.*, liquid oxygen) toward a permanent magnet.

8.2.3 FERROMAGNETISM

Ferromagnetic materials such as iron can possess large permanent magnetizations even in the absence of an applied magnetic field. The magnetic susceptibility χ_m is typically positive and very large (even infinite) and, further, depends on the applied field intensity. The relationship between the magnetization **M** and the applied magnetic field μ_o**H** is highly nonlinear. At sufficiently high fields, the magnetization **M** of the ferromagnet saturates. The origin of ferromagnetism is the quantum mechanical exchange interaction (discussed later) between the constituent atoms that results in regions of the material possessing permanent magnetization. Figure 8.15 depicts a region of the Fe crystal, called a **magnetic domain,** that has a net magnetization vector **M** due to the alignment of the magnetic moments of all Fe atoms in this region. This crystal domain has **magnetic ordering** as all the atomic magnetic moments have been aligned parallel to each other. Ferromagnetism occurs below a critical temperature called the Curie temperature T_C. At temperatures above T_C, ferromagnetism is lost and the material becomes paramagnetic.

8.2.4 ANTIFERROMAGNETISM

Antiferromagnetic materials such as chromium have a small but positive susceptibility. They cannot possess any magnetization in the absence of an applied field, in contrast to ferromagnets. Antiferromagnetic materials possess a magnetic ordering in which the magnetic moments of alternating atoms in the crystals align in opposite directions, as schematically depicted in Figure 8.16. The opposite alignments of atomic magnetic moments are due to quantum mechanical exchange forces (described later in Section 8.3). The net result is that in the absence of an applied field, there is no net magnetization. Antiferromagnetism occurs below a critical temperature called the **Néel temperature** T_N. Above T_N, antiferromagnetic material becomes paramagnetic.

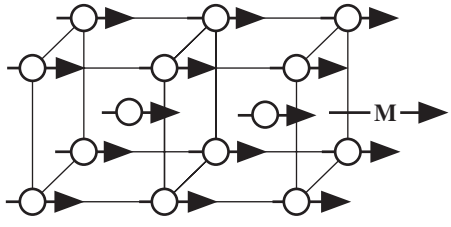


Figure 8.15 In a magnetized region of a ferromagnetic material such as iron, all the magnetic moments are spontaneously aligned in the same direction.

There is a strong magnetization vector **M** even in the absence of an applied field.

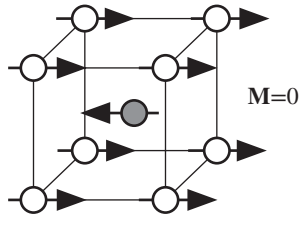


Figure 8.16 In this antiferromagnetic BCC crystal (Cr), the magnetic moment of the center atom is canceled by the magnetic moments of the corner atoms (one-eighth of the corner atom belongs to the unit cell).

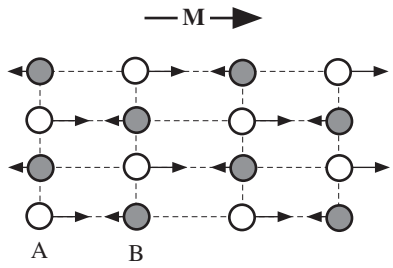


Figure 8.17 Illustration of magnetic ordering in the ferrimagnetic crystal.

All A atoms have their spins aligned in one direction and all B atoms have their spins aligned in the opposite direction. As the magnetic moment of an A atom is greater than that of a B atom, there is net magnetization **M** in the crystal.

8.2.5 FERRIMAGNETISM

Ferrimagnetic materials such as ferrites (*e.g.*, Fe_3O_4) exhibit magnetic behavior similar to ferromagnetism below a critical temperature called the Curie temperature T_C. Above T_C they become paramagnetic. The origin of ferrimagnetism is based on magnetic ordering, as schematically illustrated in Figure 8.17. All A atoms have their spins aligned in one direction and all B atoms have their spins aligned in the opposite direction. As the magnetic moment of an A atom is greater than that of a B atom, there is net magnetization **M** in the crystal. Unlike the antiferromagnetic case, the oppositely directed magnetic moments have different magnitudes and do not cancel. The net effect is that the crystal can possess magnetization even in the absence of an applied field. Since ferrimagnetic materials are typically nonconducting and therefore do not suffer from eddy current losses, they are widely used in high-frequency electronics applications.

All useful magnetic materials in electrical engineering are invariably ferromagnetic or ferrimagnetic.

8.3 FERROMAGNETISM ORIGIN AND THE EXCHANGE INTERACTION

The transition metals iron, cobalt, and nickel are all ferromagnetic at room temperature. The rare earth metals gadolinium and dysprosium are ferromagnetic below room temperature. Ferromagnetic materials can exhibit permanent magnetization even in the absence of an applied field; that is, they possess a susceptibility that is infinite.

In a magnetized iron crystal, all the atomic magnetic moments are aligned in the same direction, as illustrated in Figure 8.15, where the moments in this case have all been aligned along the [100] direction, which gives net magnetization along this direction. It may be thought that the reason for the alignment of the moments is the magnetic forces between the moments, just as bar magnets will tend to align head to tail in an SNSN . . . fashion. This is not, however, the cause, as the magnetic potential energy of interaction is small, indeed smaller than the thermal energy.

The iron atom has the electron structure $[Ar]3d^64s^2$. An isolated iron atom has only the 3*d* subshell with four of the five orbitals unfilled. By virtue of Hund's rule, the electrons try to align their spins so that the five 3*d* orbitals contain two paired



Figure 8.18 The isolated Fe atom has four unpaired spins and a spin magnetic moment of 4β.

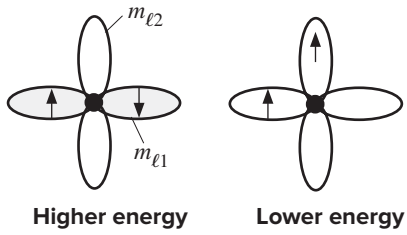


Figure 8.19 Hund's rule for an atom with many electrons is based on the exchange interaction.

electrons and four unpaired electrons, as in Figure 8.18. The isolated atom has four parallel electron spins and hence a spin magnetic moment of 4β.

The origin of Hund's rule, visualized in Figure 8.19, lies in the fact that when the spins are parallel (same m_s), as a requirement of the Pauli exclusion principle, the electrons must occupy orbitals with different m_ℓ and hence possess different spatial distributions (recall that m_ℓ determines the orientation of an orbit). Different m_ℓ values result in a smaller Coulombic repulsion energy between the electrons compared with the case where the electrons have opposite spins (different m_s), where they would be in the same orbital (same m_ℓ), that is, in the same spatial region. It is apparent that even though the interaction energy between the electrons has nothing to do with magnetic forces, it does depend nonetheless on the orientations of their spins (m_s), or on their spin magnetic moments, and it is less when the spins are parallel. Two electrons parallel their spins not because of the direct magnetic interaction between the spin magnetic moments but because of the **Pauli exclusion principle** and the **electrostatic interaction energy.** Together they constitute what is known as an **exchange interaction,** which forces two electrons to take m_s and m_ℓ values that result in the minimum of electrostatic energy. In an atom, the exchange interaction therefore forces two electrons to take the same m_s but different m_ℓ if this can be done within the Pauli exclusion principle. This is the reason an isolated Fe atom has four unpaired spins in the 3*d* subshell.

In the crystal, of course, the outer electrons are no longer strictly confined to their parent Fe atoms, particularly the 4*s* electrons. The electrons now have wavefunctions that belong to the whole solid. Something like Hund's rule also operates at the crystal level for Fe, Co, and Ni. If two 3*d* electrons parallel their spins and occupy different wavefunctions (and hence different negative charge distributions), the resulting mutual Coulombic repulsion between them and also with all the other electrons and the attraction to the positive Fe ions result in an overall reduction of potential energy. This reduction in energy is again due to the exchange interaction and is a direct consequence of the Pauli exclusion principle and the Coulombic forces. Thus, the majority of 3*d* electrons spontaneously parallel their spins without the need for the application of an external magnetic field. The number of electrons that actually parallel their spins depends on the strength of the exchange interaction, and for the iron crystal this turns out to be about 2.2 electrons per atom. Since typically the wavefunctions of the 3*d* electrons in the whole iron crystal show

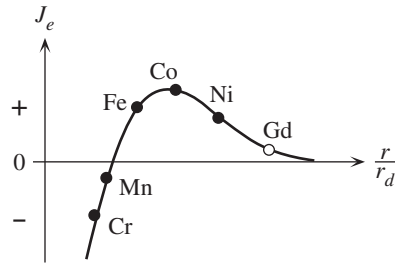


Figure 8.20 The exchange integral as a function of r/r_d, where r is the interatomic distance and r_d the radius of the d orbit (or the average d subshell radius).
Cr to Ni are transition metals. For Gd, the x-axis is r/r_f, where r_f is the radius of the f orbit.

localization around the iron ions, some people prefer to view the 3d electrons as spending the majority of their time around Fe atoms, which explains the reason for drawing the magnetized iron crystal as in Figure 8.15.

It may be thought that all solids should follow the example of Fe and become spontaneously ferromagnetic since paralleling spins would result in different spatial distributions of negative charge and probably a reduction in the electrostatic energy, but this is not generally the case at all. We know that, in the case of covalent bonding, the electrons have the lowest energy when the two electrons spin in opposite directions. In covalent bonding in molecules, the exchange interaction does not reduce the energy. Making the electron spins parallel leads to spatial negative charge distributions that result in a net mutual electrostatic repulsion between the positive nuclei.

In the simplest case, for two atoms only, the exchange energy depends on the interatomic separation between two interacting atoms and the relative spins of the two outer electrons (labeled as 1 and 2). From quantum mechanics, the exchange interaction can be represented in terms of an exchange energy E_{ex} as

$$E_{\text{ex}} = -2J_e\mathbf{S}_1 \cdot \mathbf{S}_2 \qquad [8.25]$$

where $\mathbf{S}_1$ and $\mathbf{S}_2$ are the spin angular momenta of the two electrons and J_e is a numerical quantity called the **exchange integral** that involves integrating the wavefunctions with the various potential energy interaction terms. It therefore depends on the electrostatic interactions and hence on the interatomic distance. For the majority of solids, J_e is negative, so the exchange energy is negative if $\mathbf{S}_1$ and $\mathbf{S}_2$ are in the opposite directions, that is, the spins are antiparallel (as we found in covalent bonding). This is the antiferromagnetic state. For Fe, Co, and Ni, however, J_e is positive. E_{ex} is then negative if $\mathbf{S}_1$ and $\mathbf{S}_2$ are parallel. Spins of the 3d electrons on the Fe atoms therefore spontaneously align in the same direction to reduce the exchange energy. This spontaneous magnetization is the phenomenon of ferromagnetism. Figure 8.20 illustrates how J_e changes with the ratio of interatomic separation to the radius of the 3d subshell (r/r_d). For the transition metals Fe, Co, and Ni, the r/r_d is such that J_e is positive.[3] In all other cases, it is negative and does not produce ferromagnetic behavior. It should be mentioned that Mn, which is not ferromagnetic,

[3] According to H. P. Myers, *Introductory Solid State Physics* 2nd ed., London: Taylor and Francis Ltd., 1997, p. 362, there have been no theoretical calculations of the exchange integral J_e for any real magnetic substance.

can be alloyed with other elements to increase r/r_d and hence endow ferromagnetism in the alloy.

EXAMPLE 8.3

SATURATION MAGNETIZATION IN IRON The maximum magnetization, called **saturation magnetization** M_{sat}, in iron is about 1.75×10^6 A m^{-1}. This corresponds to all possible net spins aligning parallel to each other. Calculate the effective number of Bohr magnetons per atom that would give M_{sat}, given that the density and relative atomic mass of iron are 7.86 g cm^{-3} and 55.85, respectively.

SOLUTION

The number of Fe atoms per unit volume is

$$n_{at} = \frac{\rho N_A}{M_{at}} = \frac{(7.86 \times 10^3 \text{ kg m}^{-3})(6.022 \times 10^{23} \text{ mol}^{-1})}{55.85 \times 10^{-3} \text{ kg mol}^{-1}}$$

$$= 8.48 \times 10^{28} \text{ atoms m}^{-3}$$

If each Fe atom contributes x number of net spins, then since each net spin has a magnetic moment of β, we have,

$$M_{sat} = n_{at}(x\beta)$$

so

$$x = \frac{M_{sat}}{n_{at}\beta} = \frac{1.75 \times 10^6}{(8.48 \times 10^{28})(9.27 \times 10^{-24})} \approx 2.2$$

In the solid, each Fe atom contributes only 2.2 Bohr magnetons to the magnetization even though the isolated Fe atom has 4 Bohr magnetons. There is no orbital contribution to the magnetic moment per atom in the solid because all the outer electrons, 3*d* and 4*s* electrons, can be viewed as belonging to the whole crystal, or being in an energy band, rather than orbiting individual atoms. A 3*d* electron is attracted by various Fe ions in the crystal and therefore does not experience a central force, in contrast to the 3*d* electron in the isolated Fe atom that orbits the nucleus. The orbital momentum in the crystal is said to be quenched.

We should note that when the magnetization is saturated, all atomic magnetic moments are aligned. The resulting magnetic field within the iron specimen in the absence of an applied magnetizing field ($H = 0$) is

$$B_{sat} = \mu_o M_{sat} = 2.2 \text{ T}$$

8.4 SATURATION MAGNETIZATION AND CURIE TEMPERATURE

The maximum magnetization in a ferromagnet when all the atomic magnetic moments have been aligned as much as possible is called the saturation magnetization M_{sat}. In the iron crystal, for example, this corresponds to each Fe atom with an effective spin magnetic moment of 2.2 Bohr magnetons aligning in the same direction to give a magnetic field $\mu_o M_{sat}$ or 2.2 T. As we increase the temperature, lattice vibrations become more energetic, which leads to a frequent disruption of the alignments of the spins. The spins cannot align perfectly with each other as the temperature

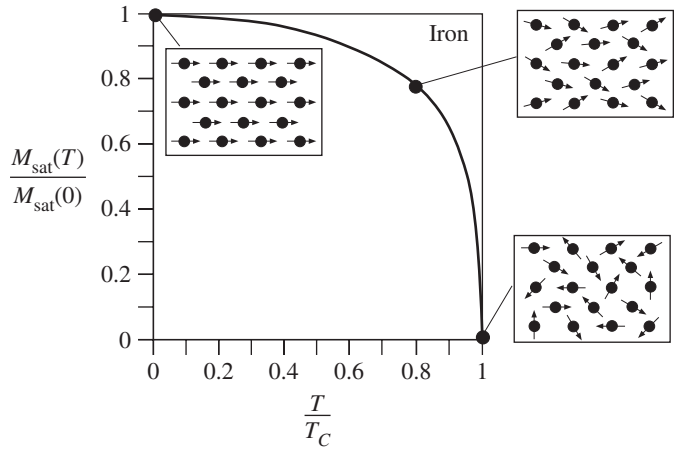


Figure 8.21 Normalized saturated magnetization versus reduced temperature T/T_C where T_C is the Curie temperature (1043 K).

increases due to lattice vibrations randomly agitating the individual spins. When an energetic lattice vibration passes through a spin site, the energy in the vibration may be sufficient to disorientate the spin of the atom. The ferromagnetic behavior disappears at a critical temperature called the **Curie temperature,** denoted by T_C, when the thermal energy of lattice vibrations in the crystal can overcome the potential energy of the exchange interaction and hence destroy the spin alignments. Above the Curie temperature, the crystal behaves as if it were paramagnetic. The saturation magnetization M_{sat}, therefore, decreases from its maximum value $M_{sat}(0)$ at absolute zero of temperature to zero at the Curie temperature. Figure 8.21 shows the dependence of M_{sat} on the temperature when M_{sat} has been normalized to $M_{sat}(0)$ and the temperature is the reduced temperature, that is, T/T_C. At $T/T_C = 1$, $M_{sat} = 0$. When plotted in this way, the ferromagnets cobalt and nickel follow closely the observed behavior for iron. We should note that since for iron $T_C = 1043$ K, at room temperature, $T/T_C = 0.29$ and M_{sat} is very close to its value at $M_{sat}(0)$.

Since at the Curie temperature, the thermal energy, of the order of kT_C, is sufficient to overcome the energy of the exchange interaction E_{ex} that aligns the spins, we can take kT_C as an order of magnitude estimate of E_{ex}. For iron, E_{ex} is ~0.09 eV and for cobalt this is ~0.1 eV.

Table 8.3 summarizes some of the important properties of the ferromagnets Fe, Co, Ni, and Gd (rare earth metal).

Table 8.3 Properties of the ferromagnets Fe, Co, Ni, and Gd

	Fe	Co	Ni	Gd
Crystal structure	BCC	HCP	FCC	HCP
Bohr magnetons per atom	2.22	1.72	0.62	7.1
$M_{sat}(0)$ (MA m^{-1})	1.75	1.45	0.50	2.0
$B_{sat} = \mu_o M_{sat}$(T)	2.2	1.82	0.64	2.5
T_C	770 °C	1127 °C	358 °C	16 °C
	1043 K	1400 K	631 K	289 K

8.5 MAGNETIC DOMAINS: FERROMAGNETIC MATERIALS

8.5.1 MAGNETIC DOMAINS

A single crystal of iron does not necessarily possess a net permanent magnetization in the absence of an applied field. If a magnetized piece of iron is heated to a temperature above its Curie temperature and then allowed to cool in the absence of a magnetic field, it will possess no net magnetization. The reason for the absence of net magnetization is due to the formation of magnetic domains that effectively cancel each other, as discussed below. A **magnetic domain** is a region of the crystal in which all the spin magnetic moments are aligned to produce a magnetic moment in one direction only.

Figure 8.22a shows a single crystal of iron that has a permanent magnetization as a result of ferromagnetism (aligning of all atomic spins). The crystal is like a bar magnet with magnetic field lines around it. As we know, there is potential energy (*PE*), called **magnetostatic energy,** stored in a magnetic field, and we can reduce this energy in the external field by dividing the crystal into two domains where the magnetizations are in the opposite directions, as shown in Figure 8.22b. The external magnetic field lines are reduced and there is now less potential energy stored in the magnetic field. There are only field lines at the ends. This arrangement is energetically favorable because the magnetostatic energy has been reduced by decreasing the external field lines. However, there is now a boundary, called a **domain wall** (or **Bloch wall**), between the two domains where the magnetization changes from one direction to the opposite direction and hence the atomic spins do, also. It requires

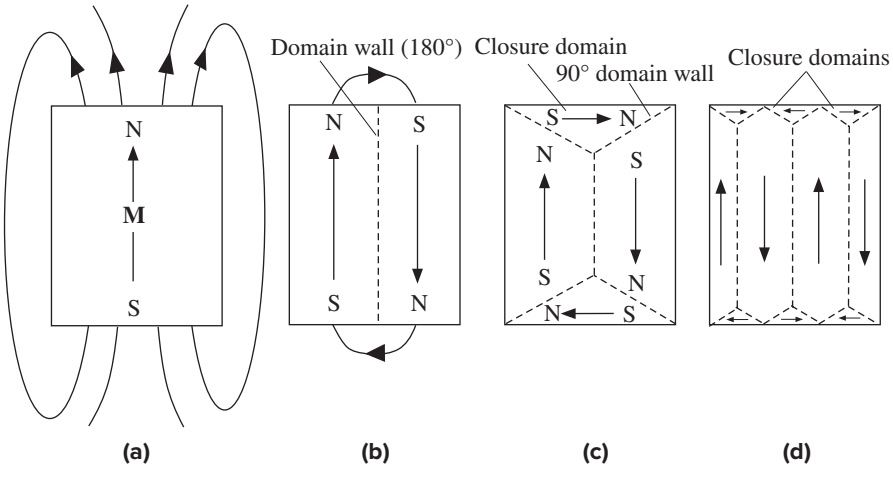


Figure 8.22 (a) Magnetized bar of ferromagnet in which there is only one domain and hence an external magnetic field. (b) Formation of two domains with opposite magnetizations reduces the external field. There are, however, field lines at the ends. (c) Domains of closure fitting at the ends eliminate the external fields at the ends. (d) A specimen with several domains and closure domains. There is no external magnetic field and the specimen appears unmagnetized.

energy to rotate the atomic spin through 180° with respect to its neighbor because the exchange energy favors aligning neighboring atomic spins (0°). The wall in Figure 8.22b is a 180° wall inasmuch as the magnetization through the wall is rotated by 180°. It is apparent that the wall region where the neighboring atomic spins change their relative direction (or orientation) from one domain to the neighboring one has higher *PE* than the bulk of the domain, where all the atomic spins are aligned. As we will show below, the domain wall is not simply one atomic spacing but has a finite thickness, which for iron is typically of the order of 0.1 μm, or several hundred atomic spacings. The excess energy in the wall increases with the area of the wall.

The magnetostatic energy associated with the field lines at the ends in Figure 8.22b can be further reduced by eliminating these external field lines by closing the ends with sideway domains with magnetizations at 90°, as shown in Figure 8.22c. These end domains are **closure domains** and have walls that are 90° walls. The magnetization is rotated through 90° through the wall. Although we have reduced the magnetostatic energy, we have increased the potential energy in the walls by adding additional walls. The creation of magnetic domains continues (spontaneously) until the potential energy reduction in creating an additional domain is the same as the increase in creating an additional wall. The specimen then possesses minimum potential energy and is in equilibrium with no net magnetization. Figure 8.22d shows a specimen with several domains and no net magnetization. The sizes, shapes, and distributions of domains depend on a number of factors, including the size and shape of the whole specimen. For iron particles of dimensions less than of the order of 0.01 μm, the increase in the potential energy in creating a domain wall is too costly and these particles are single domains and hence always magnetized.

The magnetization of each domain is normally along one of the preferred directions in which the atomic spin alignments are easiest (the exchange interaction is the strongest). For iron, the magnetization is easiest along any one of six ⟨100⟩ directions (along cube edges), which are called **easy directions.** The domains have magnetizations along these easy directions. The magnetization of the crystal along an applied field occurs, in principle, by the growth of domains with magnetizations (or components of **M**) along the applied field (**H**), as illustrated in Figure 8.23a and b. For simplicity, the magnetizing field is taken along an easy direction. The Bloch wall between the domains A and B migrates toward the right, which enlarges the domain

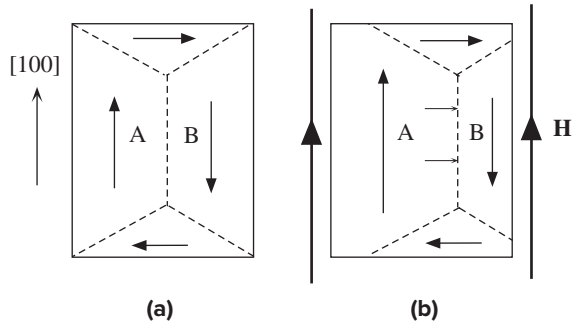


Figure 8.23 (a) An unmagnetized crystal of iron in the absence of an applied magnetic field. Domains A and B are the same size and have opposite magnetizations. (b) When an external magnetic field is applied, the domain wall migrates into domain B, which enlarges A and shrinks B. The result is that the specimen now acquires net magnetization.

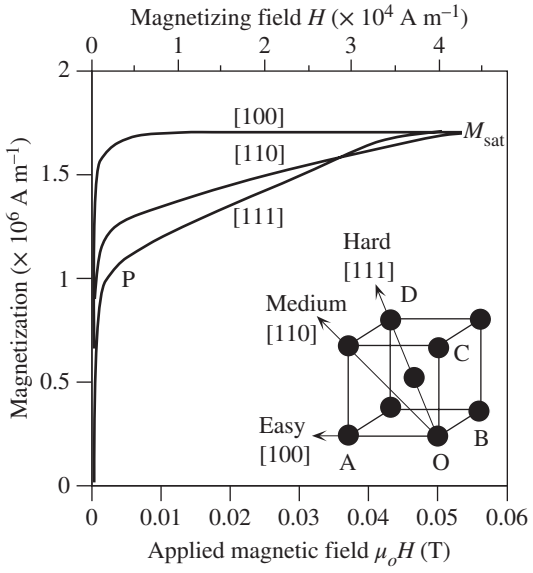


Figure 8.24 Magnetocrystalline anisotropy in a single iron crystal.

M versus *H* depends on the crystal direction and is easiest along [100] and hardest along [111].

A and shrinks domain B, with the net result that the crystal has an effective magnetization **M** along **H**. The migration of the Bloch wall is caused by the spins in the wall, and also spins in section B adjacent to the wall, being gradually rotated by the applied field (they experience a torque). The magnetization process therefore involves the motions of Bloch walls in the crystal.

8.5.2 MAGNETOCRYSTALLINE ANISOTROPY

Ferromagnetic crystals characteristically exhibit magnetic anisotropy, which means that the magnetic properties are different along different crystal directions. In the case of iron (BCC), the spins in a domain are most easily aligned in any of the six [100] type directions, collectively labeled as ⟨100⟩, and correspond to the six edges of the cubic unit cell. The exchange interactions are such that spin magnetic moments are most easily aligned with each other if they all point in one of the six ⟨100⟩ directions. Thus ⟨100⟩ directions in the iron crystal constitute the easy directions for magnetization. When a magnetizing field **H** along a [100] direction is applied, as illustrated in Figure 8.23a and b, domain walls migrate to allow those domains (*e.g.*, A) with magnetizations along **H** to grow at the expense of those domains (*e.g.*, B) with magnetizations opposing **H**. The observed *M* versus *H* behavior is shown in Figure 8.24. Magnetization rapidly increases and saturates with an applied field of less than 0.01 T.

On the other hand, if we want to magnetize the crystal along the [111] direction by applying a field along this direction, then we have to apply a stronger field than that along [100]. This is clearly shown in Figure 8.24, where the resulting magnetization along [111] is smaller than that along [100] for the same magnitude of applied field. Indeed, saturation is reached at an applied field that is about a factor of 4 greater

Table 8.4 Exchange interaction, magnetocrystalline anisotropy energy K, and saturation magnetostriction coefficient λ_{sat}

Material	Crystal	$E_{ex} \approx kT_C$ (meV)	Easy	Hard	K (mJ cm^{-3})	λ_{sat} ($\times 10^{-6}$)
Fe	BCC	90	<100>; cube edge	<111>; cube diagonal	48	20 [100] −20 [111]
Co	HCP	120	// to c axis	⊥ to c axis	450	
Ni	FCC	50	<111>; cube diagonal	<100>; cube edge	5	−46 [100] −24 [111]

NOTE: K is the magnitude of what is called the first anisotropy constant (K_1) and is approximately the magnitude of the anisotropy energy. E_{ex} is an estimate from kT_C, where T_C is the Curie temperature. All approximate values are from various sources. (Further data can be found in Jiles, D., *Introduction to Magnetism and Magnetic Materials*, London, England: Chapman and Hall, 1991.)

than that along [100]. The [111] direction in the iron crystal is consequently known as the **hard direction.** The M versus H behavior along [100], [110], and [111] directions in an iron crystal and the associated anisotropy are shown in Figure 8.24.

When an external field is applied along the diagonal direction OD in Figure 8.24, initially all those domains with **M** along OA, OB, and OC, that is, those with magnetization components along OD, grow by consuming those with **M** in the wrong direction and eventually take over the whole specimen. This is an easy process (similar to the process along [100]) and requires small fields and represents the processes from 0 to P on the magnetization curve for [111] in Figure 8.24. However, from P onwards, the magnetizations in the domains have to be rotated away from their easy directions, that is, from OA, OB, and OC toward OD. This process consumes substantial energy and hence needs much stronger applied fields.

It is apparent that the magnetization of the crystal along [100] needs the least energy, whereas that along [111] consumes the greatest energy. The excess energy required to magnetize a unit volume of a crystal in a particular direction with respect to that in the easy direction is called the **magnetocrystalline anisotropy energy** and is denoted by K. For iron, the anisotropy energy is zero for [100] and largest for the [111] direction, about 48 kJ m^{-3} or 3.5×10^{-6} eV per atom. For cobalt, which has the HCP crystal structure, the anisotropy energy is at least an order of magnitude greater. Table 8.4 summarizes the easy and hard directions, and the anisotropy energy K for the hard direction.

8.5.3 DOMAIN WALLS

We recall that the spin magnetic moments rotate across a domain wall. We mentioned that the wall is not simply one atomic spacing wide, as this would mean two neighboring spins being at 180° to each other and hence possessing excessive exchange interaction. A schematic illustration of the structure of a typical 180° Bloch wall, between two domains A and B, is depicted in Figure 8.25. It can be seen that the neighboring spin magnetic moments are rotated gradually, and over several hundred atomic spacings the magnetic moment reaches a rotation of 180°. Exchange forces between neighboring atomic spins favor very little relative rotation.

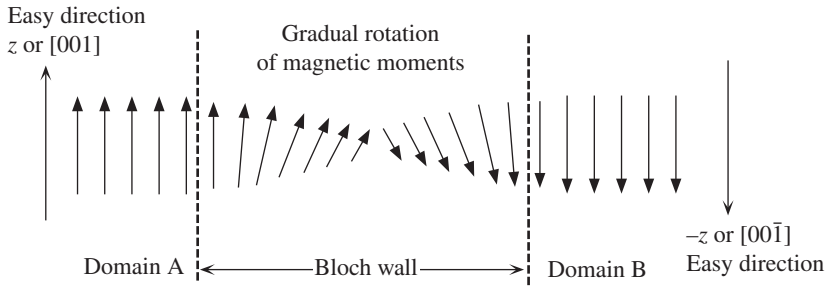


Figure 8.25 In a Bloch wall, the neighboring spin magnetic moments rotate gradually, and it takes several hundred atomic spacings to rotate the magnetic moment by 180°.

Had it been left to exchange forces alone, relative rotation of neighboring spins would be so minute that the wall would have to be very thick (infinitely thick) to achieve a 180° rotation.

However, magnetic moments that are oriented away from the easy direction possess excess energy, called the anisotropy energy (K). If the wall is thick, then it will contain many magnetic moments rotated away from the easy direction and there would be a substantial anisotropy energy in the wall. Minimum anisotropy energy in the wall is obtained when the magnetic moment changes direction by 180° from the easy direction along $+z$ to that along $-z$ in Figure 8.25 without any intermediate rotations away from z. This requires a wall of one atomic spacing. In reality, the wall thickness is a compromise between the exchange energy, demanding a thick wall, and anisotropy energy, demanding a thin wall. The equilibrium wall thickness is that which minimizes the total potential energy, which is the sum of the exchange energy *and* the anisotropy energy within the wall. This thickness turns out to be ∼0.1 μm for iron and less for cobalt, in which the anisotropy energy is greater.

EXAMPLE 8.4

MAGNETIC DOMAIN WALL ENERGY AND THICKNESS The Bloch wall energy and thickness depend on two main factors: the exchange energy E_{ex} (J atom^{-1}) and magnetocrystalline energy K (J m^{-3}). Suppose that we consider a Bloch wall of unit area, and thickness δ, and calculate the potential energy U_{wall} in this wall due to the exchange energy and the magnetocrystalline anisotropy energy. The spins change by 180° across the thickness δ of the Bloch wall as in Figure 8.25. The contribution $U_{exchange}$ from the exchange energy arises because it takes energy to rotate one spin with respect to another. If the thickness δ is large, then the angular change from one spin to the next will be small, and the exchange energy contribution $U_{exchange}$ will also be small. Thus, $U_{exchange}$ is inversely proportional to δ. $U_{exchange}$ is also directly proportional to E_{ex} which gauges the magnitude of this exchange energy; it costs E_{ex} to rotate the two spins 180° to each other. Thus, $U_{exchange} \propto E_{ex}/\delta$.

The anisotropy energy contribution $U_{anisotropy}$ arises from having spins point away from the easy direction. If the thickness δ is large, there are more and more spin moments that are aligned away from the easy direction, and the anisotropy energy contribution $U_{anisotropy}$ is also large. Thus, $U_{anisotropy}$ is proportional to δ, and also, obviously, to the anisotropy energy K that gauges the magnitude of this energy. Thus, $U_{anisotropy} \propto K\delta$.

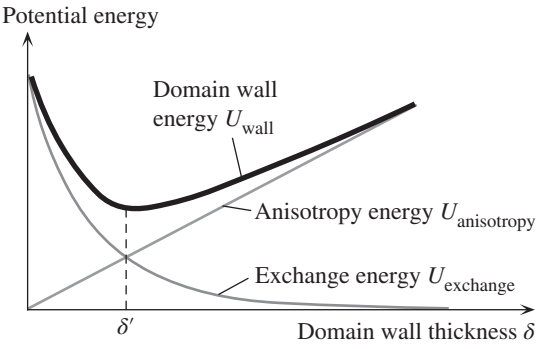


Figure 8.26 The potential energy of a domain wall depends on the exchange and anisotropy energies.

Figure 8.26 shows the contributions of the exchange and anisotropy energies, $U_{exchange}$ and $U_{anisotropy}$, to the total Bloch wall energy as a function of wall thickness δ. It is clear that exchange and anisotropy energies have opposite (or conflicting) requirements on the wall thickness. There is, however, an optimum thickness δ' that *minimizes* the Bloch wall energy, that is, a thickness that balances the requirements of exchange and anisotropy forces.

If the interatomic spacing is a, then there would be $N = \delta/a$ atomic layers in the wall. Since the spin moment angle changes by 180° across δ, we can calculate the relative spin orientations $(180°/N)$ of adjacent atomic layers, and hence we can find the exact contributions of exchange and anisotropy energies. We do not need the exact mathematics, but the final result is that the potential energy U_{wall} per unit area of the wall is approximately

Potential energy of a Bloch wall

$$U_{wall} \approx \frac{\pi^2 E_{ex}}{2a\delta} + K\delta$$

The first term on the right is the exchange energy contribution (proportional to E_{ex}/δ), and the second is the anisotropy energy contribution (proportional to $K\delta$); both have the features we discussed.

Show that the minimum energy occurs when the wall has the thickness

Bloch wall thickness

$$\delta' = \left(\frac{\pi^2 E_{ex}}{2aK}\right)^{1/2}$$

Taking $E_{ex} \approx kT_C$, where T_C is the Curie temperature, and for iron, $K \approx 50$ kJ m^{-3}, and $a \approx 0.3$ nm, estimate the thickness of a Bloch wall and its energy per unit area.

SOLUTION

We can differentiate U_{wall} with respect to δ,

$$\frac{dU_{wall}}{d\delta} = -\frac{\pi^2 E_{ex}}{2a\delta^2} + K$$

and then set it to zero for $\delta = \delta'$ to find,

$$\delta' = \left(\frac{\pi^2 E_{ex}}{2aK}\right)^{1/2}$$

Since $T_C = 1043$ K, $E_{ex} = kT_C = (1.38 \times 10^{-23}\ \text{J K}^{-1})(1043\ \text{K}) = 1.4 \times 10^{-20}$ J, so that

$$\delta' = \left(\frac{\pi^2 E_{ex}}{2aK}\right)^{1/2} = \left[\frac{\pi^2(1.4 \times 10^{-20})}{2(0.3 \times 10^{-9})(50{,}000)}\right]^{1/2} = 6.8 \times 10^{-8}\ \text{m} \quad \text{or} \quad 68\ \text{nm}$$

and $$U_{\text{wall}} = \frac{\pi^2 E_{\text{ex}}}{2a\delta'} + K\delta' = \frac{\pi^2(1.4 \times 10^{-20})}{2(0.3 \times 10^{-9})(6.8 \times 10^{-8})} + (50 \times 10^3)(6.8 \times 10^{-8})$$

$$= 0.007 \text{ J m}^{-2} \quad \text{or} \quad 7 \text{ mJ m}^{-2}$$

A better calculation gives δ' and U_{wall} as 40 nm and 3 mJ m^{-2}, respectively, about the same order of magnitude.[4] The Bloch wall thickness is roughly 70 nm or $\delta/a = 230$ atomic layers. It is left as an exercise to show that when $\delta = \delta'$, the exchange and anisotropy energy contributions are equal.

8.5.4 MAGNETOSTRICTION

If we were to strain a ferromagnetic crystal (by applying a suitable stress) along a certain direction, we would change the interatomic spacing not only along this direction but also in other directions and hence change the exchange interactions between the atomic spins. This would lead to a change in the magnetization properties of the crystal. In the converse effect, the magnetization of the crystal generates strains or changes in the physical dimensions of the crystal. For example, in very qualitative terms, when an iron crystal is magnetized along the [111] direction by a strong field, the atomic spins within domains are rotated from their easy directions toward the hard [111] direction. These electron spin rotations involve changes in the electron charge distributions around the atoms and therefore affect the interatomic bonding and hence the interatomic spacing. When an iron crystal is placed in a magnetic field along an easy direction [100], it gets longer along this direction but contracts in the transverse directions [010] and [001], as depicted in Figure 8.27. The reverse is true for nickel. The longitudinal strain $\Delta\ell/\ell$ along the direction of magnetization is called the **magnetostrictive constant,** denoted by λ. The magnetostrictive constant depends on the crystal direction and may be positive (extension) or negative (contraction). Further, λ depends on the applied field and can even change sign as the field is increased; for example, λ for iron along the [110] direction is initially positive and then, at higher fields, becomes negative. When the crystal reaches saturation magnetization, λ also reaches saturation, called **saturation magnetostriction strain** λ_{sat}, which is typically 10^{-6}–10^{-5}. Table 8.4 summarizes the λ_{sat} values for Fe and Ni along the easy and hard directions. The crystal lattice strain energy associated with magnetostriction is called the **magnetostrictive energy,** which is typically less than the anisotropy energy.

Magnetostriction is responsible for the transformer hum noise one hears near power transformers. As the core of a transformer is magnetized one way and then in the opposite direction under an alternating voltage, the alternating changes in the longitudinal strain vibrate the surrounding environment, air, oil, and so forth, and generate an acoustic noise at twice the main frequency, or 120 Hz, and its harmonics. (Why?)

The magnetostrictive constant can be controlled by alloying metals. For example, λ_{sat} along the easy direction for nickel is negative and for iron it is positive, but for the alloy 85% Ni–15% Fe, it is zero. In certain magnetic materials, λ can be quite

[4] See, for example, Jiles, D., *Introduction to Magnetism and Magnetic Materials*, London, England: Chapman and Hall, 1991.

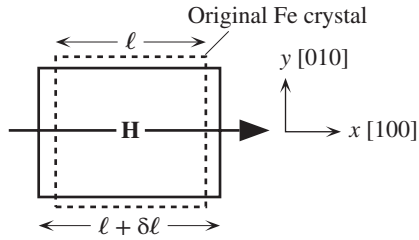


Figure 8.27 Magnetostriction means that the iron crystal in a magnetic field along *x*, an easy direction, elongates along *x* but contracts in the transverse directions (in low fields).

large, greater than 10^{-4}, which has opened up new areas of sensor applications based on the magnetostriction effect. For example, it may be possible to develop torque sensors for automotive steering applications by using Co-ferrite type magnetic materials[5] (*e.g.*, $CoO–Fe_2O_3$ or similar compounds) that have λ_{sat} of the order of 10^{-4}.

8.5.5 DOMAIN WALL MOTION

The magnetization of a single ferromagnetic crystal involves the motions of domain boundaries to allow the favorably oriented domains to grow at the expense of domains with magnetizations directed away from the field (Figure 8.23). The motion of a domain wall in a crystal is affected by crystal imperfections and impurities and is not smooth. For example, in a 90° Bloch wall, the magnetization changes direction by 90° across the boundary. Due to magnetostriction (Figure 8.27), there is a change in the distortion of the lattice across the 90° boundary, which leads to a complicated strain and hence stress distribution around this boundary. We also know that crystal imperfections such as dislocations and point defects also have strain and stress distributions around them. Domain walls and crystal imperfections therefore interact with each other. Dislocations are line defects that have a substantial volume of strained lattice around them. Figure 8.28 visualizes a dislocation with tensile and compressive strains around it and a domain wall that has a tensile strain on the side of the dislocation. If the wall gets close to the dislocation, the tensile and compressive strains cancel, which results in an unstrained lattice and hence a lower strain energy. This energetically favorable arrangement keeps the domain boundary close to the dislocation. It now takes greater magnetic field to snap away the boundary from the dislocation. Domain walls also interact with nonmagnetic impurities and inclusions. For example, an inclusion that finds itself in a domain becomes magnetized and develops south and north poles, as shown in Figure 8.29a. If the domain wall were to intersect the inclusion and if there were to be two neighboring domains around the inclusion, as in Figure 8.29b, then the magnetostatic energy would be lowered—energetically a favorable event. This reduction in magnetostatic potential energy means that it now takes greater force to move the domain wall past the impurity, as if the wall were "pinned" by the impurity.

The motion of a domain wall in a crystal is therefore not smooth but rather jerky. The wall becomes pinned somewhere by a defect or an impurity and then needs a greater applied field to break free. Once it snaps off, the domain wall is moved until

[5] See, for example, D. Jiles and C. C. H. Lo, *Sensors and Actuators*, A106, 3, 2003.

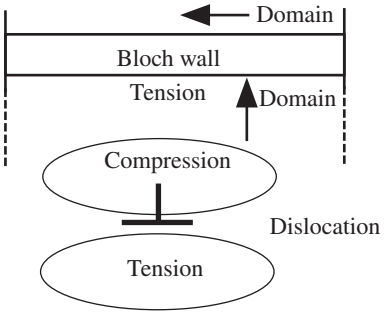


Figure 8.28 Stress and strain distributions around a dislocation and near a domain wall.

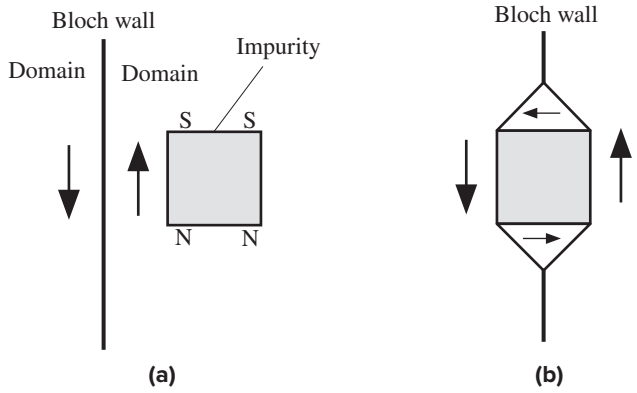


Figure 8.29 Interaction of a Bloch wall with a nonmagnetic (no permanent magnetization) inclusion. (a) The inclusion becomes magnetized and there is magnetostatic energy. (b) This arrangement has lower potential energy and is thus favorable.

it is attracted by another type of imperfection, where it is held until the field increases further to snap it away again. Each time the domain wall is snapped loose, lattice vibrations are generated, which means loss of energy as heat. The whole domain wall motion is nonreversible and involves energy losses as heat to the crystal.

8.5.6 POLYCRYSTALLINE MATERIALS AND THE *M* VERSUS *H* BEHAVIOR

The majority of the magnetic materials used in engineering are polycrystalline and therefore have a microstructure that consists of many grains of various sizes and orientations depending on the preparation and thermal history of the component. In an unmagnetized polycrystalline sample, each crystal grain will possess domains, as depicted in Figure 8.30. The domain structure in each grain will depend on the size and shape of the grain and, to some extent, on the magnetizations in neighboring grains. Although very small grains, perhaps smaller than 0.1 μm, may be single domains, in most cases the majority of the grains will have many domains. Overall, the structure will possess no net magnetization, provided that it was not previously subjected to an applied magnetic field. We can assume that the component was heated to a temperature above the Curie point and then allowed to cool to room temperature without an applied field.

Suppose that we start applying a very small external magnetic field ($\mu_o H$) along some direction, which we can arbitrarily label as $+x$. The domain walls within various grains begin to move small distances, and favorably oriented domains (those with a component of M along $+x$) grow a little larger at the expense of those pointing away from the field, as indicated by point a in Figure 8.31. The domain walls that are pinned by imperfections tend to bow out. There is a very small but net magnetization along the field, as indicated by the Oa region in the magnetization versus magnetizing field (M versus H) behavior in Figure 8.31. As we increase the magnetizing field, the domain motions extend larger distances, as shown for point b

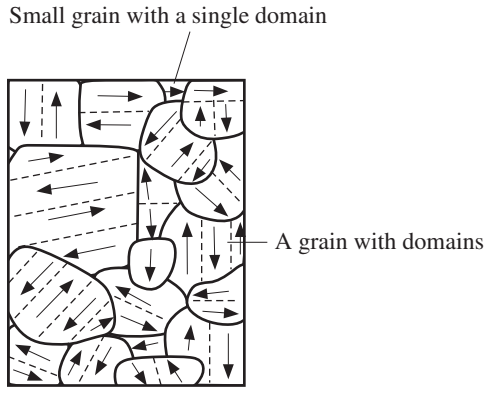


Figure 8.30 Schematic illustration of magnetic domains in the grains of an unmagnetized polycrystalline iron sample.
Very small grains have single domains.

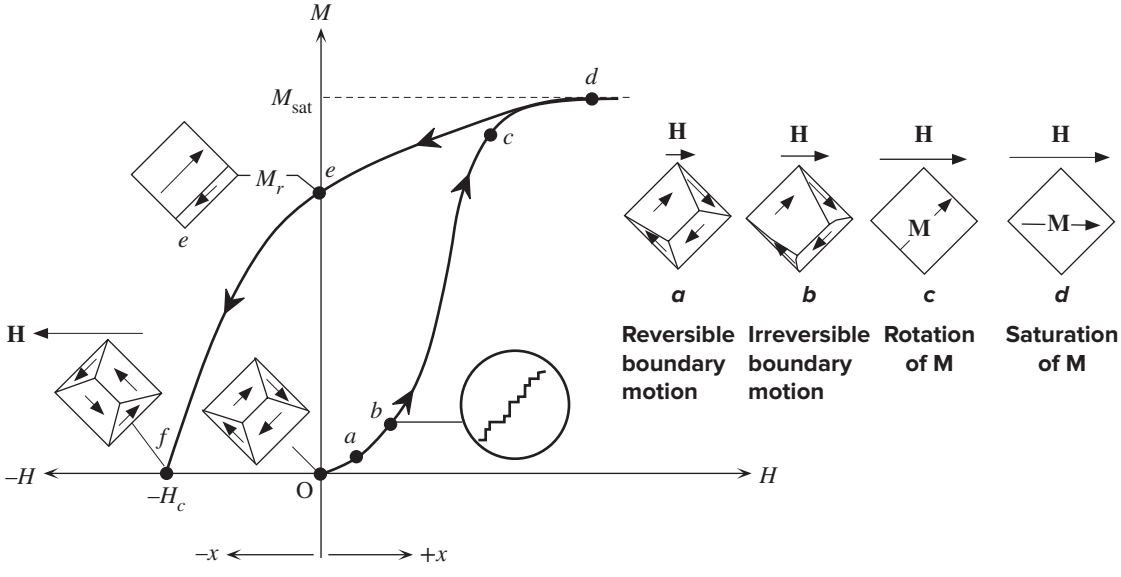


Figure 8.31 *M* versus *H* behavior of a previously unmagnetized polycrystalline iron specimen.
An example grain in the unmagnetized specimen is that at O. (a) Under very small fields, the domain boundary motion is reversible. (b) The boundary motions are irreversible and occur in sudden jerks. (c) Nearly all the grains are single domains with saturation magnetizations in the easy directions. (d) Magnetizations in individual grains have to be rotated to align with the field *H*. (e) When the field is removed, the specimen returns along *d* to *e*. (f) To demagnetize the specimen, we have to apply a magnetizing field of H_c in the reverse direction.

in Figure 8.31, and walls encounter various obstacles such as crystal imperfections, impurities, second phases, and so on, which tend to attract the walls and thereby hinder their motions. A domain wall that is stuck (or pinned) at an imperfection at a given field cannot move until the field increases sufficiently to provide the necessary force to snap the wall free, which then suddenly surges forward to the next obstacle. As a wall suddenly snaps free and shoots forward to the next obstacle, essentially two causes lead to heat generation. Sudden changes in the lattice distortion,

due to magnetostriction, create lattice waves that carry off some of the energy. Sudden changes in the magnetization induce eddy currents that dissipate energy via Joule heating (domains have a finite electrical resistance). These processes involve energy conversion to heat and are irreversible. Sudden jerks in the wall motions lead to small jumps in the magnetization of the specimen as the magnetizing field is increased; the phenomenon is known as the **Barkhausen effect.** If we could examine the magnetization precisely with a highly sensitive instrument, we would see jumps in the M versus H behavior, as shown in the inset in Figure 8.31.

As we increase the field, magnetization continues to increase by jerky domain wall motions that enlarge domains with favorably oriented magnetizations and shrink away those with magnetizations pointing away from the applied field. Eventually domain wall motions leave each crystal grain with a single domain and magnetization in one of the easy directions, as indicated by point c in Figure 8.31. Although some grains would be oriented to have the easy direction and hence M along the applied field, the magnetization in many grains will be pointing at some angle to H as shown for point c in Figure 8.31. From then until point d, the increase in the applied field forces the magnetization in a grain, such as that at point c to rotate toward the direction of H. Eventually the applied field is sufficiently strong to align M along H, and the specimen reaches saturation magnetization M_{sat}, directed along H or $+x$, as at point d in Figure 8.31.

If we were to decrease and remove the magnetizing field, the magnetization in each grain would rotate to align parallel with the nearest easy direction in that grain. Further, in some grains, additional small domains may develop that reduce the magnetization within that grain, as indicated at point e in Figure 8.31. This process, from point d to point e, leaves the specimen with a permanent magnetization, called the **remanent** or **residual magnetization** and denoted by M_r.

If we were now to apply a magnetizing field in the reverse direction $-x$, the magnetization of the specimen, still along $+x$, would decrease and eventually, at a sufficiently large applied field M would be zero and the sample would have been totally demagnetized. This is shown as point f in Figure 8.31. The magnetizing field H_c required to totally demagnetize the sample is called the **coercivity** or the **coercive field.** Some authors and various data sheets define H_c as the **intrinsic coercivity.** It represents the resistance of the sample to demagnetization. We should note that at point f in Figure 8.31, the sample again has grains with many domains, which means that during the demagnetization process, from point e to point f, new domains had to be generated. The demagnetization process invariably involves the nucleation of various domains at various crystal imperfections to cancel the overall magnetization. The treatment of the nucleation of domains is beyond the scope of this book; we will nonetheless, accept it as required process for the demagnetization of the crystal grains.

If we continue to increase the applied magnetic field along $-x$, as illustrated in Figure 8.32a, the process from point f onward becomes similar to that described for magnetization from point a to point d in Figure 8.31 along $+x$ except that it is now directed along $-x$. At point g, the sample reaches saturation magnetization along the $-x$ direction. The full M versus H behavior as the magnetizing field is cycled between $+x$ to $-x$ has a closed loop shape, shown in Figure 8.32a, called the **hysteresis loop.** We observe that in both $+x$ and $-x$ directions, the magnetization reaches saturation

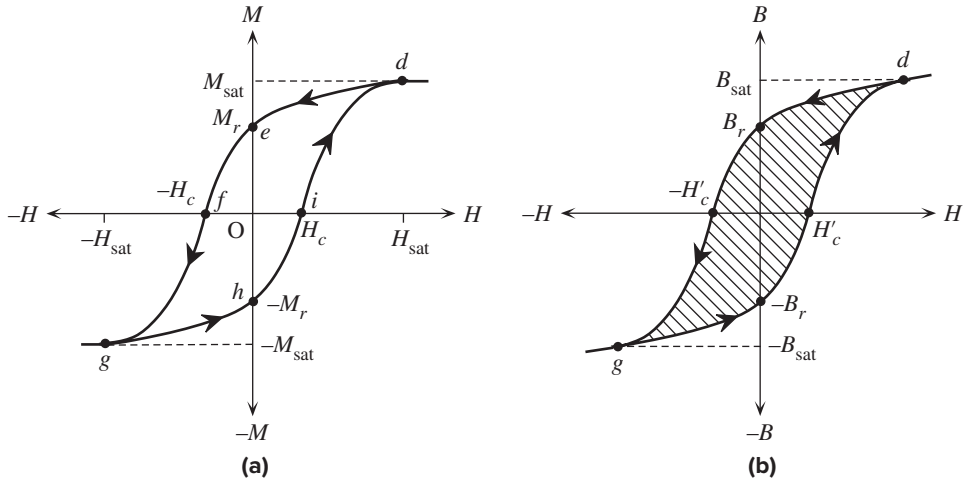


Figure 8.32 (a) A typical *M* versus *H* hysteresis curve. (b) The corresponding *B* versus *H* hysteresis curve. The shaded area inside the hysteresis loop is the energy loss per unit volume per cycle.

M_{sat} when H reaches H_{sat}, and on removing the applied field, the specimen retains an amount of permanent magnetization, represented by points *e* and *h* and denoted by M_r. The necessary applied field of magnitude H_c that is needed to demagnetize the specimen is the coercivity (or coercive field), which is represented by points *f* and *i*. The initial magnetization curve, O*abcd* in Figure 8.31, which starts from an unmagnetized state, is called the **initial magnetization curve.**

We can, of course, monitor the magnetic field B instead of M, as in Figure 8.32b, where

$$B = \mu_o M + \mu_o H \qquad [8.26]$$

which leads to a hysteresis loop in the B versus H behavior. The very slight increase in B with H when M is in saturation is due to the permeability of free space ($\mu_o H$). The area enclosed within the B versus H hysteresis loop, shown as the hatched region in Figure 8.32b, represents the energy dissipated per unit volume per cycle of applied field variation. Notice that the magnetizing field H_c for $M = 0$ is different than H'_c for $B = 0$ in the material. We will call H'_c the **coercivity on the *B*–*H* loop**.[6] H'_c is smaller than H_c because we are trying to make $B = 0$ in Equation 8.26, and this occurs at a finite (and negative) M, before we reach point *f* on path *def* in Figure 8.32a.

Suppose we do not take a magnetic material to saturation but still subject the specimen to a cyclic applied field alternating between the $+x$ and $-x$ directions. Then the hysteresis loop would be different than that when the sample is taken all the way to saturation, as shown in Figure 8.33. The magnetic field in the material does not reach B_{sat} (corresponding to M_{sat}) but instead reaches some maximum value B_m when the magnetizing field is H_m. There is still a hysteresis effect because the

[6] Unfortunately there is no accepted consensus on the exact terminology for H_c and H'_c, which adds to confusion. Nonetheless, intrinsic coercivity H_c defined on the *M*–*H* curve seems a reasonable definition. H_{ci} is also used for H_c.

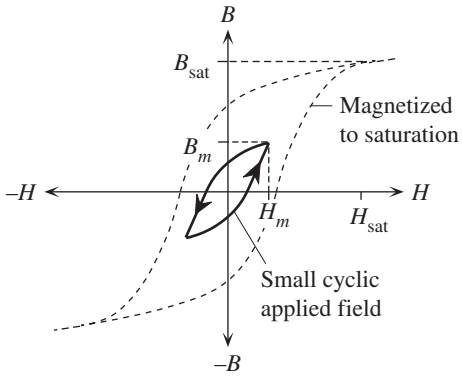


Figure 8.33 The *B* versus *H* hysteresis loop depends on the magnitude of the applied field in addition to the material and sample shape and size.

magnetization and demagnetization processes are nonreversible and do not retrace each other. The shape of the hysteresis loop depends on the magnitude of the applied field in addition to the material and sample shape and size. The area enclosed within the loop is still the energy dissipated per unit volume per cycle of applied field oscillation. The hysteresis loop taken to saturation, as in Figure 8.32a and b, is called the **saturation (major) hysteresis loop.** It is apparent from Figure 8.33 that the remanence and coercivity exhibited by the sample depend on the *B–H* loop. The quoted values normally correspond to the saturation hysteresis loop.

Ferrimagnetic materials exhibit properties that closely resemble those of ferromagnetic materials. One can again identify distinct magnetic domains and domain wall motions during magnetization and demagnetization that also lead to *B–H* hysteresis curves with the same characteristic parameters, namely, saturation magnetization (M_{sat} and B_{sat} at H_{sat}), remanence (M_r and B_r), coercivity (H_c), hysteresis loss, and so on.

8.5.7 DEMAGNETIZATION

The *B–H* hysteresis curves, as in Figure 8.32b, that are commonly given for magnetic materials represent *B* versus *H* behavior observed under repeated cycling. The applied field intensity *H* is cycled back and forward between the $-x$ and $+x$ directions. If we were to try and demagnetize a specimen with a remanent magnetization at point *e* in Figure 8.34 by applying a reverse field intensity, then the magnetization would move along from point *e* to point *f*. If at point *f* we were to suddenly switch off the applied field, we would find that *B* does not actually remain zero but recovers along *f* to point e' and attains some value B_r'. The main reason is that small domain wall motions are reversible and as soon as the field is removed, there is some reversible domain wall motion "bouncing back" the magnetization along f–e'. We can anticipate this recovery and remove the field intensity at some point f' so that the sample recovers along f'O and the magnetization ends up being zero. However, to remove the field intensity at point f', we need to know not only the exact *B–H* behavior but also the exact location of point f' (or the recovery behavior). The simplest method to demagnetize the sample is first to cycle *H* with ample magnitude to reach saturation and then to continue cycling *H* but with a gradually decreasing magnitude, as

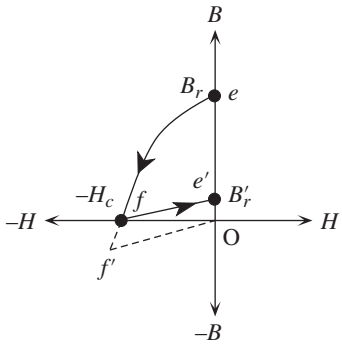


Figure 8.34 Removal of the demagnetizing field at point *f* does not necessarily result in zero magnetization as the sample recovers along *f*–*e*′.

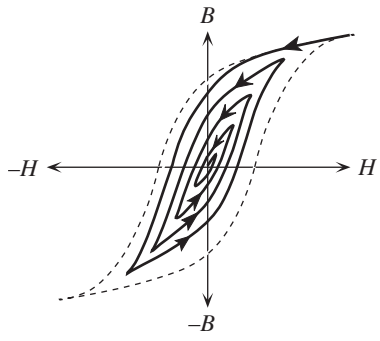


Figure 8.35 A magnetized specimen can be demagnetized by cycling the field intensity with a decreasing magnitude, that is, tracing out smaller and smaller *B*–*H* loops until the origin is reached, $H = 0$.

depicted in Figure 8.35. As H is cycled with a decreasing magnitude, the sample traces out smaller and smaller B–H loops until the B–H loops are so small that they end up at the origin when H reaches zero. The demagnetization process in Figure 8.35 is commonly known as **deperming.** Undesirable magnetization of various magnetic devices such as recording heads is typically removed by this deperming process (for example, a demagnetizing gun brought close to a magnetized recording head implements deperming by applying a cycled H with decreasing magnitude).

EXAMPLE 8.5 **ENERGY DISSIPATED PER UNIT VOLUME AND THE HYSTERESIS LOOP** Consider a toroidal coil with an iron core that is energized from a voltage supply through a rheostat, as shown in Figure 8.11. Suppose that by adjusting the rheostat we can adjust the current i supplied to the coil and hence the magnetizing field H in the core material. H and i are simply related by Ampere's law. However, the magnetic field B in the core is determined by the B–H characteristics of the core material. From electromagnetism (see Example 8.2), we know that the battery has to do work dE_{vol} per unit volume of core material to increase the magnetic field by dB, where

$$dE_{vol} = H\, dB$$

Work done per unit volume during magnetization

so that the total energy or work involved per unit volume in changing the magnetic field from an initial value B_1 to a final value B_2 in the core is

$$E_{vol} = \int_{B_1}^{B_2} H\, dB \qquad [8.27]$$

where the integration limits are determined by the initial and final magnetic fields.

Equation 8.27 corresponds to the area between the B–H curve and the B axis between B_1 and B_2. Suppose that we take the iron core in the toroid from point P on the hysteresis curve to Q, as shown in Figure 8.36. This is a magnetization process for which energy is put into the sample. The work done per unit volume from P to Q is the area $PQRS$, shown as

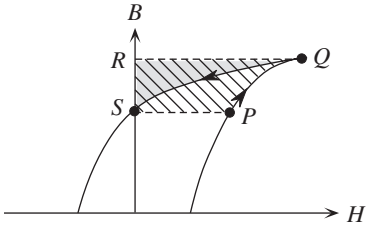


Figure 8.36 The area between the *B–H* curve and the *B* axis is the energy absorbed per unit volume in magnetization or released during demagnetization.

hatched. On returning the sample to the same initial magnetization (same magnetic field B as we had at P), taking it from Q to S, energy is returned from the core into the electric circuit. This energy per unit volume is the area QRS, shown as gray, and is less than $PQRS$ during magnetization. The difference is the energy dissipated in the sample as heat (moving domain walls and so on) and corresponds to the hysteresis loop area PQS. Over one full cycle, the energy dissipated per unit volume is the total hysteresis loop area.

The hysteresis loop and hence the energy dissipated per unit volume per cycle depend not only on the core material but also on the magnitude of the magnetic field (B_m), as apparent in Figure 8.33. For example, for magnetic steels used in transformer cores, the hysteresis **power loss** P_h per unit volume of core is empirically expressed in terms of the maximum magnetic field B_m and the ac frequency f as[7]

Hysteresis power loss per m^3

$$P_h = KfB_m^n \qquad [8.28]$$

where K is a constant that depends on the core material (typically, $K = 150.7$), f is the ac frequency (Hz), B_m is the maximum magnetic field (T) in the core (assumed to be in the range 0.1–1.5 T), and $n = 1.6$. According to Equation 8.28, the hysteresis loss can be decreased by operating the transformer with a reduced magnetic field.

8.6 SOFT AND HARD MAGNETIC MATERIALS

8.6.1 DEFINITIONS

Based on their *B–H* behavior, engineering materials are typically classified into soft and hard magnetic materials. Their typical *B–H* hysteresis curves are shown in Figure 8.37. Soft magnetic materials are easy to magnetize and demagnetize and hence require relatively low magnetic field intensities. Put differently, their *B–H* loops are narrow, as shown in Figure 8.37. The hysteresis loop has a small area, so the hysteresis power loss per cycle is small. Soft magnetic materials are typically suitable for applications where repeated cycles of magnetization and demagnetization are involved, as in electric motors, transformers, and inductors, where the magnetic field varies cyclically. These applications also require low hysteresis losses, or small hysteresis loop area. Electromagnetic relays that have to be turned on and off require the relay iron to be magnetized and demagnetized and therefore need soft magnetic materials.

Hard magnetic materials, on the other hand, are difficult to magnetize and demagnetize and hence require relatively large magnetic field intensities, as apparent

[7] This is the power engineers Steinmetz equation for commercial magnetic steels. It has been applied not only to silicon irons (Fe + few percent Si) but also to a wide range of magnetic materials.

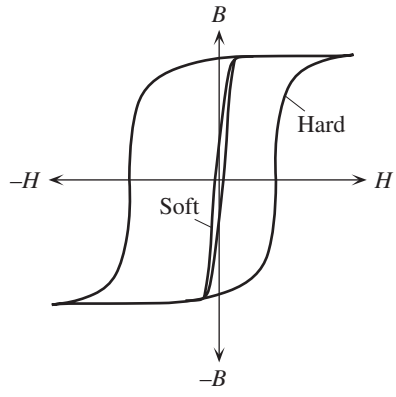


Figure 8.37 Soft and hard magnetic materials.

in Figure 8.37. Their *B–H* curves are broad and almost rectangular. They possess relatively large coercivities, which means that they need large applied fields to be demagnetized. The coercive field for hard materials can be millions of times greater than those for soft magnetic materials. Their characteristics make hard magnetic materials useful as permanent magnets in a variety of applications. It is also clear that the magnetization can be switched from one very persistent direction to another very persistent direction, from $+B_r$ to $-B_r$, by a suitably large magnetizing field intensity. As the coercivity is strong, both the states $+B_r$ and $-B_r$ persist until a suitable (large) magnetic field intensity switches the field from one direction to the other. It is apparent that hard magnetic materials can also be used in magnetic storage of digital data, where the states $+B_r$ and $-B_r$ can be made to represent 1 and 0 (or vice versa).

8.6.2 Initial and Maximum Permeability

It is useful to characterize the magnetization of a material by a relative permeability μ_r, since this simplifies magnetic calculations. For example, inductance calculations become straightforward if one could represent the magnetic material by μ_r alone. But it is clear from Figure 8.38a that

$$\mu_r = \frac{B}{\mu_o H}$$

is not even approximately constant because it depends on the applied field and the magnetic history of the sample. Nonetheless, we still find it useful to specify a relative permeability to compare various materials and even use it in various calculations. The definition $\mu_r = B/(\mu_o H)$ represents the slope of the straight line from the origin O to the point *P*, as shown in Figure 8.38a. This is a maximum when the line becomes a tangent to the *B–H* curve at *P*, as in the figure. Any other line from O to the *B–H* curve that is not a tangent does not yield a maximum relative permeability (the mathematical proof is left to the reader, though the argument is intuitively acceptable from the figure). The **maximum relative permeability,** as defined in Figure 8.38a, is denoted by $\mu_{r,\max}$ and serves as a useful magnetic parameter.

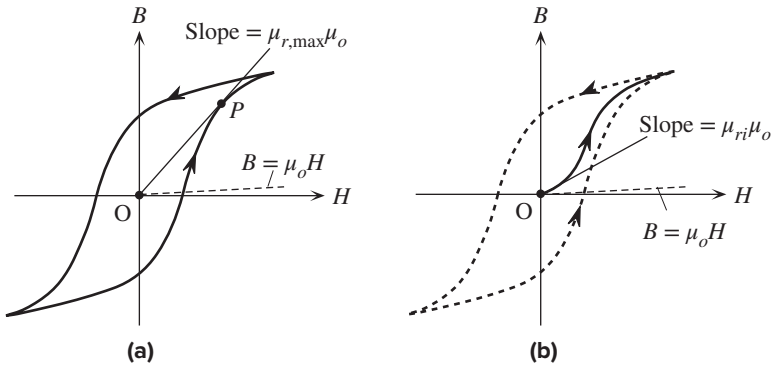


Figure 8.38 Definitions of (a) maximum permeability and (b) initial permeability.

The point P in Figure 8.38a that defines the maximum permeability corresponds to what is called the "knee" of the B–H curve. Many transformers are designed to operate with the maximum magnetic field in the core reaching this knee point. For pure iron, $\mu_{r,\max}$ is less than 10^4, but for certain soft magnetic materials such as supermalloys (a nickel–iron alloy), the values of $\mu_{r,\max}$ can be as high as 10^6.

Initial relative permeability, denoted as μ_{ri}, represents the initial slope of the initial B versus H curve as the material is first magnetized from an unmagnetized state, as illustrated in Figure 8.38b. This definition is useful for soft magnetic materials that are employed at very low magnetic fields (*e.g.*, small signals in electronics and communications engineering). In practice, weak applied magnetic fields where μ_{ri} is useful are typically less than 10^{-4} T. In contrast, $\mu_{r,\max}$ is useful when the magnetic field in the material is not far removed from saturation. Initial relative permeability of a magnetically soft material can vary by orders of magnitude. For example, μ_{ri} for iron is 150, whereas for supernumetal-200, a commercial alloy of nickel and iron, it is about 2×10^5.

8.7 SOFT MAGNETIC MATERIALS: EXAMPLES AND USES

Table 8.5 identifies what properties are desirable in soft magnetic materials and also lists some typical examples with various applications. An *ideal* soft magnetic material would have zero coercivity (H_c), a very large saturation magnetization (B_{sat}), zero remanent magnetization (B_r), zero hysteresis loss, and very large $\mu_{r,\max}$ and μ_{ri}. A number of example materials, from pure iron to ferrites, which are ferrimagnetic, are listed in Table 8.5. Pure iron, although soft, is normally not used in electric machines (except in a few specific relay-type applications) because its good conductivity allows large eddy currents to be induced under varying fields. Induced eddy currents in the iron lead to Joule losses (RI^2), which are undesirable. The addition of a few percentages of silicon to iron (silicon–iron), known typically as silicon–steels, increases the resistivity and hence reduces the eddy current losses. Silicon–iron is widely used in power transformers and electric machinery.

Table 8.5 Selected soft magnetic materials and some typical values and applications

Magnetic Material	$\mu_o H_c$ (T)	B_{sat} (T)	B_r (T)	μ_{ri}	$\mu_{r,max}$	W_h (J m^{-3})	Typical Applications
Ideal soft	0	Large	0	Large	Large	0	Transformer cores, inductors, electric machines, electromagnet cores, relays, magnetic recording heads.
Iron (commercial) grade, 0.2% impurities	$<10^{-4}$	2.2	<0.1	150	10^4	250	Large eddy current losses. Generally not preferred in electric machinery except in some specific applications (*e.g.*, some electromagnets and relays).
Silicon iron (Fe: 2–4% Si)	$<10^{-4}$	2.0	0.5–1	10^3	10^4–4×10^5	30–100	Higher resistivity and hence lower eddy current losses. Wide range of electric machinery (*e.g.*, transformers, motors, generators).
Supermalloy (79% Ni–15.5% Fe–5% Mo–0.5% Mn)	2×10^{-7}	0.7–0.8	<0.1	10^5	10^6	<0.5	High permeability, low-loss electric devices, *e.g.*, specialty transformers, magnetic amplifiers.
78 Permalloy (78.5% Ni–21.5% Fe)	5×10^{-6}	0.86	<0.1	8×10^3	10^5	<0.1	Low-loss electric devices, audio transformers, HF transformers, recording heads, filters, inductors.
Glassy metals, Fe–Si–B	2×10^{-6}	1.6	$<10^{-6}$	—	10^5	20	Low-loss transformer cores.
Ferrites, Mn–Zn ferrite.	10^{-5}	0.4	<0.01	2×10^3	5×10^3	<0.01	HF low-loss applications. Low conductivity ensures negligible eddy current losses. HF transformers, inductors (*e.g.*, pot cores, E and U cores), antenna rods, recording heads.

NOTE: W_h is the hysteresis loss, energy dissipated per unit volume per cycle in hysteresis losses, J m^{-3} cycle^{-1}, typically at $B_m = 1$ T.

The nickel–iron alloys with compositions around 77% Ni–23% Fe constitute an important class of soft magnetic materials with low coercivity, low hysteresis losses, and high permeabilities (μ_{ri} and $\mu_{r,max}$). High μ_{ri} makes these alloys particularly useful in low magnetic field applications that are typically found in high-frequency work in electronics (*e.g.*, audio and wide-band transformers). They have found many engineering uses in sensitive relays, pulse and wide-band transformers, current transformers, magnetic recording heads, magnetic shielding, and so forth. Alloying iron with nickel increases the resistivity and hence reduces eddy current losses. The magnetocrystalline anisotropy energy is least at these nickel compositions, which leads to easier domain wall motions and hence smaller hysteresis losses. There are a number of commercial nickel–iron alloys whose application depends on the exact composition (which may also have a few percentages of Mo, Cu, or Cr) and the method of preparation (*e.g.*, mechanical rolling). For example, supermalloy (79% Ni–16% Fe–5% Co) has $\mu_{ri} \approx 10^5$, compared with commercial grade iron, which has μ_{ri} less than 10^3.

Amorphous magnetic metals, as the name implies, have no crystal structure (they only have short-range order) and consequently possess no crystalline imperfections such as grain boundaries and dislocations. They are prepared by rapid solidification of the melt by using special techniques such as melt spinning (as described in Chapter 1). Typically they are thin ribbons by virtue of their preparation method. Since they have no crystal structure, they also have no magnetocrystalline anisotropy energy, which means that all directions are easy. The absence of magnetocrystalline anisotropy and usual crystalline defects which normally impede domain wall motions, leads to low coercivities and hence to soft magnetic properties. The coercivity, however, is not zero inasmuch as there is still some magnetic anisotropy due to the directional nature of the strains frozen in the metal during rapid solidification. By virtue of their disordered structure, these metallic glasses also have higher resistivities and hence they have smaller eddy current losses. Although they are ideally suited for various transformer and electric machinery applications, their limited size and shape, at present, prevent their use in power applications.

Ferrites are ferrimagnetic materials that are typically oxides of mixed transition metals, one of which is iron. For example, Mn ferrite is $MnFe_2O_4$ and MgZn ferrite is $Mn_{1-x}Zn_xFe_2O_4$. They are normally insulators and therefore do not suffer from eddy current losses. They are ideal as magnetic materials for high-frequency work where eddy current losses would prevent the use of any material with a reasonable conductivity. Although they can have high initial permeabilities and low losses, they do not possess as large saturation magnetizations as ferromagnets, and further, their useful temperature range (determined by the Curie temperature) is lower. There are many types of commercial ferrites available depending on the application, tolerable losses, and the required upper frequency of operation. MnZn ferrites, for example, have high initial permeabilities (*e.g.*, 2×10^3) but are only useful up to about 1 MHz, whereas NiZn ferrites have lower initial permeability (*e.g.*, 10^2) but can be used up to 200 MHz. Generally, the initial permeability in the high-frequency region decreases with frequency.

Garnets are ferrimagnetic materials that are typically used at the highest frequencies that cover the microwave range (1–300 GHz). The yttrium iron garnet, YIG, which is $Y_3Fe_5O_{12}$, is one of the simplest garnets with a very low hysteresis loss at microwave frequencies. Garnets have excellent dielectric properties with high resistivities and hence low losses. The main disadvantages are the low saturation magnetization, which is 0.18 T for YIG, and low Curie temperature, 280 °C for YIG. The compositions of garnets depend on the properties required for the particular microwave application. For example, $Y_{2.1}Gd_{0.98}Fe_5O_{12}$ is a garnet that is used in X-band (8–12 GHz) three-port circulators handling high microwave powers (*e.g.*, peak power 200 kW and average power 200 W).

EXAMPLE 8.6

AN INDUCTOR WITH A FERRITE CORE Consider a toroidal coil with a ferrite core. Suppose that the coil has 200 turns and is used in HF work with small signals. The mean diameter of the toroid is 2.5 cm and the core diameter is 0.5 cm. If the core is a MnZn ferrite with $\mu_r = 2 \times 10^3$, what is the approximate inductance of the coil?

SOLUTION

The inductance L of a toroidal coil is given by

$$L = \frac{\mu_{ri}\mu_o N^2 A}{\ell}$$

so

$$L = \frac{(2 \times 10^3)(4\pi \times 10^{-7}\ \text{H m}^{-1})(200)^2 \pi \left(\frac{0.005}{2}\ \text{m}\right)^2}{(\pi\, 0.025\ \text{m})} = 0.025\ \text{H} \quad \text{or} \quad 25\ \text{mH}$$

Had the core been air, the inductance would have been 1.26×10^{-5} H or 12.6 μH. The main assumption is that B is uniform in the core, and this will be only so if the diameter of the toroid (2.5 cm) is much greater than the core diameter (0.5 cm). Here this ratio is 5 and the calculation is only approximate.

8.8 HARD MAGNETIC MATERIALS: EXAMPLES AND USES

An ideal hard magnetic material, as summarized in Table 8.6, has very large coercivity and remanent magnetic field. Further, since they are used as permanent magnets, the energy stored per unit volume in the external magnetic field should be as large as possible since this is the energy available to do work. This energy density (J m^{-3})

Table 8.6 Selected hard magnetic materials and typical values

Magnetic Material	$\mu_o H_c$ (T)	B_r (T)	$(BH)_{max}$ (kJ m^{-3})	Examples and Uses
Ideal hard	Large	Large	Large	Permanent magnets in various applications.
Alnico (Fe–Al–Ni–Co–Cu)	0.05–0.1	1.0	40–50	Wide range of permanent magnet applications.
Alnico (Columnar)	0.075	1.35	60	
Strontium ferrite (sintered)	0.3–0.5	0.3–0.5	20–35	Starter motors, dc motors, loudspeakers, telephone receivers, various toys.
Rare earth cobalt, *e.g.*, Sm_2Co_{17} (sintered)	0.9–1.2	1.1	200–250	Servo motors, stepper motors, couplings, clutches, quality audio headphones.
NdFeB magnets	1.0–1.5	1.0–1.4	300–350	Wide range of applications, small motors (*e.g.*, in hand tools), audio equipment, hard drives, MRI body scanners.
Hard particles, γ-Fe_2O_3	0.03	0.2		Audio and video tapes, floppy disks.

NOTE: H_c is the intrinsic coercivity.

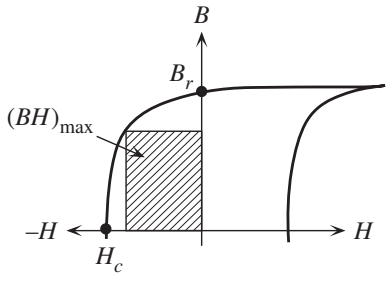


Figure 8.39 Hard magnetic materials and $(BH)_{max}$.

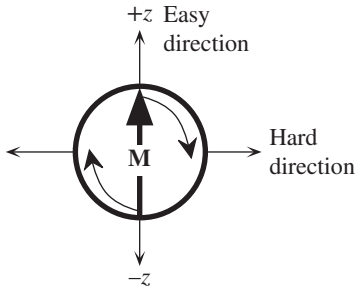


Figure 8.40 A single domain fine particle.

in the external field depends on the maximum value of the product BH in the second quadrant of the B–H characteristics and is denoted as $(BH)_{max}$. It corresponds to the largest rectangular area that fits the B–H curve in the second quadrant, as shown in Figure 8.39.

When the size of a ferromagnetic sample falls below a certain critical dimension, of the order of 0.1 μm for cobalt, the whole sample becomes a single domain, as depicted in Figure 8.40, because the cost of energy in generating a domain wall is too high compared with the reduction in external magnetostatic energy. These small particle-like pieces of magnets are called **single domain fine particles.** Their magnetic properties depend not only on the crystal structure of the particle but also on the shape of the particle because different shapes give rise to different external magnetic fields. For a spherical iron particle, the magnetization **M** will be in an easy direction, for example, along [100] taken along $+z$. To reverse the magnetization from $+z$ to $-z$ by an applied field, we have to rotate the spins around past the hard direction, as shown in Figure 8.40, since we cannot generate reverse domains (or move domain walls). The rotation of magnetization involves substantial work due to the magnetocrystalline anisotropic energy, and the result is high coercivity. The higher the magnetocrystalline anisotropy energy, the greater the coercivity. The energy involved in creating a domain wall increases with the magnetocrystalline anisotropy energy. The critical size below which a particle becomes a single domain therefore increases with the crystalline anisotropy. Barium ferrite crystals have the hexagonal structure and hence have a high degree of magnetocrystalline anisotropy. Critical size for single domain barium ferrite particles is about 1–1.5 μm, and the coercivity $\mu_o H_c$ of small particles can be as high as 0.3 T, compared with values 0.02–0.1 T in multidomain barium ferrite pieces.

Particles that are not spherical may even have higher coercivity as a result of shape anisotropy. Consider an ellipsoid (elongated) fine particle, shown in Figure 8.41a. If the magnetization **M** is along the long axis (along z), then the potential energy in the external magnetic field is less than if **M** were along the minor axis (along y), as compared in Figure 8.41a and b. Thus, we have to do work to rotate **M** from the long to the short axis, or from Figure 8.41a to b. An elongated fine particle therefore has its magnetization along its length, and the effect is called **shape anisotropy.** If we have to reverse the magnetization from $+z$ to $-z$ by applying a reverse field, then

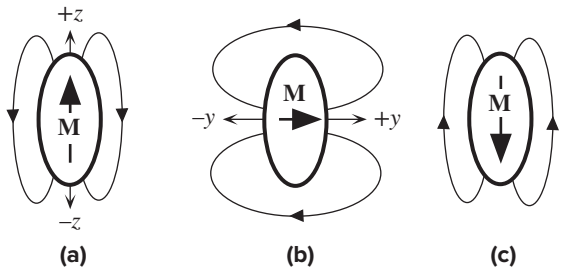
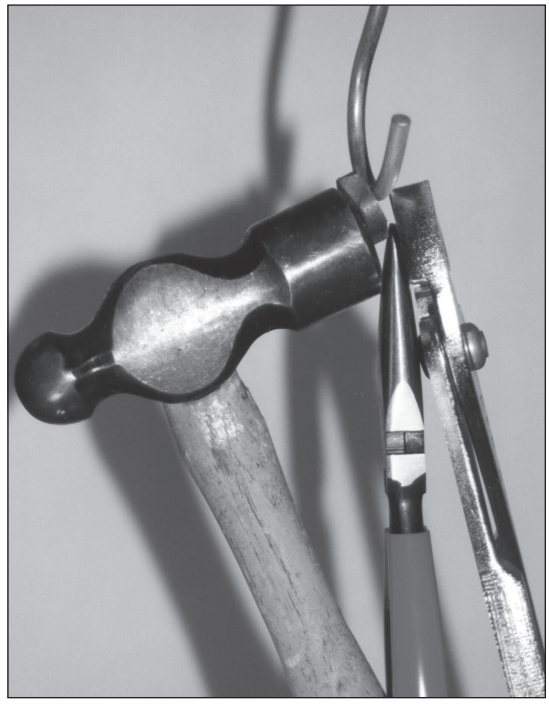


Figure 8.41 A single domain elongated particle.

Due to shape anisotropy, magnetization prefers to be along the long axis as in (a). Work has to be done to change **M** from (a) to (b) to (c).



This small neodymium-iron-boron permanent magnet (diameter about the same as one-cent coin) is capable of lifting up to 10 pounds. Nd-Fe-B magnets typically have large $(BH)_{max}$ values (200–275 kJ m^{-3}).

| Photo by S. Kasap.

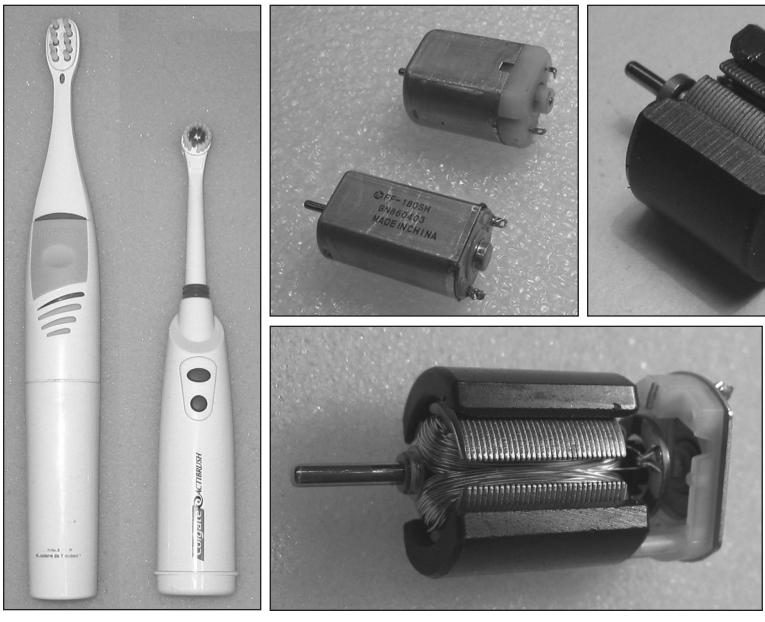
we can only do so by rotating the magnetization, as shown in Figure 8.41a to c. **M** has to be rotated around through the minor axis, and this involves substantial work. Thus the coercivity is high. In general, the greater the elongation of the particle with respect to its width, the higher the coercivity. Small spherical Fe–Cr–Co particles have a coercivity $\mu_o H_c$ at most 0.02 T, but elongated and aligned particles can have a coercivity as high as 0.075 T due to shape anisotropy.

High coercivity magnets can be fabricated by having elongated fine particles dispersed by precipitation in a structure. Fine particles will be single domains. Alnico is a popular permanent magnet material that is an alloy of the metals Al, Ni, Co, and Fe (hence the name). Its microstructure consists of fine elongated Fe–Co rich particles, called the α'-phase, dispersed in a matrix that is Ni–Al rich and called the α-phase. The structure is obtained by an appropriate heat treatment that allows fine α' particles to precipitate out from a solid solution of the alloy. The α' particles are

strongly magnetic, whereas the α-phase matrix is weakly magnetic. When the heat treatment is carried out in the presence of a strong applied magnetic field, the α' particles that are formed have their elongations (or lengths) and hence their magnetizations along the applied field. The demagnetization process requires the rotations of the magnetizations in single domain elongated α' particles, which is a difficult process (shape anisotropy), and hence the coercivity is high. The main drawback of the Alnico magnet is that the alloy is mechanically hard and brittle and cannot be shaped except by casting or sintering before heat treatment. There are, however, other alloy permanent magnets that can be machined.

A variety of permanent magnets are made by compacting high-coercivity particles by using powder metallurgy (*e.g.*, powder pressing or sintering). The particles are magnetically hard because they are sufficiently small for each to be of single domain or they possess substantial shape anisotropy (elongated particles may be ferromagnetic alloys, *e.g.*, Fe–Co, or various hard ferrites). These are generically called powdered solid permanent magnets. An important class is the **ceramic magnets** that are made by compacting barium ferrite, $BaFe_{12}O_9$, or strontium ferrite, $SrFe_{12}O_9$, particles. The barium ferrite has the hexagonal crystal structure with a large magnetocrystalline anisotropy, which means that barium ferrite particles have high coercivity. The ceramic magnet is typically formed by wet pressing ferrite powder in the presence of a magnetizing field, which allows the easy directions of the particles to be aligned, and then drying and carefully sintering the ceramic. They are used in many low-cost applications.

Rare earth cobalt permanent magnets based on samarium–cobalt (Sm–Co) alloys have very high $(BH)_{max}$ values and are widely used in many applications such as dc motors, stepper and servo motors, traveling wave tubes, klystrons, and



One important application of permanent magnets is in small dc motors. Toothbrushes that operate from batteries use dc motors with strong permanent magnets to get the required torque to drive the brushes.

| Photo by S. Kasap.

gyroscopes. The intermetallic compound $SmCo_5$ has a hexagonal crystal structure with high magnetocrystalline anisotropy and hence high coercivity. The $SmCo_5$ powder is pressed in the presence of an applied magnetic field to align the magnetizations of the particles. This is followed by careful sintering to produce a solid powder magnet. The Sm_2Co_{15} magnets are more recent and have particularly high values of $(BH)_{max}$ up to about 250 kJ m^{-3}. Sm_2Co_{15} is actually a generic name and the alloy may contain other transition metals substituting for some of the Co atoms.

The more recent **neodymium–iron–boron,** NdFeB, powdered solid magnets can have very large $(HB)_{max}$ values up to about 350 kJ m^{-3}. The tetragonal crystal structure has the easy direction along the long axis and possesses high magnetocrystalline anisotropic energy. This means that we need a substantial amount of work to rotate the magnetization around through the hard direction, and hence the coercivity is also high. The main drawback is the lower Curie temperature, typically around 300 °C, whereas for Alnico and rare earth cobalt magnets, the Curie temperatures are above 700 °C. Another method of preparing NdFeB magnets is by the recrystallization of amorphous NdFeB at an elevated temperature in an applied field. The grains in the recrystallized structure are sufficiently small to be single domain grains and therefore possess high coercivity.

EXAMPLE 8.7 **$(BH)_{max}$ FOR A PERMANENT MAGNET** Consider the permanent magnet in Figure 8.42. There is a small air gap of length ℓ_g where there is an external magnetic field that is available to do work. For example, if we were to insert an appropriate coil in the gap and pass a current through the coil, it would rotate as in a moving coil panel meter. Show that the magnetic energy per unit volume stored in the gap is proportional to the maximum value of BH. How does $(BH)_{max}$ vary with the magnetizing field?

SOLUTION

Let ℓ_m be the mean length of the magnet from one end to the other, as shown in Figure 8.42. We assume that the cross-sectional area A is constant throughout. There are no windings around the magnet and no current, $I = 0$. Ampere's law for H involves integrating H along a closed path or around the mean path length $\ell_m + \ell_g$. Suppose that H_m and H_g are the magnetic field intensities in the permanent magnet and in the gap, respectively. Then $H\,d\ell$ integrated around $\ell_m + \ell_g$ is

$$\oint H\,d\ell = H_m\ell_m + H_g\ell_g = 0$$

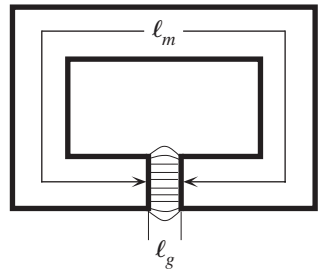


Figure 8.42 A permanent magnet with a small air gap.

so that

$$H_g = -H_m \frac{\ell_m}{\ell_g}$$

and hence

$$B_g = -\mu_o \frac{\ell_m}{\ell_g} H_m \qquad [8.29]$$

B–H for air gap

Equation 8.29 is a relationship between B_g in the gap and H_m in the magnet. In addition, we have the B–H relationship for the magnetic material itself between the magnetic field B_m and intensity H_m in the magnet, that is,

$$B_m = f(H_m) \qquad [8.30]$$

B–H for magnet material

The magnetic flux in the magnet and in the air gap must be continuous. Since we assumed a uniform cross-sectional area, the continuity of flux across the air gap implies that $B_m = B_g$. Thus we need to equate Equation 8.29 to Equation 8.30. Equation 8.29 is a straight line with a negative slope in a B_g versus H_m plot, as shown in Figure 8.43a. Equation 8.30 is, of course, the B–H characteristics of the material. The two intersect at point P, as shown in Figure 8.43a, where $B_g = B_m = B'_m$ and $H_m = H'_m$.

We know that there is magnetic energy in the air gap given by

$$\begin{aligned} E_{\text{mag}} &= (\text{Gap volume})(\text{Magnetic energy density in the gap}) \\ &= (A\ell_g)\left(\frac{1}{2}B_g H_g\right) = \frac{1}{2}(A\ell_g)B'_m H'_m\left(\frac{\ell_m}{\ell_g}\right) \\ &= \frac{1}{2}(A\ell_m)B'_m H'_m \\ &= \frac{1}{2}(\text{Magnet volume})B'_m H'_m \end{aligned} \qquad [8.31]$$

Energy in air gap of a magnet

Thus, the external magnetic energy depends on the magnet volume and the *product* of B'_m and H'_m of the magnet characteristics at the operating point P. For a given magnet size, the magnetic energy in the gap is proportional to the rectangular area $B'_m H'_m$, $OB'_m P H'_m$ in Figure 8.43a, and we have to maximize this area for the best energy extraction. Figure 8.43b

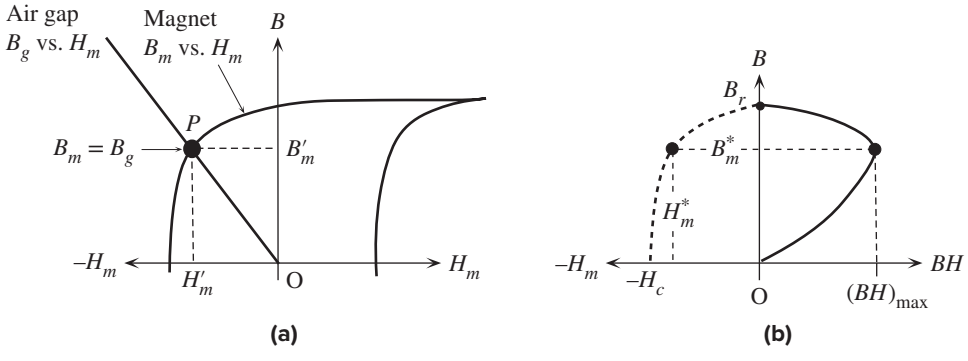


Figure 8.43 (a) Point P represents the operating point of the magnet and determines the magnetic field inside and outside the magnet. (b) Energy density in the gap is proportional to BH, and for a given geometry and size of gap, this is a maximum at a particular magnetic field B^*_m or B^*_g.

shows how the product BH varies with B in a typical magnetic material. BH is maximum at $(BH)_{max}$, when the magnetic field is B_m^* and the field intensity is H_m^*. We can appropriately choose the air-gap size to operate at these values, in which case we will be only limited by the $(BH)_{max}$ available for that magnetic material. It is clear that $(BH)_{max}$ is a good figure of merit for comparing hard magnetic materials. According to Table 8.6, we can extract four to five times more work from a rare earth cobalt magnet than from an Alnico magnet of the same size if we were not limited by economics and weight. It should be mentioned that Equation 8.31 is only approximate as it neglects all fringe fields.

8.9 ENERGY BAND DIAGRAMS AND MAGNETISM

8.9.1 PAULI SPIN PARAMAGNETISM

Consider a paramagnetic metal such as sodium. The paramagnetism arises from the alignment of the spins of conduction electrons with the applied magnetic field. A conduction electron in a metal has an extended wave function and does not orbit any particular metal ion. The conduction electron's magnetic moment arises from the electron spin alone, and $\boldsymbol{\mu}_{spin}$ is in the opposite direction to the spin; $\boldsymbol{\mu}_{spin}$ can be either up $(m_s = -\frac{1}{2})$ or down $(m_s = +\frac{1}{2})$. In the absence of a magnetic field, the energies of magnetic moment up and down states (or wavefunctions) are the same and there are as many electrons with magnetic moment up as there are with magnetic moment down. Figure 8.44a shows the density of states (number of states per unit energy per unit volume) for states with magnetic moment up (↑), denoted as $g_\uparrow(E)$, and for states with magnetic moment down (↓), denoted as $g_\downarrow(E)$. Both states have the same energy and both are equally occupied. All energy levels up to the Fermi energy E_F are occupied as shown in Figure 8.44a. Effectively we are viewing the energy band of the metal as two subbands corresponding to magnetic moment up and down bands. The bands overlap in the absence of a field and are indistinguishable.

Consider what happens in the presence of an applied field B_o along the z direction. If a conduction electron's magnetic moment μ_z is *along* the field (aligned with

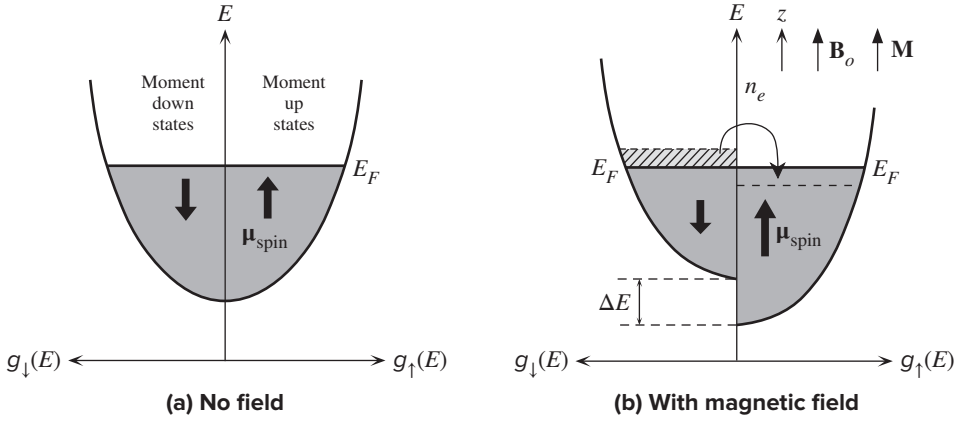


Figure 8.44 Pauli spin paramagnetism in metals due to conduction electrons.

the field), then it has a lower potential energy. Thus, those electron wavefunctions with a magnetic moment up have lower energy, whereas those wavefunctions with a magnetic moment down have higher energy. In the presence of a field B_o, therefore, all states with magnetic moment up, and hence $g_\uparrow(E)$, are lowered in energy by βB_o where β is the Bohr magneton. All states with magnetic moment down, and hence $g_\downarrow(E)$, are raised by βB_o. Both shifts are shown in Figure 8.44b. Those electrons with magnetic moment down near E_F in the $g_\downarrow(E)$ band can now find lower energy states in the $g_\uparrow(E)$ band and hence flip their spins and transfer to the $g_\uparrow(E)$ band. There are now more electrons in states with magnetic moment up in the $g_\uparrow(E)$ band than in the $g_\downarrow(E)$ band. When averaged over all conduction electrons there is now a net magnetic moment per conduction electron along the z direction or the applied field.

To find the net magnetic moment per conduction electron we have to find how many electrons transfer from the $g_\downarrow(E)$ band to the $g_\uparrow(E)$ band. The energy separation ΔE between the magnetic moment down and up states is $2\beta B_o$. All electrons, n_e per unit volume, in the $g_\downarrow(E)$ band around E_F within an energy range $\frac{1}{2}\Delta E$ transfer to the $g_\uparrow(E)$ band. ΔE is small, so n_e is approximately $g_\downarrow(E_F)(\frac{1}{2}\Delta E)$ or $\frac{1}{2}g(E_F)(\frac{1}{2}\Delta E)$ because $g(E_F)$ includes states with spin up and down, that is, $\frac{1}{2}g(E_F) = g_\downarrow(E_F)$. The magnetic moment down band decreases by n_e and the magnetic moment up band increases by n_e and the net magnetic moment per unit volume is

$$M \approx 2n_e\mu_z = 2[\tfrac{1}{2}g(E_F)(\tfrac{1}{2}\Delta E)]\beta$$
$$= 2[\tfrac{1}{2}g(E_F)(\tfrac{1}{2}2\beta B_o)]\beta = \beta^2 g(E_F)B_o$$

Using $B_o = \mu_o H$ and the definition $\chi_m = M/H$, the paramagnetic susceptibility is

Pauli spin paramagnetism

$$\chi_{\text{para}} \approx \mu_o \beta^2 g(E_F) \qquad [8.32]$$

We see that the density of states at the Fermi level determines the susceptibility.

EXAMPLE 8.8

PAULI SPIN PARAMAGNETISM OF SODIUM The Fermi energy of sodium, E_F, is 3.15 eV. Using the density of states $g(E)$ expression for the free conduction electrons in a metal, evaluate the paramagnetic susceptibility of sodium and compare with the experimental value of 9.1×10^{-6}.

SOLUTION

The density of states $g(E)$ in the free electron model is

$$g(E) = (8\pi 2^{1/2})\left(\frac{m_e}{h^2}\right)^{3/2} E^{1/2}$$

We have to evaluate $g(E)$ at the Fermi energy $E = E_F = 3.15$ eV,

$$g(E_F) = (8\pi 2^{1/2})\left(\frac{9.1 \times 10^{-31}}{(6.626 \times 10^{-34})^2}\right)^{3/2}(3.15 \times 1.6 \times 10^{-19})^{1/2} = 7.54 \times 10^{46}\ \text{J}^{-1}\ \text{m}^{-3}$$

Paramagnetic susceptibility is

$$\chi_{\text{para}} = \mu_o \beta^2 g(E_F) = (4\pi \times 10^{-7})(9.27 \times 10^{-24})^2(7.54 \times 10^{46}) = 8.16 \times 10^{-6}$$

We need to subtract the diamagnetic from the calculated paramagnetic susceptibility to obtain the net susceptibility, which would decrease the calculated value slightly. Nonetheless, given the approximate nature of the theory, the calculated value is not far out from the measured value.

8.9.2 ENERGY BAND MODEL OF FERROMAGNETISM

The energy band model of paramagnetism can be extended to explain ferromagnetism. Once we start using the energy band model, we are essentially assigning all the valence (outer shell) electrons of the atoms to a collective sharing among *all* the atoms; they no longer belong to their individual parents. These valence electrons now belong to the whole crystal. (The model is also known as the *itinerant electron model*.)

Recall that in a ferromagnetic crystal there is an internal magnetization, even in the absence of an applied field, due to a net number of unpaired spins; that is, overall, the crystal has more electrons with spins up than with spins down. The reason is the exchange energy, which causes the spin magnetic moments of two electrons to line up parallel to each other so that their energy is lowered in much the same way as Hund's rule works within an atom. In magnetic metals such as Fe, Ni, and Co, there are two bands of interest, the *s*-band and the *d*-band. The two bands overlap but the *s*-band is much wider. We can represent the density of states for magnetic moment up and magnetic moment down states separately. Consider the *d*-band. The density of states $g_{\uparrow}(E)$ for magnetic moment up states is lowered by ΔE with respect to the density of states $g_{\downarrow}(E)$ for magnetic moment down states due to the exchange energy as shown in Figure 8.45a. The energy lowering ΔE for the *s*-band can be neglected as in Figure 8.45b. All the states up to the Fermi energy are occupied. For Fe, the *d*-band magnetic moment up states are filled almost to the top of the band (this band is 96 percent full), and magnetic moment down states are filled roughly halfway. Thus, there are many more electrons with moments up than moments down; put differently there are many electrons that have aligned their spins. The spin magnetic moment alignment of electrons is exactly what is needed to generate a net magnetization. (In some books, the spin magnetic moment down band is sketched lower than the spin magnetic moment up band in contrast to Figure 8.45a. Both sketches are correct since both would also result in a net number of electrons having

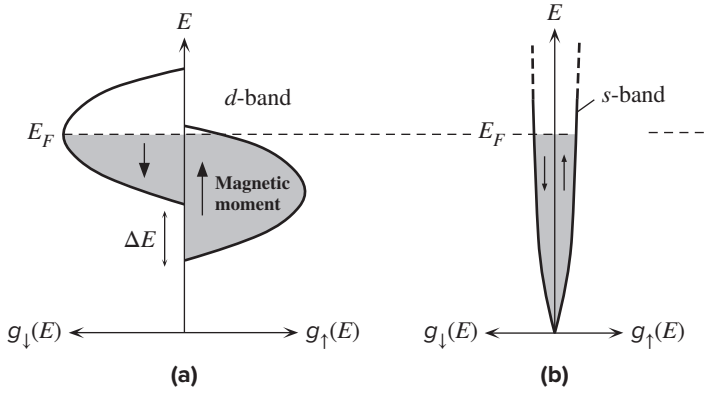


Figure 8.45 Energy band model of ferromagnetism. (a) The split *d*-band. (b) The *s*-band is not affected. The arrows in the bands are spin magnetic moments.

their spins in parallel, and hence a net magnetization within the crystal. Another way to look at it is to realize that there are two bands: one band for the "majority of spins," and another band for the "minority spins.")

The *s*-band is filled up to E_F, and there are almost equal numbers of electrons with up and down moments in this band. The ferromagnetic effect arises from the behavior of electrons mainly in the *d*-band. Electrical conduction, on the other hand, is determined by electrons in the *s*-band. The reason is that the *s*-band is very wide compared with the *d*-band, and the electron effective mass in the *s*-band is very small. Thus, electrons have a much higher mobility in the *s*-band than in the *d*-band. When an *s*-electron is scattered (by phonons, impurities, defects, etc.) into the *d*-band, it does not make any significant contribution to conduction because the drift mobility is very small in this band. The spin of the electron cannot be flipped easily in a scattering process. An *s*-electron with its moment down can be easily scattered into the empty states in the corresponding moment-down *d*-band (there are many empty states at E_F), but the moment-up electron has no states in the moment-up *d*-band into which it can be scattered. Conduction occurs by moment-up electrons; these are the *favored* electrons for conduction.

The band model is particularly useful in explaining the noninteger number of Bohr magnetons that give rise to the ferromagnetism. The isolated Fe atom has six 3*d* and two 4*s* electrons or 8 valence electrons. These electrons in the crystal become shared by all the atoms. If N is the number of atoms per unit volume, then one unit volume of crystal has $8N$ valence electrons. $8N$ electrons enter the *s* and *d* bands, filling states starting from the lowest energy.[8] The exact distribution of electrons depends on how many states are available at each energy as electrons fill the bands. We simply summarize the results of the filling process that is shown in Figure 8.45 for Fe:

$0.3N$ electrons in the moment-up *s*-band (N states available)

$0.3N$ electrons in the moment-down *s*-band (N states available)

$4.8N$ electrons in the moment-up *d*-band ($5N$ states available)

$2.6N$ electrons in the moment-down *d*-band ($5N$ states available)

To find how many electrons have parallel spin magnetic moments, we simply sum the above, which is $2.2N$ moment-up electrons per unit volume or $2.2N$ Bohr magnetons per unit volume, or 2.2 Bohr magnetons per atom. The saturation magnetization M_{sat} is then $(2.2N)\beta$ or 2.2 T. There is therefore a natural explanation for a noninteger number of spins per atom in the band model of ferromagnetism.

8.10 ANISOTROPIC AND GIANT MAGNETORESISTANCE

In general, **magnetoresistance** refers to the change in the resistance of a material (any material) when it is placed in a magnetic field. When a nonmagnetic metal such as copper is placed in a magnetic field, the change in its resistivity, and hence the sample resistance, is so small that it has no real practical use. When a magnetic

[8] $8N$ is used to emphasize that all these valence electrons belong to the crystal, *i.e.*, $8N \approx 7 \times 10^{24}$ cm^{-3}.



Albert Fert (left) and Peter Grünberg (right) were awarded the 2007 Nobel Prize "for the discovery of Giant Magnetoresistance". Alfred Fert is at Université Paris-Sud, Orsay, France and Peter Grünberg is at Forschungszentrum Jülich, Germany. This image was taken in 2007 in the auditorium of the Stockholm University.

© dpa picture alliance archive/Alamy Stock Photo.

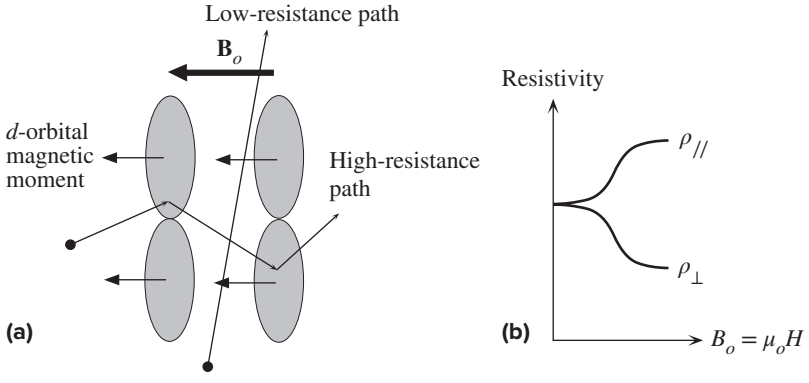


Figure 8.46 (a) The origin of anisotropic magnetoresistance (AMR). The electrons traveling along the field experience more scattering than those traveling perpendicular to the field. (b) Resistivity depends on the current flow direction with respect to the applied magnetic field.

metal, such as iron, is placed in a magnetic field, the change in the resistivity depends on the direction of the current flow with respect to the magnetic field. The resistivity $\rho_{//}$ for current flow parallel to the magnetic field decreases, and the resistivity $\rho_\perp$, perpendicular to the field, increases by roughly the same amount. The change in the resistivity due to the applied magnetic field is *anisotropic* (depends on the direction) and is called **anisotropic magnetoresistance (AMR).** The change in resistivity is limited to a few percent, but, nonetheless, is still useful. The physical origin of this phenomenon is based on the applied field being able to tilt the orbital angular momenta of the 3*d* electrons as shown in Figure 8.46a. The field rotates the 3*d* orbitals, which changes the scattering of the conduction electrons according to their direction of travel; hence $\rho_{//}$ and $\rho_\perp$ are different, as shown in Figure 8.46b.

On the other hand, a very large magnetoresistance, called **giant magnetoresistance (GMR),** has been observed in certain special multilayer structures, which exhibit substantial changes in the resistance (*e.g.*, more than 10 percent) when a magnetic field is applied.[9] The discovery of GMR in 1988 was one of the most

[9] GMR was discovered in the late 1980s by Peter Grünberg (Julich, Germany), and Albert Fert (University of Paris-Sud) and their coworkers. Magnetoresistance itself, however, has been well known, and dates back to Lord Kelvin's experiments in 1857.

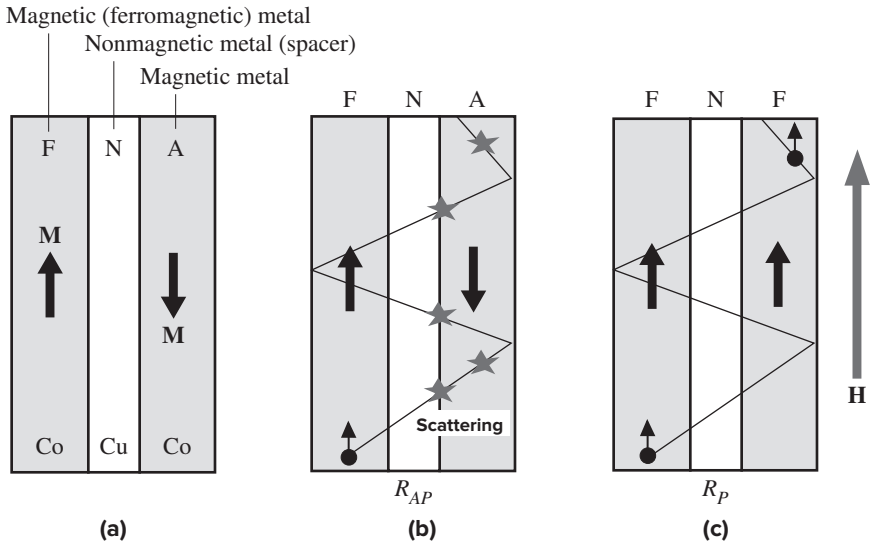


Figure 8.47 A highly simplified view of the principle of the giant magnetoresistance effect. (a) The basic trilayer structure. (b) Antiparallel magnetic layers with high resistance R_{AP}. (c) An external field aligns layers; parallel alignment has a lower resistance R_P.

important developments in magnetic devices. GMR based devices are widely used in the read heads of hard disk drives, and also in various magnetic field sensors.

The special multilayer structure in its simplest form has two **ferromagnetic layers** (such as Fe or Co or their alloys, etc.) separated by a nonmagnetic transition metal layer (such as Cu), called the **spacer,** as shown in Figure 8.47a. The magnetic layers are thin (less than 10 nm), and the nonmagnetic layer is even thinner. The magnetizations of the two ferromagnetic layers are not random; they depend on the thickness of the spacer because the two layers are "coupled" indirectly through this thin spacer.[10] In the absence of an external field, two magnetic layers are coupled in such a way that their magnetizations are *antiparallel* or in opposite directions; this arrangement is also called an *antiferromagnetically* coupled configuration. We will use the notation FNA to represent the antiparallel configuration, where N stands for the nonmagnetic metal.

We can apply an external magnetic field to one of the layers and rotate its magnetization so that the two magnetizations are now in parallel as in Figure 8.47c. This parallel configuration is frequently called *ferromagnetically* coupled layers and is denoted as FNF. The two structures have a *giant* difference in their resistances, hence the term giant magnetoresistance. The resistance of the antiparallel FNA in Figure 8.47b structure is much higher than that of the parallel structure FNF in Figure 8.47c.

The current flow through this multilayer structure (whether along or perpendicular to the layers) will involve electrons crossing from one layer to another, passing through

[10] The physics of the coupling process between the two magnetic layers is an indirect exchange interaction, the details of which are not needed to understand the basics of the GMR phenomenon.

the interfaces. Recall that it is the electrons around the Fermi energy that are involved in the conduction and that their mean speed is orders of magnitude larger than the drift velocity. The electron trajectories are therefore not parallel to the current flow (and should not be confused with current flow lines).

Consider the antiparallel FNA structure. The magnetic moment up electron in the first magnetic layer is the *favored* conduction electron; that is, it suffers very little scattering. However, when this moment-up electron arrives at the A layer in which the magnetization is reversed, it finds itself with the wrong spin or wrong moment. It is now an *unfavored* electron and is subject to scattering. Thus, the moment-up electron suffers scattering not only in the bulk of A but, more significantly, as it crosses the N-layer into the A-layer, that is, at the interface as in Figure 8.47b. The antiparallel FNA structure therefore has a high resistance, denoted as R_{AP}. In contrast, when the magnetizations are parallel, the moment-up electron is the favored electron in both the layers and experiences very little scattering. The resistance R_P of this parallel (FNF) structure is smaller than R_{AP} ($R_P < R_{AP}$). The difference in the resistances R_P and R_{AP} in this simple trilayer is roughly 10 percent or less. But, in multilayered structures, which have a series of alternating magnetic and nonmagnetic layers (*e.g.*, 50 or more magnetic and nonmagnetic alternating layers as in FNANFANFA . . .), the change in the resistance can be impressively large, exceeding 100 percent at low temperature and 60–80 percent at room temperature.

The GMR effect is often measured by quoting the change in the resistance with respect to R_P,

Giant magnetoresistance effect

$$\left(\frac{\Delta R}{R_p}\right)_{\text{GMR}} = \frac{R_{\text{AP}} - R_P}{R_p} \qquad [8.33]$$

Further, the magnetoresistance effect can be measured either by passing a current that flows in the plane of the layers or perpendicular to the plane. Most experiments use the first one, in what is known as **current in plane (CIP)** measurements; but the biggest change, however, is observed for currents perpendicular to the plane of the layers. Table 8.7 summarizes typically reported $\Delta R/R_P$ values for the GMR effect in simple trilayers and multilayers.

The structures with antiparallel and parallel magnetic alignments are obviously two extreme cases. If the angle between the magnetization vectors $\mathbf{M}_1$ and $\mathbf{M}_2$ of

Table 8.7 GMR effect in trilayers and multilayers

Sample	Structure and Layer Thicknesses	$\Delta R/R_P$ (%)	Temperature (K)
CoFe/CAgCu/CoFe	Trilayer	4–7	300
NiFe/Cu/Co	Trilayer, 10/2.5/2.2 nm (spin valve)	4.6	300
$Co_{90}Fe_{10}/Cu/Co_{90}Fe_{10}$	Trilayer, 4/2.5/0.8 nm (spin valve)	7	300
$[Co/Cu]_{100}$	100 layers of Co/Cu, 1 nm / 1 nm	80	300
$[Co/Co]_{60}$	60 layers Co/Cu, 0.8 nm / 0.83 nm	115	4.2

Data from Grünberg, P., *Sensors and Actuators A,* 91, 153, 2001.

the two magnetic layers is θ, then the resistance of the structure depends on θ, with the minimum for $\theta = 0$ (FNF) and the maximum for $\theta = 180°$ (FNA) as shown in Figure 8.48. The fractional change in the resistance depends on θ as

GMR and relative magnetizations of magnetic layers

$$\frac{\Delta R}{R_P} = \left(\frac{\Delta R}{R_P}\right)_{\max} \frac{1 - \cos\theta}{2} \qquad [8.34]$$

As expected, the change is maximum when $\theta = 180°$.

One of the best applications of GMR is in a **spin valve,** in which the current flow is controlled by an external applied magnetic field. Stated differently, the resistance of the valve is controlled by an applied field. Figure 8.49a shows one possible simple spin valve structure. The magnetization of the Co magnetic layer is fixed, that is, *pinned,* by having this layer next to an antiferromagnetic layer, called the *pinning layer*. The exchange interaction between the ferromagnetic Co layer and the antiferromagnetic CoMn layer effectively pins the direction of the Co layer; it takes an enormous field to change the magnetization of the Co layer. A Cu spacer layer separates the Co and the next magnetic FeNi layer. The FeNi layer is called the *free*

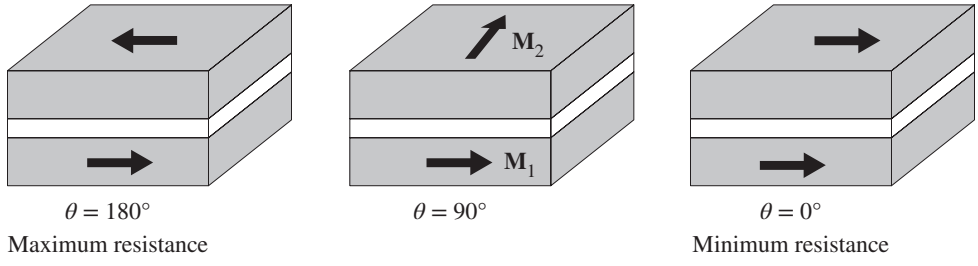


Figure 8.48 Resistance of the multilayer structure depends on the relative orientations of magnetization in the two magnetic layers.

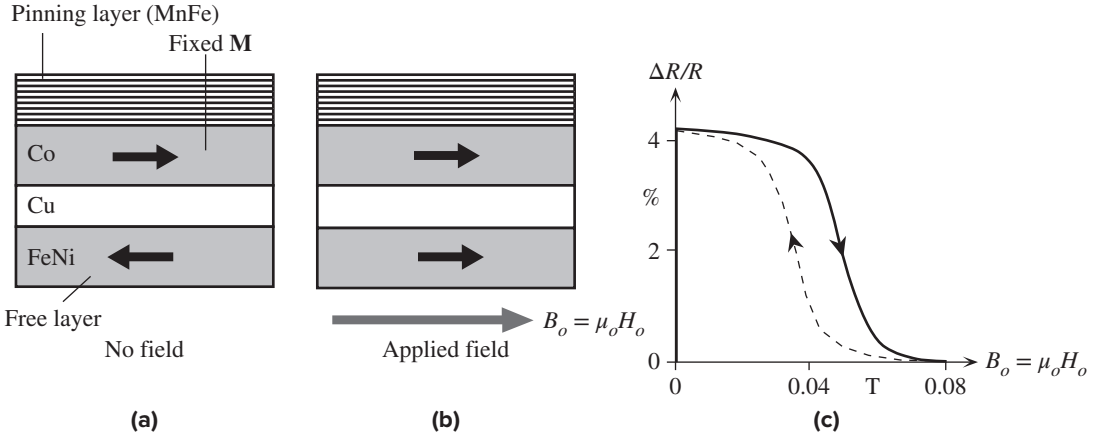


Figure 8.49 Principle of the spin valve. (a) No applied field. (b) Applied field has fully oriented the free-layer magnetization. (c) Resistance change versus applied magnetic field (schematic) for a FeNi/Cu/FeNi spin valve.

layer because its magnetization can be changed by an external magnetic field. Normally, in the absence of a field, the magnetization of the FeNi layer is antiparallel to the Co layer, and the structure has a high resistance R_{AP}. An applied external field $B_o = \mu_o H$ can rotate the FeNi layer's magnetization and can easily align FeNi's magnetization fully in parallel with that of Co so that the resistance becomes minimum, *i.e.*, R_P as in Figure 8.49b. It is clear that the external field can be used to control the flow of current through this structure. (The name spin valve reflects the fact that the valve operation relies on the spin of the electrons.) The free layer should be relatively soft to be able to respond to the applied field, whereas the pinned layer should have sufficient coercivity not to lose its magnetization. Figure 8.49c shows a typical magnetoresistance versus applied field characteristics for one particular type of spin valve. The spin valve exhibits hysteresis; that is, the signal ΔR versus H depends on the direction of magnetization as shown in the figure.

8.11 MAGNETIC RECORDING MATERIALS

8.11.1 GENERAL PRINCIPLES OF MAGNETIC RECORDING

Outside electric machinery (mainly rotating machines and transformers), magnetic materials are most widely used in magnetic recording media to store information in digital form. The deep disappointment of accidentally losing valuable stored information on the hard drive of one's computer is well known to most computer users. Magnetic materials in magnetic recording essentially fall into three categories: those used in magnetic heads to write (record), those used in read sensors, and those used in magnetic media in which the information is stored either permanently or until the next write requirement.

As a very simple example, consider magnetic recording of digital data (1s and 0s) on a magnetic disk in a hard disk drive (HDD), as shown schematically in Figure 8.50.[11] The information storage medium, that is the recording medium, is a thin film of magnetic material coated, for example, by sputtering, on a disk substrate, which rotates inside the hard drive. The substrate is called the **platter.** The information is recorded as magnetization patterns on this thin-film magnetic medium. The digital information is converted into current pulses that flow into a miniature electromagnet write element with a very small air gap. This gapped core electromagnet is called the **inductive write head** or **element.** The current modulates the magnetic field intensity in the core of the electromagnet and hence the field in the gap and around it. The recording of information is achieved by the **fringing magnetic field** around the gap region, magnetizing the magnetic medium passing under the head at a constant speed. As the fringing field changes according to the current signal, so does the magnetization of the regions that pass under the write head. Thus, the electrical signal is stored as a spatial magnetic pattern in the magnetic film in circular tracks. The fringing fields of the write head modulate the magnetization in the thin magnetic film in the direction of motion; that is, in a circular path in a disc medium.

[11] See for example Chapters 4 and 49 in the Springer Handbook of Electronic and Photonic Materials, 2nd Edition, ed. S. Kasap and P. Capper, Springer Science, New York, 2017.

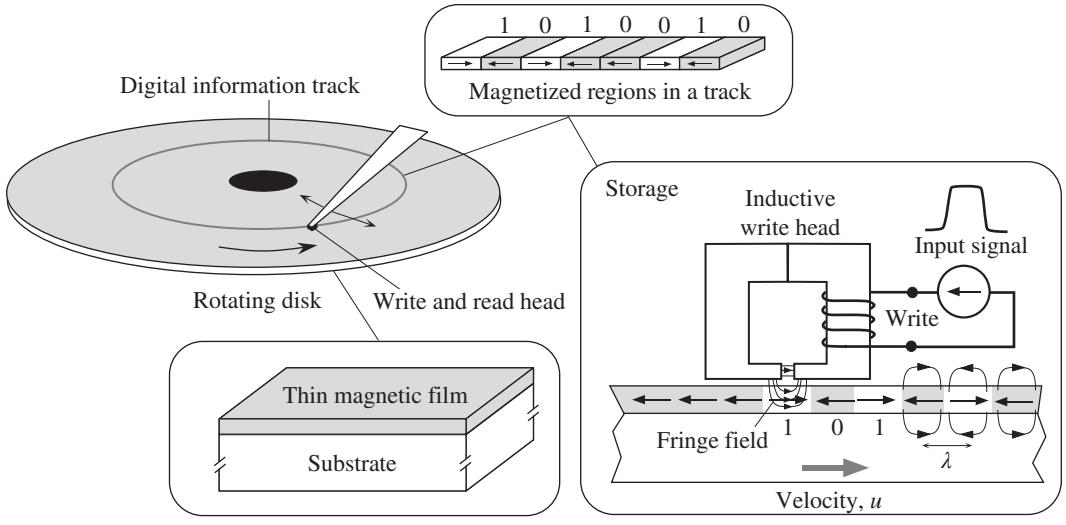


Figure 8.50 The basic principle of magnetic data storage on a disc inside a hard drive. The disk substrate is called the platter. There may be several platters with write/read heads on both sides of each disk.

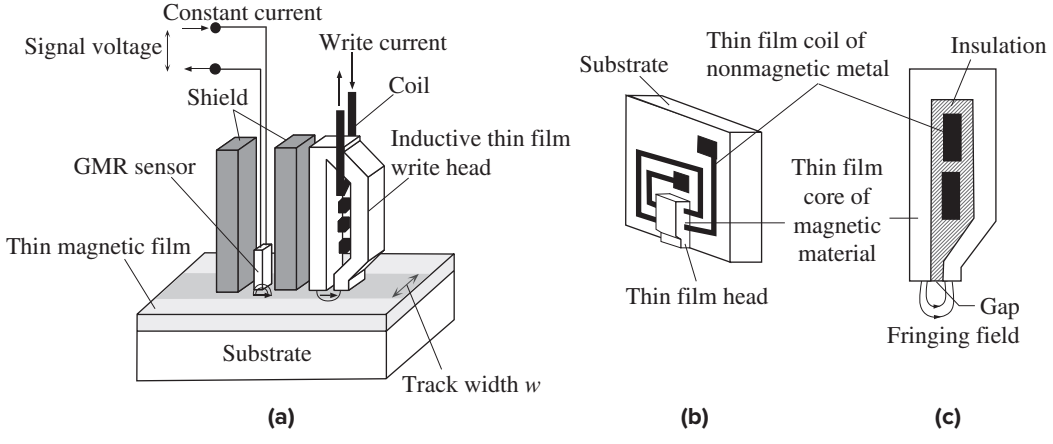


Figure 8.51 (a) A schematic illustration of the write and read heads with magnetic shielding. The write and read elements would be integrated into a single head. The GMR sensor is actually very much smaller than the inductive write head. (b) A thin film write head. (c) Magnified cross section of the write head. Usually there are more coil turns than two.

This type of magnetic information storage is called **longitudinal magnetic recording (LMR).**

The information that is written in the thin film as different orientations of magnetization is sensed by a **read element,** such as a **giant magneto resistance** (GMR) **sensor.** Figure 8.51a shows how an inductive head and a GMR sensor are used to write and read the magnetic information in the thin film. Both the write and the read heads are in a single compact assembly that moves radially across the rotating disk



Inside of a typical hard disk drive used in a laptop computer. | Photo by S. Kasap.

to write or read the information into tracks, called **magnetic bit tracks,** on the magnetic medium as shown in Figure 8.50. The read-write head is on an air bearing and the head to thin magnetic film separation is roughly 10 nm or less. GMR sensor has a width that is something like 50 nm or less (∼1000 times thinner than the human hair) so that we can squeeze more information into a given area on the magnetic storage medium.

The inductive write head is normally a **thin-film head,** which has a very small width as shown in Figure 8.51b and c. Consequently, the information can be written into a very small area on the magnetic storage medium. The write head shown in Figure 8.51b and c are fabricated from films of various ferromagnetic metals or ferrite alloys that have sufficiently small eddy current losses to be useable at high frequencies. The head is manufactured by using typical thin film deposition techniques. The magnetic core is in the form of a thin film whose thickness is a few microns and whose width determines the track width. The gap at the end of the core has the same width as the core, but its spacing is very small (*e.g.*, 100 nm) and generates the necessary fringing field. A spiral-type coil made by depositing a nonmagnetic metal thin film threads the core. The magnetic core is like a U-shaped core that is threaded by the metal strips of the coil. If the core is a metallic material, the coil metal is appropriately insulated from it by thin films of insulation. The width w of the bit-track is determined by the width of the write head in Figure 8.51b, and is typically 100 nm or less.

The resistance of the GMR sensor depends on the external magnetic field, as explained in Section 8.10. In this case, the field that influences the GMR sensor comes from that of the magnetized patch of the disk that is under the GMR sensor. The principle of the GMR is shown in Figure 8.49. The GMR sensor is a multilayered thin-film device whose resistance changes by roughly 10 percent or so in response to an applied field. This change in the resistance generates the read signal. The voltage from the sensor is maximum on locations on the film where magnetic field changes sharply (dB/dx is largest) and this corresponds to the transition region from one-bit to the next. Normally a constant current is passed through the GMR sensor, and the read signal is the voltage variation across the sensor; this voltage is due to the resistance variation induced by the field from the magnetization pattern under the sensor. Modern GMR sensors are operated in the **current perpendicular**

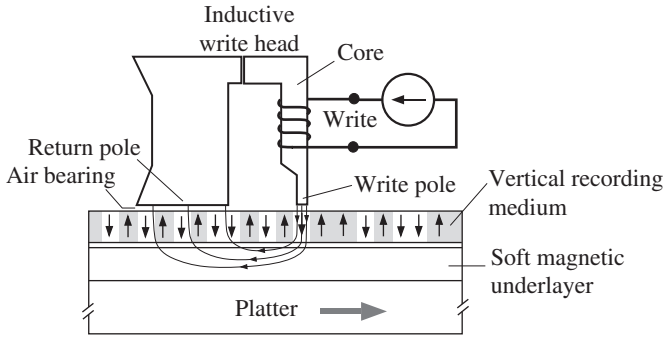


Figure 8.52 (a) A simplified illustration of perpendicular magnetic recording. (b) The magnetically soft underlayer (SUL) provides an image of opposite polarity that increases the magnetizing field though the thin film.

to the plane (CPP) mode because the current is passed perpendicular to the thin-film layers in the GMR device (Figure 8.47).

In **perpendicular magnetic recording** (PMR), the stored information in the magnetic film corresponds to magnetization directions that are perpendicular to the film surface and the disk velocity, as shown in Figure 8.52; induced **M** is either up or down. The easy direction of the grains are also perpendicular. More bits can be packed to a given surface area, for reasons explained below, and many recent magnetic HDDs use this technology. The write operation in this case is distinctly different than that in longitudinal storage. There is an inductive write head with a narrow "write pole" that brings the magnetic flux onto the film.

The magnetic thin film has a magnetically soft underlayer (SUL) that can be easily magnetized. Remember also that magnetic flux prefers to flow through high permeability regions in a medium. Thus, the flux flows from the write pole to the underlayer and then to the return pole, which has a large cross sectional area as shown in Figure 8.52.[12] It is clear that the magnetic field lines pass through the whole film perpendicularly, and the write operation does not depend on the fringe field; a distinct advantage. The magnetizing field is strong under the write pole where the cross sectional area is small, but it is weak under the return pole. The strong field at the write pole is able to magnetize the thin film and write the information, but the weak field under the return pole cannot erase this magnetization.

The magnetic thin film for storage is usually a heterogeneous granular medium. The thin film has small crystalline grains and a region between the grains that is nonmagnetic as shown in Figure 8.53a. For example, the crystalline grains could be CoCrPt and the intergrain region may be an amorphous oxide such as SiO_2 or a mixture of SiO_2–TiO_2. Notice that the information boundary between the patches is rugged because it follows the grain boundaries. If we did not have a magnetic insulation (a nonmagnetic medium) between the grains, then the exchange interaction between the atoms in two neighboring grains would force the two grains to align their magnetizations; we would not be able to magnetize a small patch on the track. The nonmagnetic intergrain region is essential.

[12] To understand the true function of the soft underlayer, we need to go into the fact that the write pole (say N at one instant) sees an induced opposite image pole (S) in the underlayer in the same way a positive charge $+Q$ on an infinite dielectric medium sees an opposite image charge $-Q$ within the dielectric. The field lines flow $+Q$ to $-Q$. It is clear though the field from the write pole cuts through the magnetic film.

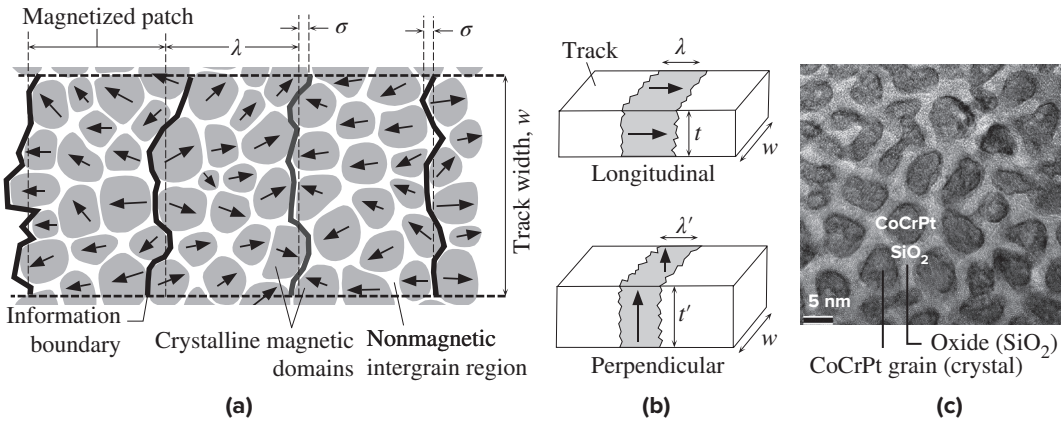


Figure 8.53 (a) A simplified view of longitudinal recording track with magnetized crystalline grains in a track. σ is the rms variation in the position of the boundary between two neighboring bits. (b) The definitions of λ, w and t involved in a bit-track with a magnetized one-bit volume in gray. (c) Transmission electron microscope image of a granular magnetic thin film medium for high density storage.
| (c) Courtesy of Kazuhiro Hono.

How small can we make one-bit patch (the magnetized region for one bit) in Figure 8.53a to store as much information as possible? Consider longitudinal recording. Let λ be the length of a one-bit patch, t be the thickness of the film and w be the track width in which information is stored as in Figure 8.53b. The volume of one-bit is λwt. Clearly, we would like λw to be as small as possible to increase the storage capacity. One possibility is to reduce the number of grains in the one-bit volume and hence the patch area. The signal-to-noise ratio (SNR) in a *granular* magnetic recording medium depends on the number of grains (domains) N in the one-bit volume (Figure 8.53a). The more grains, the higher the signal is, that is the signal is proportional to N. The noise depends on how many grains would have the wrong magnetization and is proportional to[13] $\sqrt{N}$. In terms of commonly used decibels (dB), this is

Granular noise in a recording medium

$$\text{SNR}_{\text{grain}} \approx 20 \log \sqrt{N} = 10 \log N \qquad [8.35]$$

A 20 dB SNR implies that a bit-volume should have 100 grains, which we can take very roughly as the number of minimum grains N_{min} we need; some authors use a higher N_{min}. It is also obvious that we cannot simply reduce λw to increase the storage capacity because we need at least N_{min} grains in the bit-volume. In perpendicular recording, we can reduce λw and increase t, keeping the bit volume the same, which is one of its advantages.

The boundary between two neighboring one-bit patches is quite rugged, zigzagged, because the bit boundary follows the surfaces of the grains with the same

[13] We can understand this with an analogy to the random walk example (impurity diffusion) in Section 1.8.2. If I take N random steps, my root mean square distance from the origin is proportional to $\sqrt{N}$, which is noise because the direction is random. (Remember that this is an analogy, not an explanation of the physics.) The increase in SNR with smaller grains was particularly well known in the era of photographic films.

magnetization as shown in Figure 8.53a. The root mean square variation σ in the position of the boundary represents another form of noise, **jitter noise,** inherent in a granular medium even if we had a perfect write head. The jitter noise σ increases with grain size d, and a very rough estimate gives $\sigma \approx d/3$. The signal is proportional to the bit length λ whereas noise is proportional to σ so the SNR ratio will be roughly proportional to λ/σ, that is[14]

$$\text{SNR}_{\text{jitter}} \approx 20 \log(\lambda/\sigma) \quad [8.36]$$

Approximate jitter noise

It is desirable to keep σ less than 10 percent of the bit length λ. We need to adjust our $N_{\min}$ above to reflect both granular and jitter noise because both contribute significantly to the overall SNR.

Both granular and jitter noise are important limitations in using granular media as a magnetic storage medium. We can try to reduce the grain size, and hence σ, as we try and shrink the bit-volume, but there is still another fundamental limit.

We know that the energy involved in thermal fluctuations is roughly kT. The energy involved in rotating the magnetization **M** in a magnetized grain (essentially, a domain) from one direction to the opposite direction (changing 1 to 0 or vice versa) depends on the magnetocrystalline anisotropy energy, measured in energy per unit domain volume (J m^{-3}), which was defined in Section 8.5.2. In the present case, this energy is given a special name called **uniaxial magnetocrystalline energy** K_u due to the HCP crystal structure and the shape of the grains. Both influence K_u. Thus, if V_{grain} is the average grain volume, the energy needed to rotate **M** in a grain is $K_u V_{\text{grain}}$ and this must be much greater than kT, say by a numerical factor of r (*e.g.*, $r = 40 - 60$) for a thermally stable operation. We need at least $K_u V_{\text{grain}} \approx rkT$. We cannot therefore expect to reduce the grain volume as much as we like because of this fundamental limit. The advantage of perpendicular recording is that the magnetizing field is within the main magnetic flux through the whole thickness of the film and it is stronger than in longitudinal recording; see Figure 8.52. We can therefore increase the film thickness from t to t' and shrink λ to λ' as in Figure 8.53b. More importantly, we can use a magnetic medium that has a higher K_u because the magnetizing field is stronger. This means V_{grain} can be smaller. Consequently, we can reduce the grain size (d) and still have sufficient $N_{\min}$ number of grains within a one-bit volume to avoid SNR problems.

When the grain size becomes so small that thermal energy (*i.e.*, thermal fluctuations) can easily randomize the alignments of magnetized grains, then basically the medium exhibits paramagnetic behavior as described in Section 8.2.2. This is called the **superparamagnetic state,** and represents a fundamental limit on how small we can make the domains.

8.11.2 MATERIALS FOR MAGNETIC STORAGE

The magnetic recording medium in a hard disk drive (Figure 8.50) is in the form of a magnetic thin film deposited onto hard substrate, for example, an aluminum disk.

[14] See, for example, D. Weller and T. McDaniel (Seagate), "Media for Extremely High Density Recording" in Advanced Magnetic Nanostructures, Ed D. Sellmyer and R. Skomski, Springer, New York, 2006, Chapter 11, pp. 295–325.

Table 8.8 Selected examples of materials for perpendicular magnetic recording (PMR)

Medium	Example Material	$\mu_o H_c$ (T)	$\mu_o M_r$ (T)	B_{sat} (T)	K_u (kJ m^{-3})	Comment
Recording	CoCrPt–oxide, CoCrPtB–oxide	0.4–0.5	0.60–0.65		250–500	Semihard magnetic thin film, about 20 nm. Deposited by sputtering.
Write pole	FeCo alloy			2–2.4		Generates a large field entering into the recording medium.
Soft underlayer	CoTaZr			1.4		μ_r = 600. Amorphous; thickness less than 100 nm; has low noise.

NOTE: K_u is the uniaxial magnetocrystalline anisotropy energy. Data collected from various sources.

The deposition of the magnetic thin film involves vacuum deposition techniques such as sputtering, electron beam evaporation or electroplating. Typical film thicknesses are less than 30 nm. The film is not a single phase homogenous magnetic medium. The magnetic material consists of crystalline grains (at present roughly 10 nm in size) separated by a nonmagnetic amorphous region that is usually an oxide as mentioned above and shown in Figure 8.53c; it is a phase-separated medium. Each grain is a single magnetic domain inasmuch as the grains are too small to support several domains. Table 8.8 summarizes the properties of a typical thin-film storage medium. The film must be such that it is able to retain the spatial magnetization pattern written on it after it has passed the write head. This requires high remanent magnetization M_r. High remanent magnetization is also important in the reading process because the magnetic flux that penetrates into the sensor depends on this remanent magnetization, given a particular speed of motion under the read head. Thus, the read operation also requires a medium with high M_r. Further, it should be difficult to undesirably erase the magnetic information on the disk by demagnetizing it under stray fields, and this requires high coercivity H_c. However, H_c cannot be too high because, otherwise, the inductive head will not be able to change the magnetization **M** of a magnetic grain; we need a semihard magnetic medium. Most thin films are alloys of Co because Co has a high degree of magnetocrystalline anisotropy energy and hence good coercivity H_c. Alloying Co with Cr provides good corrosion resistance and increases H_c. Alloying with Pt also increases H_c. The desired film properties can usually be obtained by alloying Co with other elements and optimizing the deposition conditions; for example CoCrPt–SiO_2 is considered to be a good magnetic storage medium but there are many others. The crystal grains have the HCP structure, which has a large K_u.

The magnetically soft underlayer (SUL) beneath the magnetic thin film in Figure 8.52 has to be sufficiently soft to be easily magnetized so that the magnetic field lines from the write head, after passing through the thin film, will be restricted to this layer. Consequently we need a soft medium with a high μ_r, *e.g.*, greater than 100, and a high M_{sat} that should match that of the write pole. There are several soft

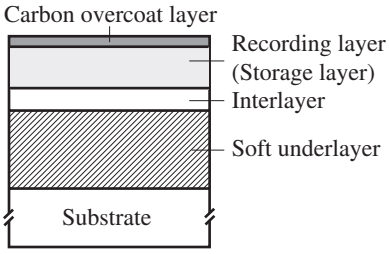


Figure 8.54 The basic multilayered structure for information storage in perpendicular magnetic recording.

magnetic media that serve as an SUL and a typical example is listed in Table 8.8. There is usually a thin **interlayer** between the storage thin film and the SUL, as shown in Figure 8.54, to magnetically separate the two layers. The interlayer can also be used to control the grain orientations and size distribution in the recording film. Further, the recording film itself may consist of several thin layers to tune the magnetic properties of this medium. The interlayer may have two sublayers to tune its properties as well. The current materials research on perpendicular recording involves optimizing the interlayer and the soft underlayer towards higher capacity. There is also a very thin top overcoat layer, usually carbon, to protect the magnetic thin film's surface.

The thin film inductive recording head in Figure 8.51c must be able to produce a strong magnetizing field. The thin film coil is normally Cu and the oxide insulation maybe SiO_2 or Al_2O_3. The magnetic core is a soft medium that can be easily magnetized such as an NiFe alloy. The narrow pole at the tip of the write head above the thin film storage medium has a large M_{sat} or B_{sat} (Figure 8.32). For example CoFe alloys can have B_{sat} around 2.4 T. What is important in recording digital information is that the write head should generate a strong magnetizing field and whose direction can be reversed by the coil. Table 8.8 summarizes some of the properties of materials involved in perpendicular magnetic recording.

So far we have only considered a granular magnetic recording medium. Within this material system, a one-bit volume has many independent grains that have to be magnetized. There is a limit to the bit-size as we need to have a certain number of grains (N_{min}); put differently, the grain size cannot be arbitrarily small. Suppose that we fabricate a recording medium in which a bit is a well-defined nanostructure, and these nanostructures are patterned to form a *periodic array* of "isolated magnetic islands" as shown in Figure 8.55a. An SEM image of such a **bit-patterned recording medium** (BPRM) is shown in Figure 8.55b. Clearly, we no longer have a granular medium and Equation 8.35 does not apply. Indeed, intuitively, we can expect an N-fold increase in storage capacity, breaking through the limits of multigrain media. Further, we can develop write and read techniques that involve synchronization with the periodicity in the bit-pattern; obviously such new techniques would require a more demanding technology for the inductive write head. This is the advantage of BPRM. The array of magnetic bits in Figure 8.55b have a pitch of 35 nm, which corresponds roughly to 0.5 Tb in^{-2}, a significant jump in areal storage density. The magnetic medium in this case is a multilayer of Co/Pd films deposited by sputtering on a patterned array of SO_2 nanoposts. Magnetic bit arrays of smaller

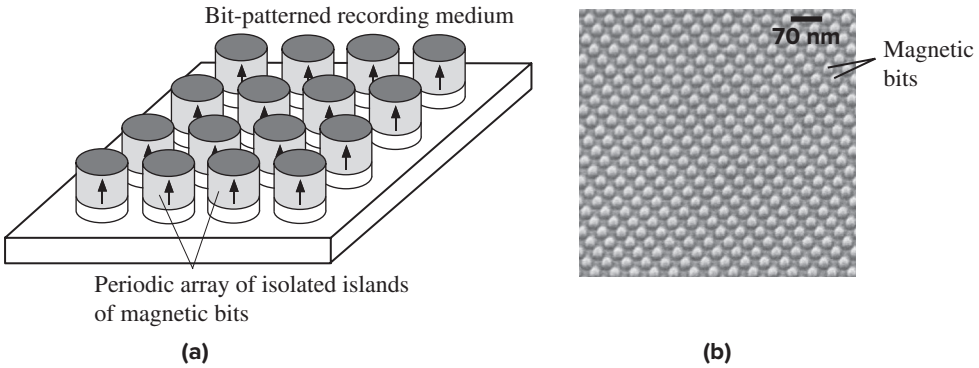


Figure 8.55 (a) A simple bit-patterned recording medium, which is a periodic array of magnetic islands. (b) SEM image of a particular bit-patterned medium. Capping each post is a multilayer of Co/Pd material deposited by sputtering. Each post represents a magnetic bit.
(b) Courtesy of Joel K.W. Yang, Singapore University of Technology and Design.

pitches have also been recorded with areal bit densities over 1 Tb in^{-2}. While the BPRM has the potential for a much higher areal density, the actual techniques used for writing and reading the bits are quite different. Further, the BPRM is not free of imperfections such as variations in the periodicity of the array of magnetic bits, which is essentially noise within this material system. Nonetheless, such BPRM have been shown to have potential areal recording densities 1–1.5 Tb in^{-2}, a factor of 10 higher than granular PRM.

EXAMPLE 8.9 **AREAL DENSITY IN GRANULAR RECORDING MEDIA** Consider a longitudinal recording medium as in Figure 8.53a. Suppose that the magnetic grains have a uniaxial magnetocrystalline anisotropy energy K_u of 500 kJ m^{-3}. The stability of magnetized grains against thermal fluctuations means that the energy involved in rotating the magnetization **M** of a grain in the wrong direction must be much greater than the thermal energy kT. Taking the ratio $r = 50$ in $K_u V_{\text{grain}} \approx rkT$ we find the minimum volume for a grain

$$V_{\text{grain}} \approx (50)(0.0259 \text{ eV})(1.602 \times 10^{-19} \text{ J/eV})/(500 \times 10^3 \text{ J m}^{-3}) = 4.15 \times 10^{-25} \text{ m}^3 \quad \text{or} \quad 415 \text{ nm}^3.$$

If d is the mean grain size, we can take d^3 to very roughly represent the grain volume. Thus, $d^3 \approx V_{\text{grain}}$ so that $d \approx 7.5$ nm.

The one-bit volume will have N grains. If p is the volume fraction (packing factor) of the grains in the film structure in Figure 8.53c, only the volume $p(\lambda wt)$ is occupied by N magnetic grains. Thus,

$$p(\lambda wt) = NV_{\text{grain}} \qquad [8.37]$$

Areal bit density in a track in granular media

from which we can find λw, the area of one-bit, and hence the areal bit density in a track

$$D_{\text{bit}} = \text{Areal bit density} = \frac{1}{\lambda w} = \frac{pt}{NV_{\text{grain}}} = \frac{ptK_u}{NrkT} \qquad [8.38]$$

This expression ignores the fact that the tracks are not side by side on the disk but have a guard band between them. The actual D_{bit} for the disk will be about 70 percent of the above

value. It is clear from Equation 8.38 that we can increase D_{bit} by increasing K_u and t, or reducing N; but N is limited by the acceptable SNR.

Further, as an estimate, we can take the packing factor $p = 0.85$, $w = 100$ nm (write head width), $t = 20$ nm (film thickness), $N = 200$ in Equations 8.37 to find $\lambda = 49$ nm, which is the size of one-bit. We can now use Equation 8.38 with $\lambda = 49$ nm and $w = 100$ nm to find $D_{info} = 205$ bits μm^{-2} or 132 Gb in^{-2} in tracks and roughly 92.4 Gb in^{-2} on the disk.

Further, from Equation 8.35,

$$SNR_{grain} = 10 \log N = 23.0 \text{ dB}.$$

Taking $\sigma \approx d/3 = 2.5$ nm, from Equation 8.36,

$$SNR_{jitter} \approx 20 \log(\lambda/\sigma) = 25.8 \text{ dB}.$$

The importance of K_u should be clearly apparent. There are magnetic media with higher K_u values than 500 kJ m^{-3} used in this example. The above estimate calculations show that there is a fundamental limit to how much information can be stored in a granular recording medium.

8.12 SUPERCONDUCTIVITY

8.12.1 ZERO RESISTANCE AND THE MEISSNER EFFECT

In 1911 Kamerlingh Onnes at the University of Leiden in Holland observed that when a sample of mercury is cooled to below 4.2 K, its resistivity totally vanishes and the material behaves as a **superconductor,** exhibiting no resistance to current flow. Other experiments since then have shown that there are many such substances, not simply metals, that exhibit superconductivity when cooled below a **critical temperature** T_c that depends on the material. On the other hand, there are also many conductors, including some with the highest conductivities such as silver, gold, and copper, that do not exhibit superconductivity. The resistivity of these **normal conductors** at low temperatures is limited by scattering from impurities and crystal defects and saturates at a finite value determined by the residual resistivity. The two distinctly different types of behavior are depicted in Figure 8.56. Between 1911 and 1986, many different metals and metal alloys had been studied, and the highest recorded critical temperature was about 23 K in a niobium–germanium compound

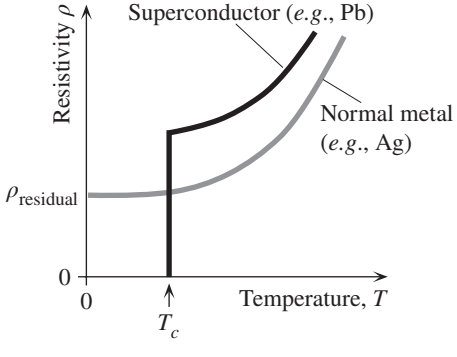


Figure 8.56 A superconductor such as lead evinces a transition to zero resistivity at a critical temperature T_c (7.2 K for Pb).

A normal conductor such as silver exhibits residual resistivity down to lowest temperatures.



In 1986 J. George Bednorz (right) and K. Alex Müller, at IBM Research Laboratories in Zurich, discovered that a copper oxide based ceramic-type compound (La-Ba-Cu-O) which normally has high resistivity becomes superconducting when cooled below 35 K. This Nobel prize winning discovery opened a new era of high-temperature-superconductivity research; now there are various ceramic compounds that are superconducting above the liquid nitrogen (an inexpensive cryogen) temperature (77 K).

© Emilio Segre Visual Archives/American Institute of Physics/Science Source.

(Nb_3Ge) whose superconductivity was discovered in the early 1970s. In 1986 Bednorz and Müller, at IBM Research Laboratories in Zürich, discovered that a copper oxide–based ceramic-type compound La–Ba–Cu–O, which normally has high resistivity, becomes superconducting when cooled below 35 K. Following this Nobel prize–winning discovery, a variety of copper oxide–based compounds (called cuprate ceramics) have been synthesized and studied. In 1987 it was found that yttrium barium copper oxide (Y–Ba–Cu–O) becomes superconducting at a critical temperature of 95 K, which is above the boiling point of nitrogen (77 K). This discovery was particularly significant because liquid nitrogen is an inexpensive cryogent that is readily liquified and easy to use compared with cryogent liquids that had to be used in the past (liquid helium). At present the highest critical temperature for a superconductor is around 130 K (−143 °C) for Hg–Ba–Ca–Cu–O. These superconductors with T_c above ∼30 K are now typically referred as **high-T_c superconductors.** The quest for a near-room-temperature superconductor goes on, with many scientists around the world trying different materials, or synthesizing them, to raise T_c even higher. There are already commercial devices utilizing high-T_c superconductors, for example, thin-film SQUIDs[15] that can accurately measure very small magnetic fluxes, high-Q filters, resonant cavities in microwave communications, superconducting power cables and superconducting fault current limiters.

The vanishing of resistivity is not the only characteristic of a superconductor. A superconductor cannot be viewed simply as a substance that has infinite conductivity below its critical temperature. A superconductor below its critical temperature expels all the magnetic field from the bulk of the sample as if it were a perfectly diamagnetic substance. This phenomenon is known as the **Meissner effect.** Suppose that we place a superconducting material in a magnetic field above T_c. The magnetic field lines will penetrate the sample, as we expect for any low μ_r medium. However, when the superconductor is cooled below T_c, it rejects all the magnetic flux in the sample, as depicted in Figure 8.57. The superconductor develops a magnetization M by developing surface currents, such that M and the applied field cancel everywhere inside the sample. Put differently $\mu_o M$ is in the *opposite* direction to the applied

[15] SQUID is a superconducting quantum interference device that can detect very small magnetic fluxes.

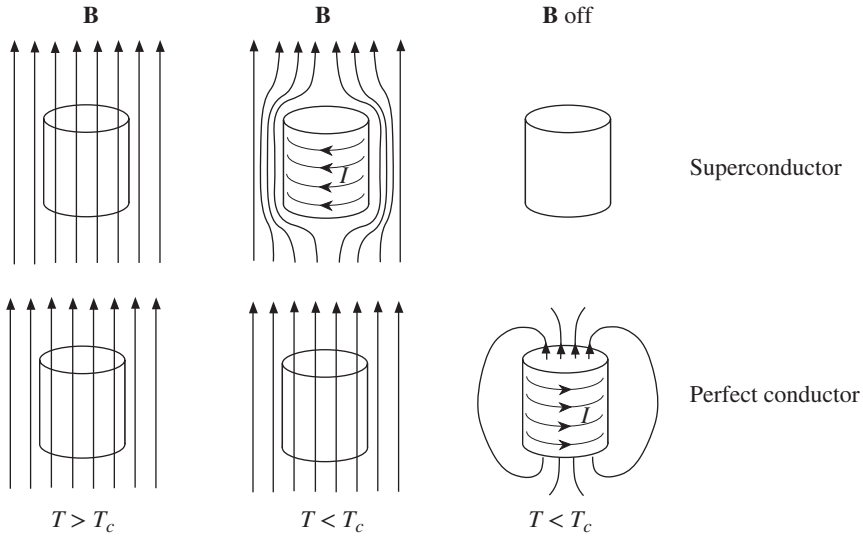
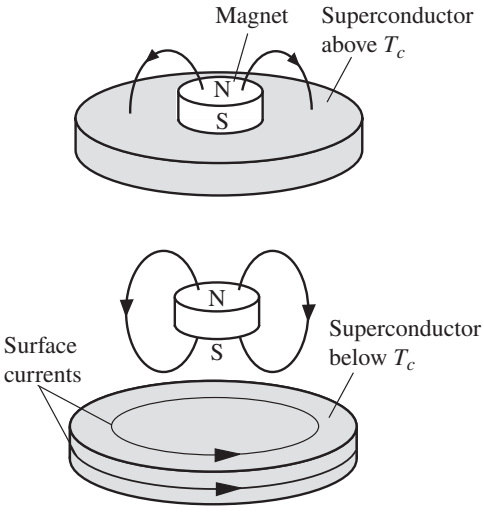


Figure 8.57 The Meissner effect.

A superconductor cooled below its critical temperature expels all magnetic field lines from the bulk by setting up a surface current. A perfect conductor ($\sigma = \infty$) shows no Meissner effect.

field and equal to it in magnitude. Thus, below T_c a superconductor is a perfectly diamagnetic substance ($\chi_m = -1$). This should be contrasted with the behavior of a perfect conductor, which only exhibits infinite conductivity, or $\rho = 0$, below T_c. If we place a perfect conductor in a magnetic field and then cool it below T_c, the magnetic field is not rejected. These two types of behavior are identified in Figure 8.57. If we switch off the field, the field around the superconductor simply disappears. But switching off the field means there is a decreasing applied field. This change in the field induces currents in the perfect conductor by virtue of Faraday's law of induction. These currents generate a magnetic field that opposes the change (Lenz's law); in other words, they generate a field along the same direction as the applied field to reenforce the decreasing field. As the current can be sustained ($\rho = 0$) without Joule dissipation, it keeps on flowing and maintaining the magnetic field. The two final situations are shown in Figure 8.57 and distinguish the Meissner effect, a distinct characteristic of a superconductor, from the behavior of a perfect conductor ($\rho = 0$ only). The photograph showing the levitation of a magnet above the surface of a superconductor (Figure 8.58) is the direct result of the Meissner effect: the exclusion of the magnet's magnetic fields from the interior of the superconductor.

The transition from the normal state to the superconducting state as the temperature falls below the critical temperature has similarities with phase transitions such as solid to liquid or liquid to vapor changes. At the critical temperature, there is a sharp change in the heat capacity as one would observe for any phase change. In the superconducting state, we cannot treat a conduction electron in isolation. The electrons behave collectively and thereby impart the superconducting characteristics to the substance, as discussed later.



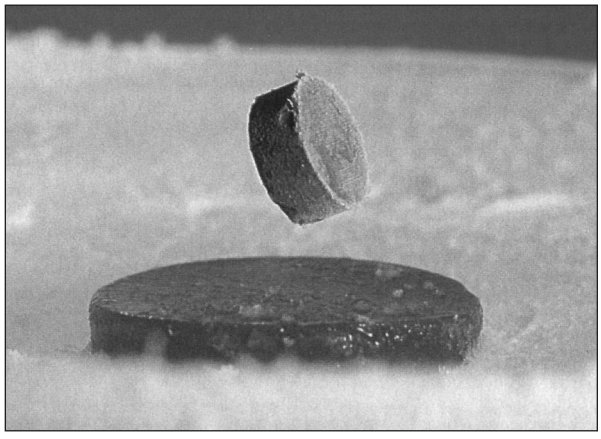


Figure 8.58 Left: A magnet over a superconductor becomes levitated. The superconductor is a perfect diamagnet which means that there can be no magnetic field inside the superconductor. Right: Photograph of a magnet levitating above a superconductor immersed in liquid nitrogen (77 K). This is the Meissner effect.
| Photo courtesy of Professor Paul C. W. Chu, University of Houston.

8.12.2 TYPE I AND TYPE II SUPERCONDUCTORS

The superconductivity below the critical temperature has been observed to disappear in the presence of an applied magnetic field exceeding a critical value denoted by B_c. This critical field depends on the temperature and is a characteristic of the material. Figure 8.59 shows the dependence of the critical field on the temperature. The critical field is maximum, $B_c(0)$, when $T = 0$ K (obtained by extrapolation[16]). As long as the applied field is below B_c at that temperature, the material is in the superconducting state, but when the field exceeds B_c, the material reverts to the normal state. We know that in the superconducting state, the applied magnetic field lines are expelled from the sample and the phenomenon is called the Meissner effect. The external field, in fact, does penetrate the sample from the surface into the bulk, but the magnitude of this penetrating field decreases exponentially from the surface. If the field at the surface of the sample is B_o, then at a distance x from the surface, the field is given by an exponential decay,

Penetration depth

$$B(x) = B_o \exp\left(-\frac{x}{\lambda}\right) \qquad [8.39]$$

where λ is a "characteristic length" of penetration, called the **penetration depth,** and depends on the temperature and T_c (or the material). At the critical temperature, the penetration length is infinite and any magnetic field can penetrate the sample and destroy the superconducting state. Near absolute zero of temperature, however,

[16] There is a third law to thermodynamics that is not as emphasized as the first two laws, which dominate all branches of engineering; that is, one can never reach the absolute zero of temperature.

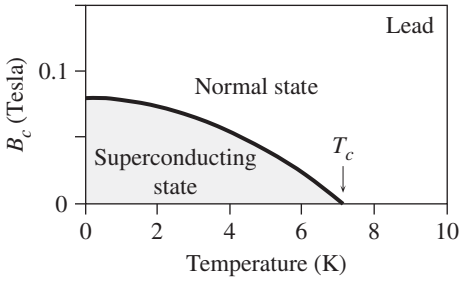


Figure 8.59 The critical field versus temperature in Type I superconductors.

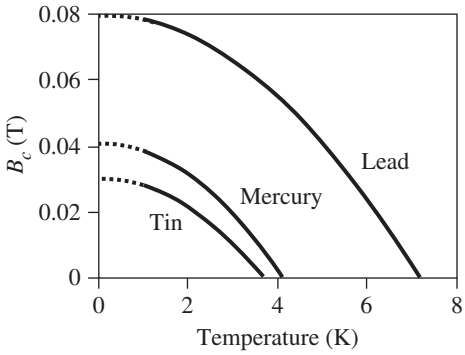


Figure 8.60 The critical field versus temperature in three examples of Type I superconductors.

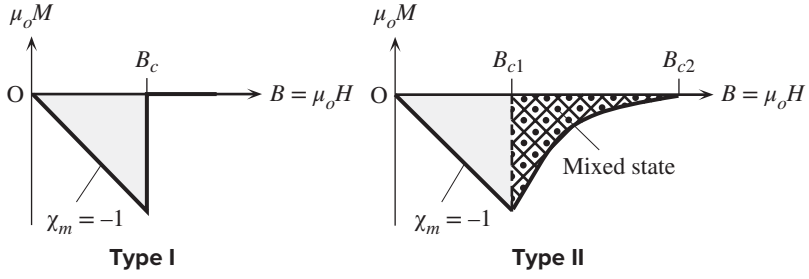


Figure 8.61 Characteristics of Type I and Type II superconductors. $B = \mu_o H$ is the applied field and M is the overall magnetization of the sample. Field inside the sample, $B_{\text{inside}} = \mu_o H + \mu_o M$, which is zero only for $B < B_c$ (Type I) and $B < B_{c1}$ (Type II).

typical penetration depths are 10–100 nm. Figure 8.60 shows the B_c versus T behavior for three example superconductors, tin, mercury, and lead.

Superconductors are classified into two types, called Type I and Type II, based on their diamagnetic properties. In Type I superconductors, as the applied magnetic field B increases, so does the opposing magnetization M until the field reaches the critical field B_c, whereupon the superconductivity disappears. At that point, the perfect diamagnetic behavior, the Meissner effect, is lost, as illustrated in Figure 8.61. A Type I superconductor below B_c is in the **Meissner state,** where it excludes all the magnetic flux from the interior of the sample. Above B_c it is in the normal state, where the magnetic flux penetrates the sample as it would normally and the conductivity is finite.

In the case of Type II superconductors, the transition does not occur sharply from the Meissner state to the normal state but goes through an intermediate phase in which the applied field is able to pierce through certain local regions of the sample. As the magnetic field increases, initially the sample behaves as a perfect diamagnet exhibiting the Meissner effect and rejecting all the magnetic flux. When the applied field increases beyond a critical field denoted as B_{c1}, the **lower critical field,** the magnetic flux lines are no longer totally expelled from the sample. The

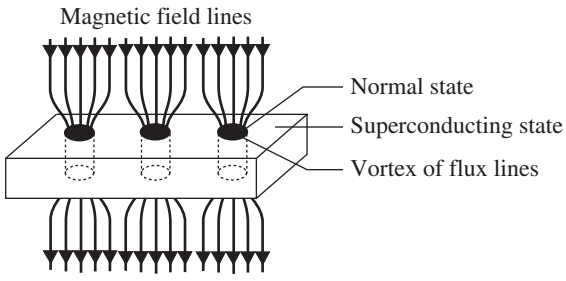


Figure 8.62 The mixed or vortex state in a Type II superconductor.

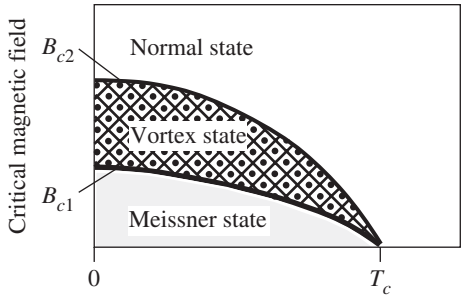


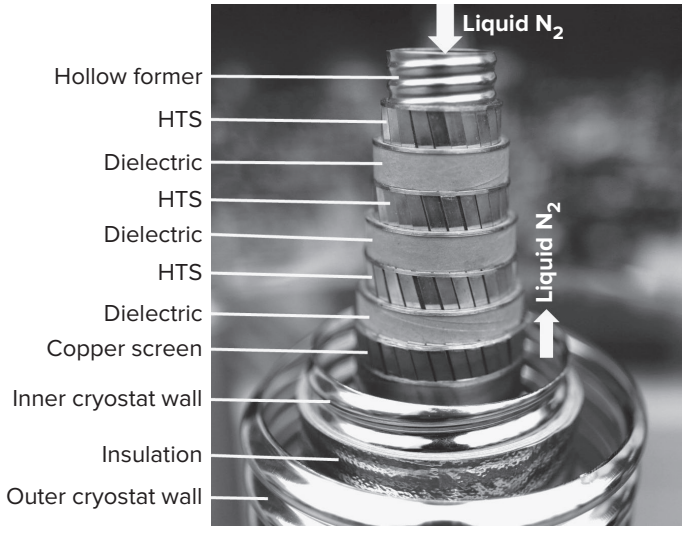
Figure 8.63 Temperature dependence of B_{c1} and B_{c2}.

overall magnetization M in the sample opposes the field, but its magnitude does not cancel the field everywhere. As the field increases, M gets smaller and more flux lines pierce through the sample until at B_{c2}, the **upper critical field,** all field lines penetrate the sample and superconductivity disappears. This behavior is shown in Figure 8.61. Type II superconductors therefore have two critical fields B_{c1} and B_{c2}.

When the applied field is between B_{c1} and B_{c2}, the field lines pierce through the sample through tubular local regions, as pictured in Figure 8.62. The sample develops local small cylindrical (filamentary) regions of normal state in a matrix of superconducting state and the magnetic flux lines go through these filaments of local normal state, as shown in Figure 8.62. The state between B_{c1} and B_{c2} is called the **mixed state** (or **vortex state**) because there are two states—normal and superconducting—mixed in the same sample. The filaments of normal state have finite conductivity and a quantized amount of flux through them. Each filament is a **vortex** of flux lines (hence the name *vortex state*). It should be apparent that there should be currents circulating around the walls of vortices. These circulating currents ensure that the magnetic flux through the superconducting matrix is zero. The sample overall has infinite conductivity due to the superconducting regions. Figure 8.63 shows the dependence of B_{c1} and B_{c2} on the temperature and identifies the regions of Meissner, mixed, and normal states. All engineering applications of superconductors invariably use Type II materials because B_{c2} is typically much greater than B_c found in Type I materials and, furthermore, the critical temperatures of Type II materials are higher than those of Type I. Many superconductors, including the recent high-T_c superconductors, are of Type II. Table 8.9 summarizes the characteristics of selected Type I and Type II superconductors.

8.12.3 CRITICAL CURRENT DENSITY

Another important characteristic feature of the superconducting state is that when the current density through the sample exceeds a critical value J_c, it is found that superconductivity disappears. This is not surprising since the current through the superconductor will itself generate a magnetic field and at sufficiently high current



A high temperature superconductor (HTS) power cable for use at 10 kV and 2,300 A. The HTS is Bi223. The cable has been installed in the city center of Essen (Germany) by a German utility company RWE Deutschland; and it has been in use since 2014. The superconductor shown is manufactured by Nexans.

© Reuters/Alamy Stock Photo.

Table 8.9 Examples of Type I and Type II superconductors

Type I	**Sn**	**Hg**	**Ta**	**V**	**Pb**	**Nb**
T_c (K)	3.72	4.15	4.47	5.40	7.19	9.2
B_c (T)	0.030	0.041	0.083	0.14	0.08	0.198

Type II	**Nb_3Sn**	**Nb_3Ge**	**$La_{1.85}Sr_{0.15}CuO_4$**	**Y-123 $YBa_2Cu_3O_7$**	**Bi-2223 $Bi_2Sr_2Ca_2Cu_3O_{10}$**	**Hg-1223 $HgBa_2Ca_2Cu_3O_8$**
T_c (K)	18.1	23.2	36.5	92	110	133
B_{c2} (Tesla) at 0 K	24.5	38	64	122	39	190
J_c (A cm^{-2}) at 0 K	$\sim 10^7$			10^4–10^7		

NOTE: Critical fields are close to absolute zero, obtained by extrapolation. Type I for pure, clean elements. B_{c2} for high-temperature superconductors depends on the crystal direction and represents the lower critical field. Values mainly from Wesche, R., "Ch 48: High-Temperature Superconductors," in Kasap, S. and Capper, P., *The Springer Handbook of Electronic and Photonic Materials*. New York, NY: Springer Science+Business Media, Inc., 2016.

densities, the magnetic field at the surface of the sample will exceed the critical field and extinguish superconductivity. This plausible direct relation between B_c and J_c is only true for Type I superconductors, whereas in Type II superconductors, J_c depends in a complicated way on the interaction between the current and the flux vortices. New high-T_c superconductors have exceedingly high critical fields, as apparent in Table 8.9, that do not seem to necessarily translate to high critical current densities. The critical current density in Type II superconductors depends not only on the temperature and the applied magnetic field but also on the preparation and hence the microstructure (*e.g.*, polycrystallinity) of the superconductor material. Critical

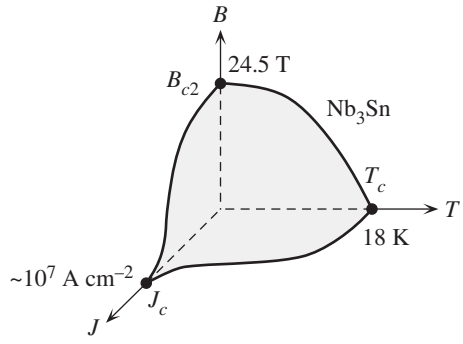


Figure 8.64 The critical surface for a niobium–tin alloy, which is a Type II superconductor.

current densities in new high-T_c superconductors vary widely with preparation conditions. For example, in Y–Ba–Cu–O, J_c may be greater than 10^7 A cm^{-2} in some carefully prepared thin films and single crystals but around 10^3–10^6 A cm^{-2} in some of the polycrystalline bulk material (*e.g.*, sintered bulk samples). In Nb_3Sn, used in superconducting solenoid magnets, on the other hand, J_c is close to 10^7 A cm^{-2} at near 0 K.

The critical current density is important in engineering because it limits the total current that can be passed through a superconducting wire or a device. The limits of superconductivity are therefore defined by the critical temperature T_c, critical magnetic field B_c (or B_{c2}), and critical current density J_c. These constitute a surface in a three-dimensional plot, as shown in Figure 8.64, which separates the superconducting state from the normal state. Any operating point (T_1, B_1, J_1) inside this surface is in the superconducting state. When the cuprate ceramic superconductors were first discovered, their J_c values were too low to allow immediate significant applications in engineering. Their synthesis over the last 20 years has advanced to a level that we can now benefit from large critical currents and fields. Over the same temperature range, ceramic cuprate superconductors now easily outperform the traditional superconductors for many applications. There are already a number of applications of these high-T_c superconductors in the commercial market.

EXAMPLE 8.10 **SUPERCONDUCTING SOLENOIDS**[17] Superconducting solenoid magnets can produce very large magnetic fields up to ~15 T or so, whereas the magnetic fields available from a ferromagnetic core solenoid is limited to ~2 T. High field magnets used in magnetic resonance imaging are based on superconducting solenoids wound using a superconducting wire. They are operated around 4 K with expensive liquid helium as the cryogen. These superconducting wires are typically Nb_3Sn or NbTi alloy filaments embedded in a copper matrix. A very large current, several hundred amperes, is passed through the solenoid winding to obtain the necessary high magnetic fields. There is, of course, no Joule heating once the current is flowing in the superconducting state. The main problem is the large forces and hence stresses in the coil due to large currents. Two wires carrying currents in the opposite direction repel each other, and the

[17] Designing a superconducting solenoid is by no means trivial, and the enthusiastic student is referred to a very readable description given by James D. Doss, *Engineer's Guide to High Temperature Superconductivity,* New York: John Wiley & Sons, 1989, ch. 4. Photographs and descriptions of catastrophic failure in high field solenoids can be found in an article by G. Broebinger, A. Passner, and J. Bevk, "Building World-Record Magnets" in Scientific American, June 1995, pp. 59–66.

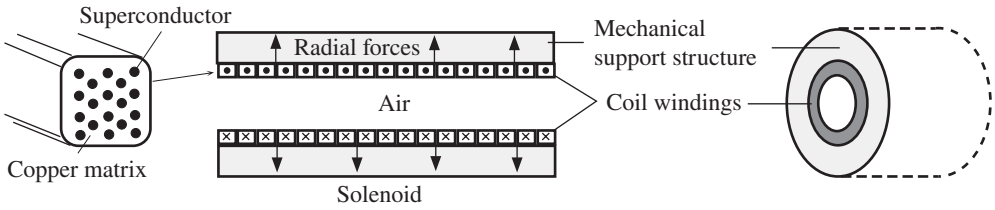
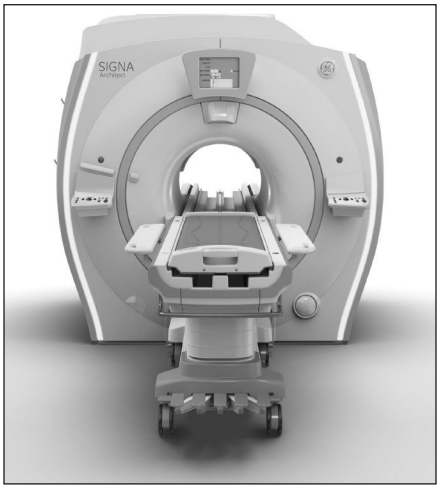


Figure 8.65 A solenoid carrying a current experiences radial forces pushing the coil apart and axial forces compressing the coil.



Magnetic Resonance Imaging (MRI) machines use a superconducting electromagnet (solenoid) similar in principle to Figure 8.65. The bore of the magnet has the patient. The magnets are cooled by liquid He and can generate the large magnetic field (3 T in this case) that is needed for MRI imaging.

| Image courtesy of GE Healthcare.

force is proportional to I^2. Thus the magnetic forces between the wires of the coil give rise to outward radial forces trying to "blow open" the solenoid, as depicted in Figure 8.65. The forces between neighboring wires are attractive and hence give rise to compressional forces squeezing the solenoid axially. The solenoid has to have a proper mechanical support structure around it to prevent mechanical fracture and failure due to large forces between the windings. The copper matrix serves as mechanical support to cushion against the stresses as well as a good thermal conductor in the event that superconductivity is inadvertently lost during operation.

Suppose that we have a superconducting solenoid that is 10 cm in diameter and 1 m in length and has 500 turns of Nb_3Sn wire, whose critical field B_c at 4.2 K (liquid He temperature) is about 20 T and critical current density J_c is 3×10^6 A cm^{-2}. What is the current necessary to set up a field of 5 T at the center of a solenoid? What is the approximate energy stored in the solenoid? Assume that the critical current density decreases linearly with the applied field. Further, assume also that the field across the diameter of the solenoid is approximately uniform (field at the windings is the same as that at the center).

SOLUTION

We can assume that we have a long solenoid, that is, length (100 cm) $\gg$ diameter (10 cm). The field at the center of a long solenoid is given by

$$B = \frac{\mu_o NI}{\ell}$$

so the current necessary for $B = 5$ T is

$$I = \frac{B\ell}{\mu_o N} = \frac{(5)(1)}{(4\pi \times 10^{-7})(500)} = 7958 \text{ A} \qquad \text{or} \qquad 7.96 \text{ kA}$$

As the coil is 1 m and there are 500 turns, the coil wire radius must be 1 mm. If all the cross section of the wire were of superconducting medium, then the corresponding current density would be

$$J_{\text{wire}} = \frac{1}{\pi r^2} = \frac{7958}{\pi(0.001)^2} = 2.5 \times 10^9 \text{ A m}^{-2} \qquad \text{or} \qquad 2.5 \times 10^5 \text{ A cm}^{-2}$$

The actual current density through the superconductors will be greater than this as the wires are embedded in a metal matrix. Suppose that 20 percent by cross-sectional area (and hence as volume percentage) is the superconductor; then the actual current density through the superconductor is

$$J_{\text{super}} = \frac{J_{\text{wire}}}{0.2} = 1.25 \times 10^6 \text{ A cm}^{-2}$$

We now need the critical current density J_c' at a field of 5 T. Assuming J_c decreases linearly with the applied field and vanishes when $B = B_c$, we can find J_c', from linear interpolation

$$J_c' = J_c \frac{B_c - B}{B_c} = (3 \times 10^6 \text{ A cm}^{-2}) \frac{20 \text{ T} - 5 \text{ T}}{20 \text{ T}} = 2.25 \times 10^6 \text{ A cm}^{-2}$$

The actual current density J_{super} through the superconductors is less than this critical value J_c'. We can assume that the superconducting solenoid will operate "safely" (with all other designs correctly implemented). It should be emphasized that accurate and reliable calculations will involve the actual J_c–B_c–T_c surface, as in Figure 8.64 for the given material.

Since the field in the solenoid is $B = 5$ T, assuming that this is uniform along the axis and the core is air, the energy density or energy per unit volume is

$$E_{\text{vol}} = \frac{B^2}{2\mu_o} = \frac{5^2}{2(4\pi \times 10^{-7})} = 9.95 \times 10^6 \text{ J m}^{-3}$$

so the total energy

$$\begin{aligned} E = E_{\text{vol}} \text{ [Volume]} &= (9.95 \times 10^6 \text{ J m}^{-3})[(1 \text{ m})(\pi 0.05^2 \text{ m}^2)]. \\ &= 7.81 \times 10^4 \text{ J} \qquad \text{or} \qquad 78.1 \text{ kJ} \end{aligned}$$

If all this energy can be converted to electrical work, it would light a 100 W lamp for 13 min (and if converted to mechanical work, it could lift a 7,900 kg truck by 1 m).

8.13 SUPERCONDUCTIVITY ORIGIN

Although superconductivity was discovered in 1911, the understanding of its origin did not emerge until 1957 when Bardeen, Cooper, and Schrieffer formulated the theory (called the **BCS theory**) in terms of quantum mechanics. The quantum mechanical treatment is certainly beyond the scope of this book, but one can nonetheless grasp an intuitive understanding, as follows. The cardinal idea is that, at sufficiently low temperatures, two oppositely spinning and oppositely traveling electrons can attract each other indirectly through the deformation of the crystal lattice

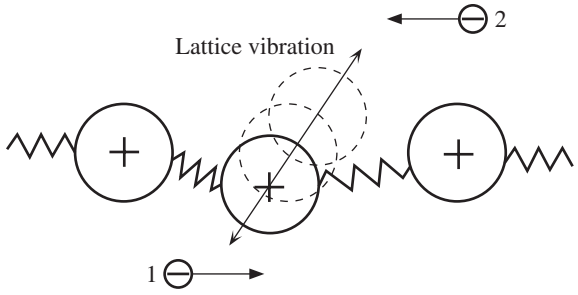


Figure 8.66 A pictorial and intuitive view of an indirect attraction between two oppositely traveling electrons via lattice distortion and vibration.

of positive metal ions. The idea is illustrated pictorially in Figure 8.66. The electron 1 distorts the lattice around it and changes its vibrations as it passes through this region. Random thermal vibrations of the lattice at low temperatures are not strong enough to randomize this induced lattice distortion and vibration. The vibrations of this distorted region now look differently to another electron, 2, passing by. This second electron feels a "net" attractive force due to the slight displacements of positive metal ions from their equilibrium positions. The two electrons interact indirectly through the deformations and vibrations of the lattice of positive ions. This indirect interaction at sufficiently low temperatures is able to overcome the mutual Coulombic repulsion between the electrons and hence bind the two electrons to each other. The two electrons are called a **Cooper pair.** The intuitive diagram in Figure 8.66, of course, does not even convey the intuition why the spins of the electrons should be opposite. The requirement of opposite spins comes from the formal quantum mechanical theory. The net spin of the Cooper pair is zero and their net linear momentum is also zero. There is a further significance to the pairing of electron spins in the Cooper pair. As a quasi-particle, or an entity, the Cooper pair has no net spin and hence the Cooper pairs do not obey the Fermi–Dirac statistics.[18] They can therefore all "condense" to the *lowest energy* state and possess one single wavefunction that can describe the whole collection of Cooper pairs. All the paired electrons are described collectively by a single coherent wavefunction Ψ, which extends over the whole sample. A crystal imperfection cannot simply scatter a single Cooper pair because all the pairs behave as a single entity—like a "huge molecule." Scattering one pair involves scattering all, which is simply not possible. An analogy may help. One can scatter an individual football player running on his own. But if all the team members got together and moved forward arm in arm as a rigid line, then the scattering of any one now is impossible, as the rest will hold him in the line and continue to move forward (don't forget, it's only an analogy!). Superconductivity is said to be a macroscopic manifestation of quantum mechanics.

The BCS theory has had good success with traditional superconductors, but it is believed that it does not apply to high-T_c superconductors, that is, lattice vibrations are not involved in the formation of Cooper pairs. The formation of a Cooper pair is still the key concept in explaining the superconductivity but the Cooper electrons are believed to be coupled by "spin waves" within the crystal. The spin of a moving

[18] In fact, the Cooper pair without a net spin behaves as if is were a **boson** particle.

electron modifies the spins of the atoms around it, generating a spin wave, which affects another nearby electron. The interactions lead to the formation of a Cooper pair. Obviously, at high temperatures, lattice vibrations have sufficient energy to disassociate the pair, and the crystal returns to the normal state.

ADDITIONAL TOPICS

8.14 JOSEPHSON EFFECT

The Josephson junction is a junction between two superconductors that are separated by a thin insulator (a few nanometers thick) as depicted in Figure 8.67. If the insulating barrier is sufficiently thin, then there is a probability that the Cooper pairs can tunnel across the junction. The wavefunction Ψ of the Cooper pair, however, changes phase by θ when it tunnels through the junction, not unexpected as the pair goes through a potential barrier. The maximum superconducting current I_c that can flow through this weak link depends on not only the thickness and area (size) of the insulator but also on the superconductor materials and the temperature. The current I, or the *supercurrent,* through the junction due to Cooper pair tunneling is determined by the phase angle θ,

Josephson junction supercurrent

$$I = I_c \sin \theta \qquad [8.40]$$

where I_c is the maximum current or the critical current. If the current through the junction is controlled by an external circuit, then the tunneling Cooper pairs on either side of the junction (in the superconductors) adjust their respective phases to maintain the phase change to satisfy Equation 8.40. If we plot the *I–V* characteristics of this junction as in Figure 8.68, we would find that for $I < I_c$, the behavior follows the vertical *OC* line with no voltage across the junction.

If the current through the junction exceeds I_c, then the Cooper pairs cannot tunnel through the insulator because Equation 8.40 cannot be satisfied. There is still a current through the junction, but it is due to the tunneling of normal, that is, single electrons as represented by the curve *OABD* in Figure 8.68. Thus, the current switches from point *C* to point *B* and then follows the normal tunneling curve *B* to *D.* At point *B*, a *voltage* develops across the junction and increases with the current. The normal tunneling current in the range *OA* is negligible and rises suddenly when the voltage exceeds V_a. The reason is that a certain amount of voltage (corresponding

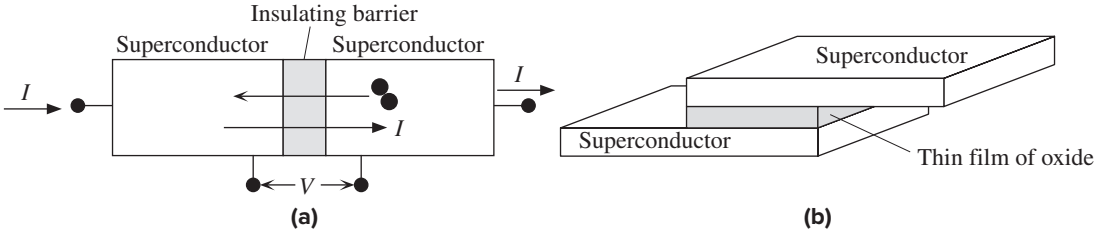


Figure 8.67 (a) A Josephson junction is a junction between two superconductors separated by a thin insulator. (b) In practice, thin-film technology is used to fabricate a Josephson junction.

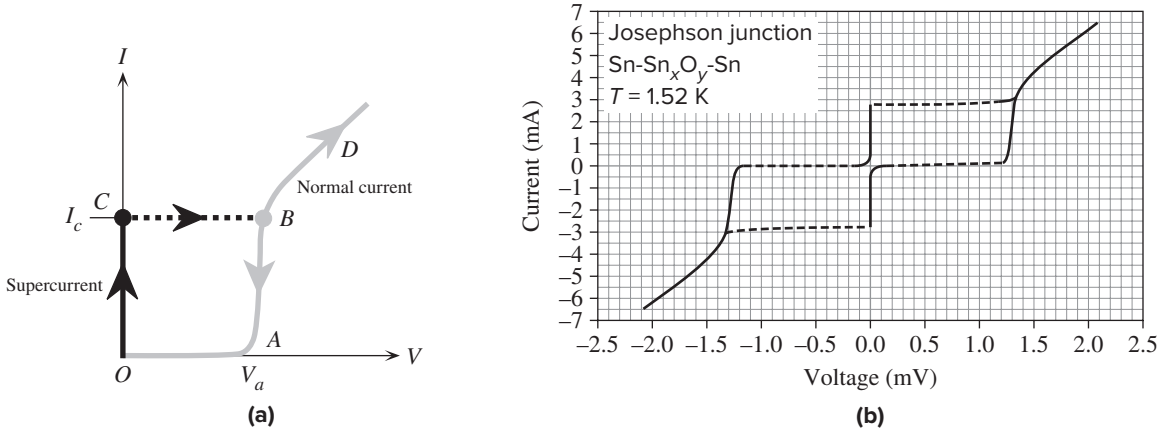


Figure 8.68 (a) *I–V* characteristics of a Josephson junction for positive currents when the current is controlled by an external circuit. (b) Experimental *I–V* characteristics of an Sn-Sn_xO_y-Sn Josephson junction at $T = 1.52$ K. Sn_xO_y is tin oxide, the weak link. | Data extracted from Balsamo et al., *Physical Review,* 10, 1881, 1974.

to a potential energy eV_a) is needed to provide the necessary energy to disassociate the tunneling single electron from its Cooper pair. It is apparent that the thin insulation acts as a weak superconductor or as a **weak link** in the superconductor; weak with regard to the currents that can flow in the superconductor itself. The *I–V* characteristic in Figure 8.68a is symmetric about *O*, and is called the **dc characteristic of the Josephson junction.** In addition, the *I–V* behavior exhibits hysteresis; that is, if we were to decrease the current, the behavior does not follow *DBC* down to *O*, but follows the *DBA* curve. When the current is decreased nearly to zero, the normal tunneling current switches to the supercurrent. The Josephson junction is bistable; that is, it has two states corresponding to the superconducting state *OC* and normal state *ABD*. Thus, the device behaves as an electronic switch whose switching time, in theory, is determined by tunneling times, in the picoseconds range. In practice the switching time (~10 ps) is limited by the junction capacitance. Figure 8.68b shows the experimental *I* versus *V* characteristics for a Josephson junction that is made of two tin superconductors with tin oxide as the weak link; it closely follows the expected behavior in Figure 4.68a.

If, on the other hand, a dc voltage is applied across the Josephson junction, then the phase change θ is modulated by the applied voltage. The most interesting and surprising aspect is that the voltage modulates the rate of change of the phase through the barrier, that is,

Applied voltage modulates phase

$$\frac{d\theta}{dt} = \frac{2eV}{\hbar}$$

When we integrate this, we find that θ is time and voltage dependent, so, according to Equation 8.40, the current is a sinusoidal function of time and voltage, that is,

$$I = I_c \sin\left(\theta_o - \frac{2\pi(2eV)t}{h}\right)$$

or

$$I = I_o \sin(2\pi ft)$$

where I_o is a new constant incorporating θ_o and the frequency of the oscillations of the current is given by

ac Josephson effect

$$f = \frac{2eV}{h} \qquad [8.41]$$

The Josephson junction therefore generates an oscillating current of frequency f when there is a dc voltage V across it. This is called the **ac Josephson effect,** a remarkable phenomenon originally predicted by Josephson as a graduate student at Cambridge (1962). According to the ac Josephson effect, the junction generates an ac current at a frequency of $2e/h$ Hz per volt or 483.6 MHz per microvolt. Furthermore, the frequency of the current has nothing to do with the material properties of the junction but is only determined by the applied voltage through e and h. The ac Josephson effect has been adopted to define the voltage standard: One volt is the voltage that, when applied to a Josephson junction, will generate an ac current and hence an electromagnetic radiation of frequency 483,597.9 GHz.

8.15 FLUX QUANTIZATION

Consider a ring of a superconducting material above its T_c. Suppose that the ring is immersed in magnetic flux lines from a magnet placed above it as shown in Figure 8.69a. When we cool the ring to below T_c, the magnetic flux lines are excluded from the ring itself, due to the Meissner effect, but they go through the hole, as shown in Figure 8.69b. If we now remove the magnet, we may think that the magnetic flux lines simply disappear, but this is not the case. A persistent current is set up on the inside surface of the superconducting ring that flows to maintain the flux constant in the hollow. This supercurrent generates flux lines in the hollow as if to replace those taken away by the removal of the magnet, as depicted in Figure 8.69c. Since the current can flow indefinitely in the ring, the overall effect is that the magnetic flux is *trapped* within the ring. Indeed, if we were to bring back the magnet, the current in the ring would disappear to ensure that the magnetic flux in the hollow remains unchanged. The origin of flux trapping can be appreciated by

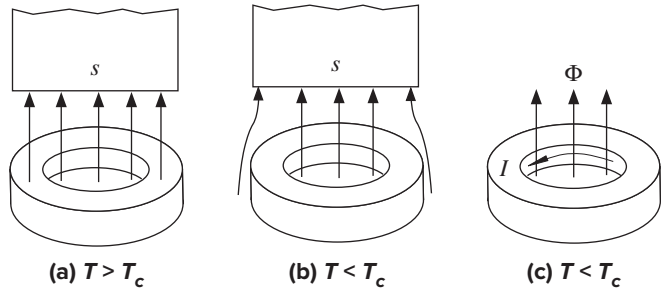


Figure 8.69 (a) Above T_c, the flux lines enter the ring. (b) The ring and magnet are cooled through T_c. The flux lines do not enter the superconducting ring but stay in the hole. (c) Removing the magnet does not change the flux in the hole.

considering what would happen if the flux were allowed to change, that is, $d\Phi/dt \neq 0$. A changing flux would induce a voltage $V = -d\Phi/dt$ around the ring that would drive an infinite current $I = V/R$ where $R = 0$. This is not possible, and hence the flux cannot change, which means we must have $d\Phi/dt = 0$. One should also note that there can be no electric field inside a superconductor because

$$E = \frac{J}{\sigma} = 0$$

since the conductivity σ is infinite.

What would happen if we have a superconducting ring (below T_c) that initially had no flux in the hole? If we were to bring a magnet to it, then the flux lines would now be excluded from both the ring itself and also the hole since the trapped flux within the ring is zero.

It turns out that the trapped flux Φ inside the ring is quantized by virtue of superconductivity being a quantum phenomenon. The smallest quantized amount of flux is called the **magnetic flux quantum** and is given by $h/2e$ or 2.0679×10^{-15} Wb. The flux Φ in the ring is an integer multiple n of this quantum,

$$\Phi = n\frac{h}{2e} \qquad [8.42]$$

Trapped flux is quantized

DEFINING TERMS

Antiferromagnetic materials have crystals in which alternating permanent atomic spin magnetic moments are equal in magnitude but point in opposite directions (antiparallel), which leads to no net magnetization of the crystal.

Bloch wall is a magnetic domain wall.

Bohr magneton (β) is a useful elementary unit of magnetic moment on the atomic scale. It is equal to the magnetic moment of one electron spin along an applied magnetic field $\beta = e\hbar/2m_e$.

Coercivity or **coercive field** (H_c) measures the ability of a magnetized material to resist demagnetization. It is the required reverse applied field that would remove any remanent magnetization, that is, demagnetize the material.

Cooper pair is a quasi-particle formed by the mutual attraction of two electrons with opposite spins and opposite linear momenta below a critical temperature. It has a charge of $-2e$ and a mass of $2m_e$ but no net spin. It does *not* obey Fermi–Dirac statistics. The electrons are held together by the induced distortions and vibrations of the lattice of positive metal ions with which the electrons interact.

Critical magnetic field (B_c) is the maximum field that can be applied to a superconductor without destroying the superconducting behavior. B_c decreases from its maximum value at absolute zero to zero at T_c.

Critical temperature (T_c) is a temperature that separates the superconducting state from the normal state. Above T_c, the substance is in the normal state with a finite resistivity, but below T_c, it is in the superconducting state with zero resistivity.

Curie temperature (T_C) is the critical temperature at which the ferromagnetic and ferrimagnetic properties are lost. Above the Curie temperature, the material behaves as if it were paramagnetic.

Diamagnetic material has a negative magnetic susceptibility and reduces or repels applied magnetic fields. Superconductors are perfect diamagnets that repel the applied field. Many substances possess weak diamagnetism, so the applied field is slightly decreased within the material.

Domain wall is a region between two neighboring magnetic domains of differing orientations of magnetization.

Domain wall energy is the excess energy in the domain wall as a result of the gradual orientations of the neighboring spin magnetic moments of atoms through the wall region. It is the excess energy due to the excess exchange interaction energy, magnetocrystalline anisotropy energy, and magnetostrictive energy in the wall region.

Easy direction is the crystal direction along which the atomic magnetic moments (due to spin) are spontaneously and most easily aligned. Exchange interaction energy is lowest (hence favorable) when the alignment of atomic spin magnetic moments is in this direction in the crystal. For the iron crystal, it is one of the six [100] directions (cube edge).

Eddy current loss is the Joule energy loss (I^2R) in a ferromagnetic material subjected to changing magnetic fields (in ac fields). The varying magnetic field induces voltages in the ferromagnetic material that drive currents (called eddy currents) that generate Joule heating due to I^2R.

Eddy currents are the induced conduction currents flowing in a ferromagnetic material as a result of varying (ac) magnetic fields.

Exchange interaction energy (E_{ex}) is a kind of Coulombic interaction energy between two neighboring electrons and positive metal ions that depends on the relative spin orientations of the electrons as a consequence of the Pauli exclusion principle. Its exact origin is quantum mechanical. Qualitatively, different spins lead to different electron wavefunctions, different negative charge distributions, and hence different Coulombic interactions. In ferromagnetic crystals, E_{ex} is negative when the neighboring electron spins are parallel.

Ferrimagnetic materials possess crystals that contain two sets of atomic magnetic moments that oppose each other, but one set has greater strength and therefore there is a net magnetization of the crystal. An unmagnetized ferrimagnetic substance normally has many magnetic domains whose magnetization vectors add to give no overall magnetization.

Ferrites are ferrimagnetic materials that are ceramics with insulating properties. They are therefore used in HF applications where eddy current losses are significant. Their general composition is $(MO)(Fe_2O_3)$, where M is typically a divalent metal. For magnetically soft ferrites, M is typically Fe, Mn, Zn, or Ni, whereas for magnetically hard ferrites, M is typically Sr or Ba. Hard ferrites such as $BaOFe_2O_3$ have the hexagonal crystal structure with a high degree of magnetocrystalline anisotropy and therefore possess high coercivity (difficult to demagnetize).

Ferromagnetic materials have the ability to possess large permanent magnetizations even in the absence of an applied field. An unmagnetized ferromagnetic material normally has many magnetic domains whose magnetization vectors add to give no overall magnetization. However, in a sufficiently strong magnetizing field, the whole ferromagnetic substance becomes one magnetic domain in which all the atomic spin magnetic moments are aligned to give a large magnetization along the field. Some of this magnetization is retained even after the removal of the field.

Giant magnetoresistance (GMR) is the large change in the resistance of a special multilayer structure when a magnetic field is applied; the simplest structure usually consists of two thin ferromagnetic layers (*e.g.*, Fe) sandwiching an even thinner nonmagnetic metal (*e.g.*, Cu).

Hard direction is the crystal direction along which it is hardest to align the atomic spin magnetic moments relative to the easy direction. Exchange interaction energy E_{ex} favors the easy direction most (E_{ex} is most negative) and favors the hard direction least (E_{ex} is least negative).

Hard magnetic materials characteristically have high remanent magnetizations (B_r) and high coercivities (H_c), so once magnetized, they are difficult to demagnetize. They are suitable for permanent magnet applications. They have broad B–H hysteresis loops.

Hard magnetic particles are small particles of various shapes that have high coercivity due to having a single magnetic domain with high magnetocrystalline anisotropy energy, or possessing substantial shape anisotropy (aspect ratio—length-to-width ratio).

Hysteresis loop is the magnetization (M) versus applied magnetic field intensity (H) or B versus H behavior of a ferromagnetic (or ferrimagnetic) substance through one cycle as it is repeatedly magnetized and demagnetized.

Hysteresis loss is the energy loss involved in magnetizing and demagnetizing a ferromagnetic (or ferrimagnetic) substance. It arises from various energy losses involved in the irreversible motions of the domain walls. Hysteresis loss per unit volume of specimen is the area of the B–H hysteresis loop.

Initial permeability ($\mu_{ri}\mu_o$) is the initial slope of the B versus H characteristic of an unmagnetized ferromagnetic (or ferrimagnetic) material and typically represents the magnetic permeability under very small applied magnetic fields. Initial relative permeability (μ_{ri}) is the relative permeability of an unmagnetized ferromagnetic (or ferrimagnetic) material under very small applied fields.

Magnetic dipole moment ($\boldsymbol{\mu}_m$) is defined as $IA\mathbf{u}_n$, where I is the current flowing in a circuit loop of area A and $\mathbf{u}_n$ is the unit vector in the direction of an advance of a screw when it is turned in the direction of the circulating current. Qualitatively, it measures the strength of the magnetic field created by a current loop and also the extent of interaction of the current loop with an externally applied magnetic field. $\boldsymbol{\mu}_m$ is normal to the surface of the loop. Magnetic moment in a magnetic field experiences a torque that tries to rotate $\boldsymbol{\mu}_m$ to align it with the field. In a nonuniform field, the magnetic moment experiences a force that attracts it to a greater field.

Magnetic domain is a region of a ferromagnetic (or ferrimagnetic) crystal that has spontaneous magnetization, that is, magnetization in the absence of an applied field, due to the alignment of all magnetic moments in that region.

Magnetic field, magnetic induction, or **magnetic flux density (B)** is a field that is generated by a current-carrying conductor that produces a force on a current-carrying conductor elsewhere. Equivalently, we can define it as the field generated by a moving charge that acts to produce a force on a moving charge elsewhere. The force is called the Lorentz force and is given by $\mathbf{F} = q\mathbf{v} \times \mathbf{B}$ where $\mathbf{v}$ is the velocity of the particle with charge q. The magnetic field $\mathbf{B}$ in a material is the sum of the applied field $\mu_o\mathbf{H}$, and that due to the magnetization of the material $\mu_o\mathbf{M}$, that is, $\mathbf{B} = \mu_o(\mathbf{H} + \mathbf{M})$.

Magnetic field intensity or **magnetizing field (H)** gauges the magnetic strength of external conduction currents (*e.g.*, currents flowing in the windings) in the absence of a material medium. It excludes the magnetization currents that become induced on the surfaces of any material placed in a magnetic field. $\mu_o H$ is the magnetic field in free space and is considered to be the *applied magnetic field*. The terms *intensity* or *strength* distinguish $\mathbf{H}$ from $\mathbf{B}$, which is simply called the magnetic field.

Magnetic flux (Φ) represents to what extent magnetic field lines are flowing through a given area perpendicular to the field lines. If δA is a small area perpendicular to the magnetic field B and B is constant over δA, then the flux $\delta\Phi$ through δA is defined by $\delta\Phi = B\,\delta A$. Total flux through any closed surface is zero.

Magnetic permeability (μ) is the magnetic field generated per unit magnetizing field, that is, $\mu = B/H$. Permeability gauges the effectiveness of a medium in generating as much magnetic field as possible per unit magnetizing field. Permeability of free space is the absolute permeability μ_o, which is the magnetic field generated in a vacuum per unit magnetizing field.

Magnetic susceptibility (χ_m) indicates the ease with which the material becomes magnetized under an applied magnetic field. It is the magnetization induced in the material per unit magnetizing field, $\chi_m = M/H$.

Magnetization or **magnetization vector (M)** represents the net magnetic moment per unit volume of material. In the presence of a magnetic field, individual atomic moments tend to align with the field, which results in a net magnetization. Magnetization of a specimen can be represented by the flow of currents on the surface over a unit length of the specimen; $M = I_m$, where I_m is the surface magnetization current per unit length.

Magnetization current (I_m) is a bound current per unit length that exists on the surface of a substance due to its magnetization. It is not, however, due to the flow of free charges but arises in the presence of an applied magnetic field as a result of the orientations of the

electronic motions in the constituent atoms. In the bulk, these electronic motions cancel each other and there is no net bulk current, but on the surface, they add to give a bound surface current I_m per unit length, which is equal to the magnetization M of the substance.

Magnetocrystalline anisotropy is the anisotropy associated with magnetic properties such as the magnetization in different directions in a ferromagnetic (or ferrimagnetic) crystal. Atomic spins prefer to align along certain directions in the crystal, called easy directions. The direction along which it is most difficult to align the spins is called the hard direction. For example, in the iron crystal, all atomic spins prefer to align along one of the [100] directions (easy directions) and it is most difficult to align the spins along one of the [111] directions (hard directions).

Magnetocrystalline anisotropy energy (K) is the energy needed to rotate the magnetization of a ferromagnetic (or ferrimagnetic) crystal from its natural easy direction to a hard direction. For example, it takes an energy of about 48 mJ cm^{-3} to rotate the magnetization of an iron crystal from the easy direction [100] to the hard direction [111].

Magnetoresistance generally refers to the change in the resistance of a magnetic material when it is placed in a magnetic field. The change in the resistance of a nonmagnetic metal, such as copper, is usually very small. In a magnetic metal, the change in the resistivity due to the applied magnetic field is *anisotropic;* that is, it depends on the direction of current flow with respect to the applied field and is called **anisotropic magnetoresistance (AMR).**

Magnetostatic energy is the potential energy stored in an external magnetic field. It takes external work to establish a magnetic field, and this energy is said to be stored in the magnetic field. Magnetic energy per unit volume at a point in free space is given by

$$E_{\text{vol}}(\text{air}) = \frac{1}{2}\mu_o H^2 = \frac{B^2}{2\mu_o}$$

Magnetostriction is the change in the length of a ferromagnetic (or ferrimagnetic) crystal as a result of its magnetization. An iron crystal placed in a magnetic field along an easy direction becomes longer along this direction but contracts in the transverse direction.

Magnetostrictive energy is the strain energy in the crystal due to magnetostriction, that is, the work done in straining the crystal when it becomes magnetized.

Maximum relative permeability ($\mu_{r,\max}$) is the maximum relative permeability of a ferromagnetic (or ferrimagnetic) material.

Meissner effect is the repulsion of all magnetic flux from the interior of a superconductor. The superconductor behaves as if it were a perfect diamagnet with $\chi_m = -1$.

Paramagnetic materials have a small and positive magnetic susceptibility. In an applied field, they develop a small amount of magnetization in the direction of the applied field, so the magnetic field in the material is slightly greater. They are attracted to a higher magnetic field.

Relative permeability (μ_r) measures the magnetic field in a medium with respect to that in a vacuum, $\mu_r = B/\mu_o H$. Since B depends on the magnetization of the medium, μ_r measures the ease with which the material becomes magnetized.

Remanence or **remanent magnetization** ($\mathbf{M}_r$) is the magnetization that remains in a magnetic material after it has been fully magnetized and the magnetizing field has been removed. It measures the ability of a magnetic material to retain a portion of its magnetization after the removal of the applied field. The corresponding magnetic field ($\mu_o \mathbf{M}_r$) is the remanent magnetic field $\mathbf{B}_r$.

Saturation magnetization is the maximum magnetization that can be obtained in a ferromagnetic crystal at a given temperature when all the magnetic moments have been aligned in the direction of the applied field, when there is a single magnetic domain with its magnetization **M** along the applied field.

Shape anisotropy is the anisotropy in magnetic properties associated with the shape of the ferromagnetic (or ferrimagnetic) substance. A crystal rod that is thin and long prefers to have its magnetization **M** along the length (long axis) of the rod because this direction of magnetization creates less external magnetic fields and leads to less external magnetostatic energy compared with the case when **M** is along the width (short axis) of the rod. Reversing the

magnetization involves rotating **M** through the width of the rod, where the external magnetic field and hence magnetostatic energy are large, and requires large substantial work. It is therefore difficult to rotate magnetization around from the long axis to the short axis.

Soft magnetic materials characteristically have high saturation magnetizations (B_{sat}) but low saturation magnetizing fields (H_{sat}) and low coercivities (H_c), so they can be magnetized and demagnetized easily. They have tall and narrow *B–H* hysteresis loops.

Superconductivity is a phenomenon in which a substance loses all resistance to current flow (acquires zero resistivity) and also exhibits the Meissner effect (becomes a perfect diamagnet).

Type I superconductors have a single critical field (B_c) above which the superconducting behavior is totally lost.

Type II superconductors have a lower (B_{c1}) and an upper (B_{c2}) critical field. Below B_{c1}, the substance is in the superconducting phase with Meissner effect; all magnetic flux is excluded from the interior. Between B_{c1} and B_{c2}, magnetic flux lines pierce through local filamentary regions of the superconductor, which behave normally. Above B_{c2}, the superconductor reverts to normal behavior.

QUESTIONS AND PROBLEMS

8.1 **Inductance of a long solenoid** Consider the very long (ideally infinitely long) solenoid shown in Figure 8.70. If r is the radius of the core and ℓ is the length of the solenoid, then $\ell \gg r$. The total number of turns is N and the number of turns per unit length is $n = N/\ell$. The current through the coil wires is I. Apply Ampere's law around C, which is the rectangular circuit $PQRS$, and show that

$$B \approx \mu_o \mu_r n I$$

Further, show that the inductance is

$$L \approx \mu_o \mu_r n^2 V_{core}$$

Inductance of a long solenoid

where V_{core} is the volume of the core. How would you increase the inductance of a long solenoid?

What is the approximate inductance of an air-cored solenoid with a diameter of 1 cm, length of 20 cm, and 500 turns? What is the magnetic field inside the solenoid and the energy stored in the whole solenoid when the current is 1 A? What happens to these values if the core medium has a relative permeability μ_r of 600?

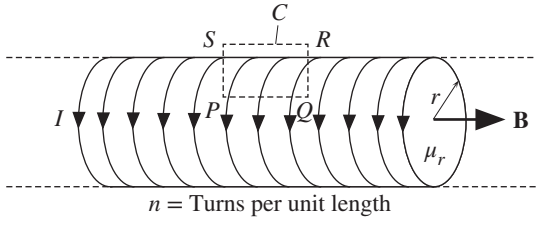


Figure 8.70

8.2 **Magnetization** Consider a long solenoid with a core that is an iron alloy (see Problem 8.1 for the relevant formulas). Suppose that the diameter of the solenoid is 2 cm and the length of the solenoid is 20 cm. The number of turns on the solenoid is 200. The current is increased until the core is magnetized to saturation at about $I = 2$ A and the saturated magnetic field is 1.5 T.

a. What is the magnetic field intensity at the center of the solenoid and the applied magnetic field, $\mu_o H$, for saturation?

b. What is the saturation magnetization M_{sat} of this iron alloy?